221 AL

CENTRE FOR ENGINEERING RESEARCH INC.

C-FER
200
Karl Clark Road
Edmonton, Alberta
Canada T6N 1H2

Tel: (403) 450-3300
Fax: (403) 450-3700

Optimization of Metal Loss Corrosion Maintenance

PIRAMID Technical Reference Manual No. 6.0

AL

Confidential to C-FER's Pipeline Program Participants

Prepared by
M. A. Nessim, Ph.D., P.Eng.
and
H. P. Hong, Dr.Eng., P.Eng.

Centre For Engineering Research Inc.

December 1996
Project 96008

NOTICE

Restriction on Disclosure

TABLE OF CONTENTS

Table of Contents

Table of Contents

LIST OF FIGURES AND TABLES

List of Figures and Tables

List of Figures and Tables

EXECUTIVE SUMMARY

This document is part of the Technical Reference Manual for the software system titled *PIRAMID* (Pipeline Risk Analysis for Maintenance and Inspection Decisions), which is being developed by C-FER as part a joint industry program aimed at applying quantitative risk analysis methods to the optimization of pipeline integrity maintenance activities. *PIRAMID* is being developed in a modular fashion; previously completed modules covered prioritization of onshore pipelines for integrity maintenance and assessment of failure consequences for onshore and offshore pipelines. These modules have been developed within a decision analysis framework based on decision influence diagrams. This document describes a module that estimates failure probabilities due to external metal loss corrosion and optimizes related maintenance activities.

The corrosion maintenance problem is modeled by an influence diagram that calculates the probabilities of failure due to corrosion considering the impact of different maintenance activities. This influence diagram is linked to the consequence analysis influence diagram developed in previous projects in order to carry out the optimization analysis and identify the optimal combination of corrosion maintenance activities. The maintenance options considered include the choice of an inspection method (high resolution or low resolution in-line inspection, or coating damage surveys), a specific tool, a repair threshold, and a time interval between inspections.

To ensure run time efficiency, the program has been designed to deal with one maintenance choice at a time. For each maintenance event, the user can carry out an initial analysis to determine whether an inspection is required and what inspection tool should be used. This analysis requires the user to input an estimate of the frequency and size distribution of existing corrosion defects. Default values of these parameters are suggested by the program based on the attributes of the line being considered. Once an inspection is carried out, the program uses a processed version of the inspection results to determine whether to carry out repairs based on the current inspection data, or to further inspect the line using more a accurate tool. When the decision is made to repair the line, the program will provide the optimal excavation and repair criteria and the optimal time interval to next inspection.

PIRAMID incorporates a model that calculates the probability of failure due to corrosion from probabilistic inputs representing the frequency, depth and length of corrosion defects, and the yield strength of the line pipe. The calculation utilizes a deterministic model that estimates pipe pressure resistance at a given defect location from the defect geometry, pipe geometry and yield strength. This model is a modified version of the well known ASME B31G model for estimating the remaining strength of corroded pipe. Modifications were made to the model to remove unnecessary conservatism, improve model accuracy and incorporate special parameters to account for model uncertainties. This model is used to calculate the probability of a pipe body failure, which will generally result in a large leak or a rupture. A separate criterion was developed to estimate the probability of small leaks. This criterion assumes that a small leak occurs when a short defect corrodes through the wall without reaching the threshold for a pipe body failure. The two failure criteria have been combined in a single model that calculates the total probability of failure and the relative frequencies of small leaks, large leaks and ruptures. Experimentation with this model shows that realistic defect size distributions result in failure

probabilities that are consistent with historical data. The approach adopted for estimating failure probabilities gives results that are highly line-specific.

A model was developed to quantify the impact of maintenance and repair on the frequency and size distributions of existing defects. This model accounts for the limitations of inspection tools including the possibility of missing some defects and the error associated with defect size estimates. Based on user-defined excavation and repair criteria, the model identifies defect sizes that are likely to be excavated and repaired and uses this information to provide final probabilistic characterizations of the depth and length of remaining defects. These estimates are used in the failure probability estimation model to calculate revised failure probabilities, thus providing a method to quantify the benefits associated maintenance.

The failure probabilities associated with the different maintenance options under consideration are used as input to the consequence assessment influence diagram to carry out the optimization analysis necessary to identify the best maintenance strategy. The corrosion analysis also provides estimates of the number of expected corrosion excavations and repairs, which are used in defining the total maintenance cost. The optimization is carried out on an annual basis by amortizing the maintenance cost over the expected time to next inspection. Special optimization output formats have been developed to account for the fact that some of the choices considered derive from continuous parameters (*e.g.*, inspection interval and repair criteria).

1.0 INTRODUCTION

1.1 Background

This document constitutes one of the deliverables associated with C-FER's joint industry program on risk-based optimization of pipeline integrity maintenance activities. The goal of this program is to develop models and software tools that can assist pipeline operators in making optimal decisions regarding integrity maintenance activities for a pipeline or pipeline segment. The software resulting from this joint industry program is called PIRAMID (Pipeline Risk Analysis for Maintenance and Inspection Decisions). This document is part of the technical reference manual for the program.

Implementation of the risk-based approach developed in this program requires quantitative estimates of both the frequency of line failure and the adverse consequences associated with failure should it occur. There is considerable uncertainty associated with the assessment of both the frequency and consequences of line failure. To find the optimal set of integrity maintenance actions in the presence of this uncertainty, a probabilistic optimization methodology based on decision influence diagrams has been adopted. A description of this approach and the reasons for its selection are given in PIRAMID Technical Reference Manual No. 1.2 (Stephens *et al.* 1995).

PIRAMID is developed as a series of individual modules. The first module developed was a consequence assessment module that estimates the impact of an (onshore) pipeline failure on cost, public safety, and the environment (see PIRAMID Technical Reference Manual No. 3.2 by Stephens *et al.* 1996). The consequence assessment module can be used to carry out a risk assessment or a decision analysis of different maintenance options, provided that the user inputs the probability of failure of the pipeline, both in its original state and after implementation of each of the candidate integrity maintenance actions.

The probability analysis modules of PIRAMID are developed individually for each failure cause. This is consistent with the fact that most integrity maintenance methods address individual failure causes (*e.g.*, magnetic flux leakage in-line inspection for metal loss corrosion, or right of way patrols for mechanical damage). The major exception to this, is hydro testing, which mitigates against in-service failures caused by any type of defect, and should therefore be assessed with respect to its cumulative benefits for different failure causes (*i.e.*, metal loss corrosion, cracks, or dents). It is recognized that other minor exceptions exist for which a given inspection method can detect more than one failure cause (for example, high resolution magnetic flux leakage tools detect girth weld cracks in addition to metal loss corrosion), but these secondary benefits are assumed not to play a major role in integrity maintenance planning.

When the PIRAMID probability module for a given failure cause is integrated with the consequence module, a decision analysis can be carried out for integrity maintenance choices aimed at reducing the chance of failures due to that cause. In this case PIRAMID would compute

the probabilities of failure from more basic pipeline attributes. For the metal loss corrosion case for example, the failure probability is computed from defect frequency, geometry and growth rates.

1.2 Objective and Scope

This document describes the PIRAMID model and influence diagram that have been developed to estimate the probability distribution of pipe performance (*i.e.*, the probabilities of safe performance, small leaks, large leaks and ruptures) with respect to metal loss corrosion, and to quantify the effect of corrosion maintenance activities on that probability. It also describes the approach developed to combine this performance analysis influence diagram with the consequence analysis influence diagram described in PIRAMID Technical Reference Manual No. 3.2 (Stephens *et al.* 1996), in an overall model that identifies the optimal corrosion inspection and repair strategies. The choices addressed in this analysis include whether or not to inspect, the inspection tool to use, the optimal interval between inspections, and the optimal defect repair threshold. The inspection methods considered include high and low resolution in-line inspection tools as well as coating damage surveys.

2.0 THE DECISION ANALYSIS INFLUENCE DIAGRAM

2.1 Review of Diagram Representation and Terminology

A decision influence diagram is a graphical representation of a decision problem that shows the interdependence between the uncertain quantities that influence the decision(s) considered. A diagram consists of a network of *chance nodes* (circles) that represent uncertain parameters and *decision nodes* (squares) that represent choices to be made. A decision influence diagram will also contain a *value node* (rounded square) that represents the objective or value function that is to be maximized to determine the optimal set of choice(s) associated with the required decision(s).

All of these nodes are interconnected by directed arcs or arrows that represent dependence relationships between node parameters. Chance nodes that receive solid line arrows are *conditional nodes* meaning that the node parameter is conditionally dependent upon the values of the nodes from which the arrows emanate (*i.e.*, direct predecessor nodes). Chance nodes that receive dashed line arrows are *functional nodes* meaning that the node parameter is defined as a deterministic function of the values of its direct predecessor nodes. The difference between these two types is that conditional node parameters must be defined explicitly for all possible combinations of the values associated with their direct conditional predecessor nodes, whereas functional node parameters are calculated directly from the values of preceding nodes. The symbolic notation adopted in drawing the influence diagrams presented in this report, and a summary of diagram terminology are given in Figure 2.1.

A detailed discussion of the steps involved in defining and solving decision influence diagrams, and a more thorough and rigorous set of node parameter and dependence relationship definitions is presented in PIRAMID Technical Reference Manual No. 2.1 (Nessim and Hong 1995). Subsequent discussions assume that the reader is familiar with the concepts described in that document.

2.2 Structure of the Influence Diagram Solution

2.2.1 Overview

An optimization analysis of corrosion-related maintenance activities involves a failure probability analysis that estimates the expected pipeline performance for different maintenance options, and a consequence analysis that defines the expected outcomes in the event of failure. The consequence analysis part of the solution was developed as a stand alone module as part of a previous PIRAMID Project (Stephens *et al.* 1996). The approach adopted in developing a complete influence diagram solution for corrosion maintenance optimization was to develop a

separate influence diagram to calculate the probability of failure for different maintenance options, and link it to the already existing consequence analysis influence diagram. The purpose of Sections 2.2.2 to 2.2.4 is to give an overview of the corrosion influence diagram and describe how it is integrated with the consequence analysis influence diagram. Details of the relationships between different diagram nodes are explained in more detail in the remainder of this report.

2.2.2 The Corrosion Analysis Influence Diagram

The corrosion analysis influence diagram is shown in Figure 2.2. This diagram includes decision nodes that describe the specific choices associated with corrosion maintenance and chance nodes that link those choices to pipe performance with respect to corrosion. The diagram shows that the performance is calculated from a series of nodes describing the dimensions of corrosion defects and their growth rates, and the pipe mechanical properties (yield strength). The diagram also shows that the impact of inspection and maintenance is taken into account by updating the corrosion defect dimensions based on the expected repairs.

The influence diagram in Figure 2.2 has four end nodes, namely, Defect Depth Before Next Inspection (node 13.8), Defect Length Before Next Inspection (node 13.9), Performance at Defect (node 3.1), and Repair Action (node 13.5). The end nodes representing Defect Depth and Length Before Next Inspection (nodes 13.8 and 13.9) are not required for the overall diagram solution. They are included only to provide defect size forecasts that can be used in planning future maintenance events.

Nodes 3.1 (Performance at Defect) and 13.5 (Repair Action) on the other hand, are the main end nodes containing the information necessary to link the corrosion influence diagram to the consequence analysis influence diagram. Performance at Defect (node 3.1) represents the pipe performance at a randomly selected defect within a specific pipeline section. This node has four possible states: safe, small leak, large leak or rupture. The Repair Action node (node 13.5), represents the action taken to investigate and/or repair a randomly selected defect. The parameter of this node has three possible states: no action, excavation and coating repair (no pipe repair), and excavation with pipe and coating repairs. The purpose of the influence diagram in Figure 2.2 is to calculate the probability distributions associated with Performance at Defect and Repair Action for any combination of choices. The linkage between these nodes and the consequence analysis influence diagram is discussed in Section 2.2.3.

2.2.3 Connections Between the Corrosion and Consequence Influence Diagrams

Once the probability distributions of the Performance at Defect and Repair Action are calculated from the influence diagram in Figure 2.2, they can be used as input to the consequence analysis influence diagram shown in Figure 2.3, which is derived by introducing minor modifications to the original consequence analysis influence diagram described in PIRAMID Technical Reference Manual 3.2 (Stephens *et al.* 1996) and shown in Figure 2.4. By solving the consequence analysis

diagram in Figure 2.3 using the inputs provided by the solution to the corrosion influence diagram in Figure 2.2, the solution to the complete corrosion maintenance decision analysis problem is reached.

Connections between the two influence diagrams occur through the nodes highlighted in Figures 2.2 and 2.3, where the nodes highlighted in Figure 2.2 provide input to the nodes highlighted in Figure 2.3. The relationships between the two diagrams are as follows:

- *Choices.* The Choices node (node 1) in the consequences influence diagram consists of all possible combinations of the choices given in each of the three choice nodes in the corrosion analysis influence diagram (nodes 1.1, 1.2 and 1.3).

- *Segment Performance.* The probability distribution of the Segment Performance node (node 3.2) in the consequence analysis influence diagram is calculated from the probability distribution of the Performance at Defect node (node 3.1) in the corrosion analysis influence diagram. This calculation involves converting the probability of failure at a single defect (node 3.1) to the probability of failure for the whole pipeline segment, using the average number of defects per unit length along the line from node 12.1 (see Section 7.3 for details). As such, calculation of Segment Performance (node 3.2) requires information from nodes 3.1 and 12.1, which belong to the corrosion analysis influence diagram.

- *Maintenance Cost.* The Maintenance Cost node (node 8.1 in the consequence analysis influence diagram) uses as input the probability distribution of repair action from node 13.5 and the number of corrosion defects from node 12.1 of the corrosion analysis influence diagram. This calculation involves adding up the defect excavation and repair costs along the line segment and including them as part of the total maintenance cost (see Section 9.0 for details). It is noted that defect repair is a separate cost from failure repair, which is included separately in node 8.2.

2.2.4 Modifications to the Consequence Analysis Influence Diagram

A number of modifications were introduced to the consequence analysis influence in Figure 2.3 in order to link it to the newly introduced corrosion analysis diagram. For comparison, Figure 2.4 gives the original influence diagram as defined in PIRAMID Technical Reference Manual No. 3.2. The modifications are as follows:

- *Pipe Performance* node (node 3) in the original diagram was renamed to Segment Performance and renumbered to node 3.2 in order to distinguish it from the Performance at Defect node (node 3.1). The probability distribution associated with the parameter of this node is no longer defined directly by the user, but is calculated by the program as described in Section 7.3.

- A conditional arrow was added from Segment Performance (node 3.2) to *Failure Section* (node 2.6). This arrow indicates that the probability distribution of the Failure Section is conditional on the parameter of the Segment Performance node (*i.e.*, the probability that a certain failure will occur on a given Section depends on the failure mode). This dependence can be understood by considering the probabilities of different failure modes for specific sections of the pipeline. Because corrosion-related attributes are allowed to vary freely from

one section to another, the relative probabilities of different failure modes (*i.e.*, small leaks, large leaks, or ruptures) can also vary between sections. It therefore follows that if a failure occurs, the probability of it being on a given section depends on the failure mode. This means that the probability distribution of Failure Section is conditional on the parameter of the Pipe Performance node. In addition to the new arrow, the node calculation for the Failure Section node (node 2.6) was also modified as discussed in Section 8.0.

- A conditional arrow was added from the Choice node to the Failure Section node (see Figure 2.3). This arrow accounts for the fact that a given choice may affect the relative failure frequencies for different pipeline sections.

- The probability distribution of the *Maintenance Cost* node (node 8.1), which was defined by direct user input in the original consequence analysis influence diagram, is now calculated using the inspection cost, the unit excavation and repair costs and the probability of excavation and/or repair obtained from the Repair Action node (node 13.5).

- The *Value* node was modified to provide additional outputs relating to the specific choices being considered in the corrosion analysis. These modifications are described in Section 10.0.

2.3 Application to Maintenance Planning

2.3.1 Sequential Decision-Making

The choices involved in defining a corrosion maintenance plan for a given pipeline segment include:

1. inspection method;

2. criteria for excavation and repair of defects identified by the inspection; and

3. times at which maintenance events (including inspection and repairs) are to be executed.

The above three choices are interrelated, because an inspection provides information that could influence repair criteria and inspection intervals. If, for example, the results of a low resolution inspection indicate that the line is in poorer condition than originally thought, a shorter interval to the following inspection would be appropriate and the inspection method may be upgraded to a high resolution tool. On the other hand, if the low resolution inspection shows that the line is in better condition than expected, a longer interval to the next inspection would be appropriate.

The decision sequence adopted to deal with the inter-relationships between individual aspects of the maintenance plan is shown in Figure 2.5, in which each square represents a separate decision. Assuming that the pipeline under consideration has not been inspected before, and that only three inspection methods are considered as listed in the figure, the decision-making sequence will be as follows:

The Decision Analysis Influence Diagram

1. *Initial inspection action.* This is represented by choice A in Figure 2.5. At this point a decision is being made regarding whether to inspect the pipeline immediately, and if so which inspection method should be used. Since the pipeline is assumed not to have been inspected in the past, initial corrosion defect characteristics used in making this choice will be defined on the basis of information from similar pipelines, possibly supplemented by subjective judgment. If the optimal choice at this point is to wait, the waiting period (or time to next decision) must be defined. Choice A would then be re-analyzed at the end of the waiting period to determine the optimal inspection choice that should be implemented after the waiting period.

2. *Action after the first inspection.* This choice corresponds to decisions B, C and D in Figure 2.5. It assumes that an analysis of choice A resulted in identifying an optimal inspection method and that the inspection has been carried out, producing information on the actual degree of corrosion damage. This new information must now be used to decide on the next step in the maintenance process. The possible choices at this stage are either to repair the line on the basis of the available inspection results, or to carry out further inspections. In general, the "repair & wait" option is expected to be optimal if the degree of damage found by the inspection is similar to that initially assumed in selecting the method for the previous inspection. This amounts to a confirmation of the assumed degree of damage and the appropriateness of the initial inspection method selected on the basis of that information. In this case a repair criterion (*e.g.*, the calculated pressure resistance at which defects must be repaired) and the time to next maintenance event must be selected.

   If the inspection data indicate more severe corrosion than originally assumed, it may be cost-effective to carry out a second inspection to obtain better information before repair decisions are made. A second inspection would only be effective if it used a more accurate method than that used in the initial inspection, and this is reflected in the choices available for decisions B, C and D in Figure 2.5. If an additional inspection is required, the analysis would be repeated using the newly acquired inspection results. As indicated in the figure, this process is repeated until the "repair & wait" option is selected over additional inspection, or until the most accurate inspection method is used. At that point the analysis would provide the optimal repair criterion and waiting period to next maintenance decision.

3. *Subsequent maintenance decisions.* The first maintenance event involves inspection and repair of critical defects as discussed in 1) and 2) above. It also produces the optimal waiting period until next maintenance event. After the waiting period, the decision cycle in 1) and 2) above can be repeated to determine the optimal inspection method, repair criterion and waiting period until subsequent maintenance events. In this case, the initial damage extent can be based on the outputs of nodes 13.8 and 13.9, which define the defect depth and length before the next inspection based on the remaining defects after the last maintenance event and the estimated defect growth rate.

It is possible to develop the maintenance plan as a series of conditional choices that depend on the different possible inspection outcomes. For example, the plan may specify the optimal choice as a three-year waiting period, followed by a low resolution inspection, and a series of subsequent optimal choices conditional on the inspection results (*e.g.*, if the inspection results show limited corrosion then wait ten years and use the same inspection method; but if the corrosion is severe, then repair defects above a specified size, wait five years and inspect again using a high resolution tool). The difficulty with this approach is that the definition of possible inspection results such as "limited" or "severe" is somewhat restrictive. In reality, corrosion

damage is characterized by the number and size distribution of defects that are detected, leading to an infinite number of possible outcomes. It is of course possible to discretize the outcomes into specific categories, but even if this approach is adopted, there will be a potentially large number of possible outcomes. Each of these outcomes would have to be analyzed to determine subsequent optimal actions. This requires a large computational effort to analyze all possibilities, especially as the number of branches multiplies near the end of the tree. In addition, it can be argued that making choices that are conditional on events that will take place several years in the future is not very useful because of the potential for significant changes in the state of related knowledge and technology. For example, new data or inspection technologies may become available that would render the basis for the initial decision sequence obsolete.

To provide an efficient and realistic solution to the optimization problem, a step-wise approach has been adopted. In this approach each decision box in Figure 2.5 is solved individually in a separate run of the program. This means that for a pipeline that has not been inspected before, the program will be initially run to determine the optimal inspection method or the waiting period until inspection is necessary (decision box A in Figure 2.5). Assuming that inspection with a low resolution tool is selected, then the user will carry out the inspection. After the results are obtained, another run of the program would be required to determine whether further inspection is necessary or whether repair should be implemented (decision box B in Figure 2.5). Assuming that the repair and wait option is optimal, the repair criterion and waiting period would be provided by the program. The user would then carry out the repair and then re-analyze the segment after the waiting period has elapsed to determine the next course of action. This approach has been adopted because of its efficiency with respect to computer time as mentioned earlier. It also allows incorporation of new information (*e.g.*, new inspection data or advances in inspection technology) that may become available between maintenance events.

2.3.2 Modes of Influence Diagram Operation

Based on the discussion in Section 2.3.1, there are two distinct modes of operation for the corrosion analysis influence diagram. These are:

- *Pre-inspection mode (mode I)* This arises at decision boxes marked with the letter A in Figure 2.5, where the objective of the user is to determine the optimal initial inspection method for the current maintenance event. It is noted that the term pre-inspection refers only to inspections within the current maintenance event. In other words, inspections carried out as part of previous maintenance events are not considered in determining whether a certain run is characterized as a pre-inspection run. In this mode, the program expects a user-defined characterization of corrosion defect frequency and dimensions.

- *Post-inspection mode (mode II).* This condition arises if the program is run subsequent to an inspection to determine the need for further inspection and, if no further inspection is required, calculate the optimal repair criterion and waiting period to next inspection. In this mode, the program expects the corrosion feature frequency and dimensions obtained from the inspection data as input.

This distinction has some implications with respect to the calculations needed to quantify different influence diagram nodes. These differences will be discussed in the context of individual node descriptions.

2.4 Compact Influence Diagram and Organization of This Manual

As previously discussed in the consequence analysis influence diagram (Technical Reference Manual No. 3.2), each node in the influence diagrams in Figures 2.2 and 2.3 represents a single parameter that influences the decision problem being analyzed. This manual describes the methods used to define each node parameter for later use in solving the diagram and identifying the optimal choices.

To facilitate understanding of the influence diagrams in Figures 2.2 and 2.3, nodes have been collected into logical groupings, resulting in the compound node influence diagram shown in Figure 2.6. Nodes 1 through 11 in the compound influence diagram existed in the consequence analysis compound influence diagram. Nodes 12, 13 and 14 have been added to accommodate the basic nodes in the new corrosion analysis influence diagram (Figure 2.2). Figure 2.6 highlights compound nodes that were added for corrosion analysis, as well as compound nodes that existed in the original consequence analysis influence diagram but involved some modifications to establish the connection between the corrosion and consequence analysis influence diagrams (see Section 2.2.3).

This manual describes node calculations for the new corrosion analysis influence diagram, and the modifications made to the original consequence analysis influence diagram. The new models or modification associated with each compound node are described in a separate section in the following order:

Section	Node group
3.0	Choices (node group 1)
4.0	Initial Damage (node group 12)
5.0	Remaining Damage (node group 13)
6.0	Mechanical Properties (node group 14)
7.0	Performance (node group 3)
8.0	Conditions at Failure (node group 2)
9.0	Repair and Interruption Costs (node group 8)
10.0	Value (node group 11)

Figures

Node Notation

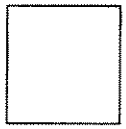

Decision node: Indicates a choice to be made

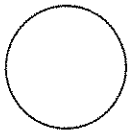

Chance node: Indicates uncertain parameter or event (discrete or continuous)

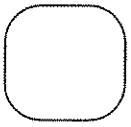

Value node: Indicates the criterion used to evaluate consequences

Arrow Notation

Solid Line Arrow: Indicates probabilistic dependence

Dashed Line Arrow: Indicates functional dependence

Other Terminology

Predecessor to node A :	Node from which a path leading to A begins
Successor to node A:	Node to which a path leading to A begins
Functional predecessor:	Predecessor node from which a functional arrow emanates
Conditional predecessor:	Predecessor node from which a conditional arrow emanates
Direct predecessor to A:	Predecessor node that immediately precedes A (i.e. the path from it to A does not contain any other nodes)
Direct successor to A:	Successor node that immediately succeeds A (i.e. the path from A to it does not contain any other nodes)
Direct conditional predecessor to A: (A must be a functional node)	A predecessor node from which the path to node A contains only one conditional arrow (may contain functional arrows)
Functional node:	A chance node that receives only functional arrows
Conditional node:	A chance node that receives only conditional arrows
Orphan node:	A node that does not have any predecessors

Figure 2.1 Influence diagram notation and terminology

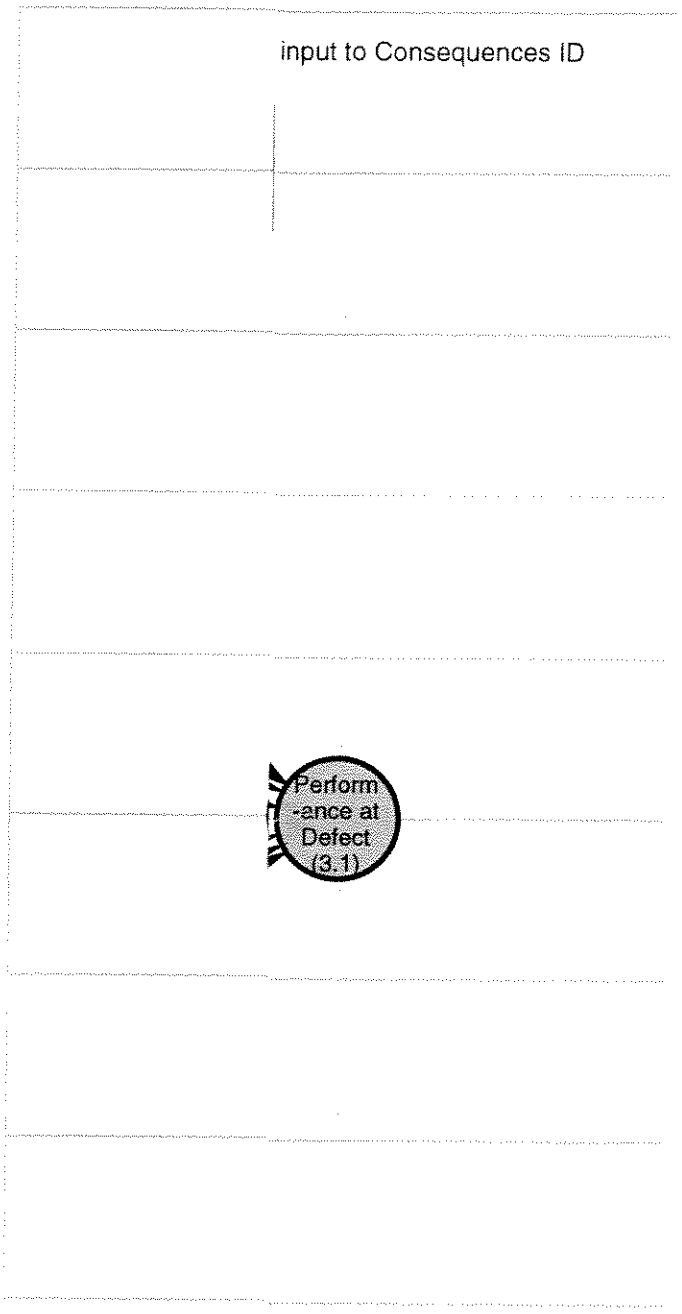
input to Consequences ID
Perform
-ance at
Defect
(3.1)

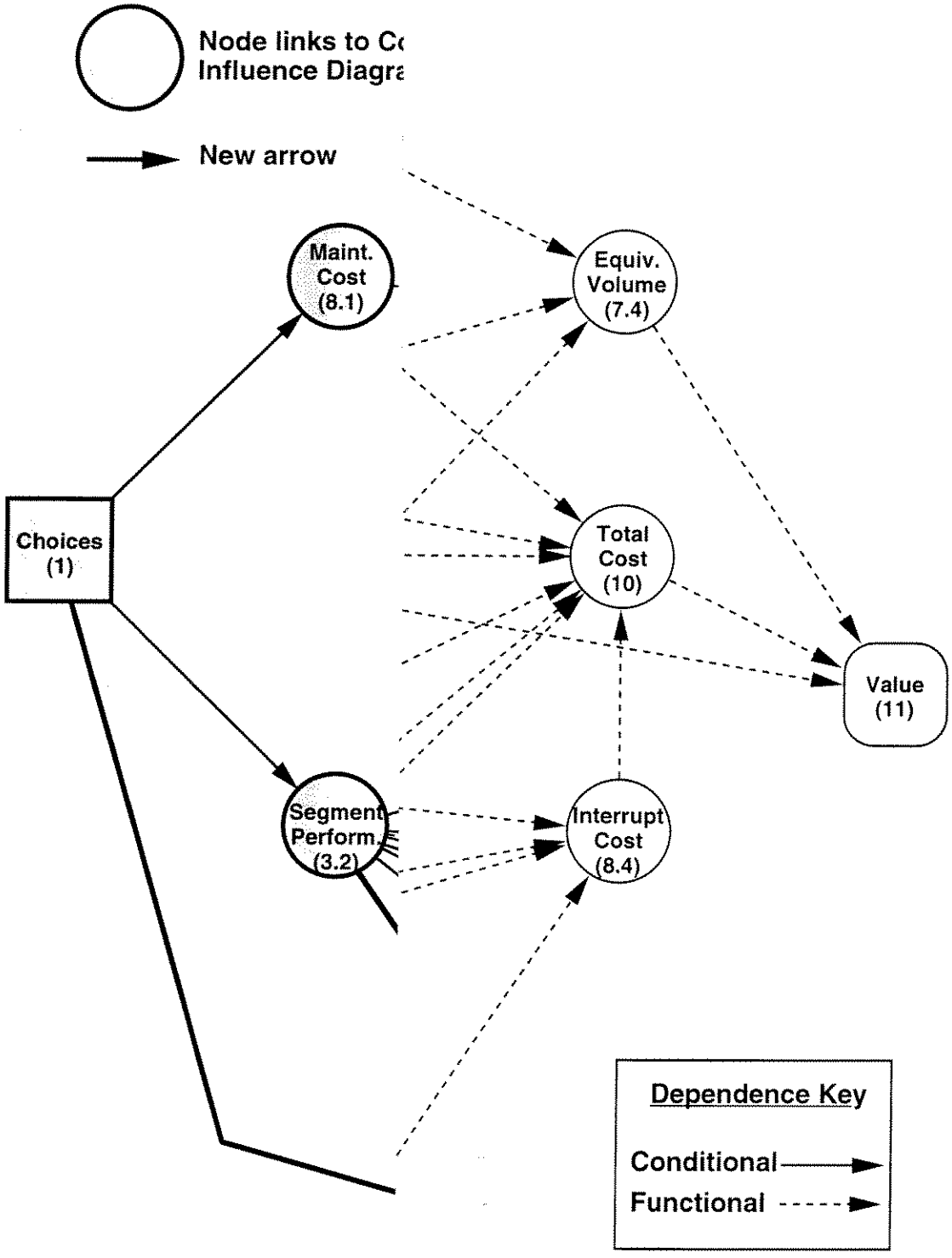
Node links to C
Influence Diagra
New arrow
Maint.
Cost
(8.1)
Equiv.
Volume
(7.4)
Choices
(1)
Total
Cost
(10)
Value
(11)
Segment
Perform.
(3.2)
Interrupt
Cost
(8.4)
Dependence Key
Conditional
Functional

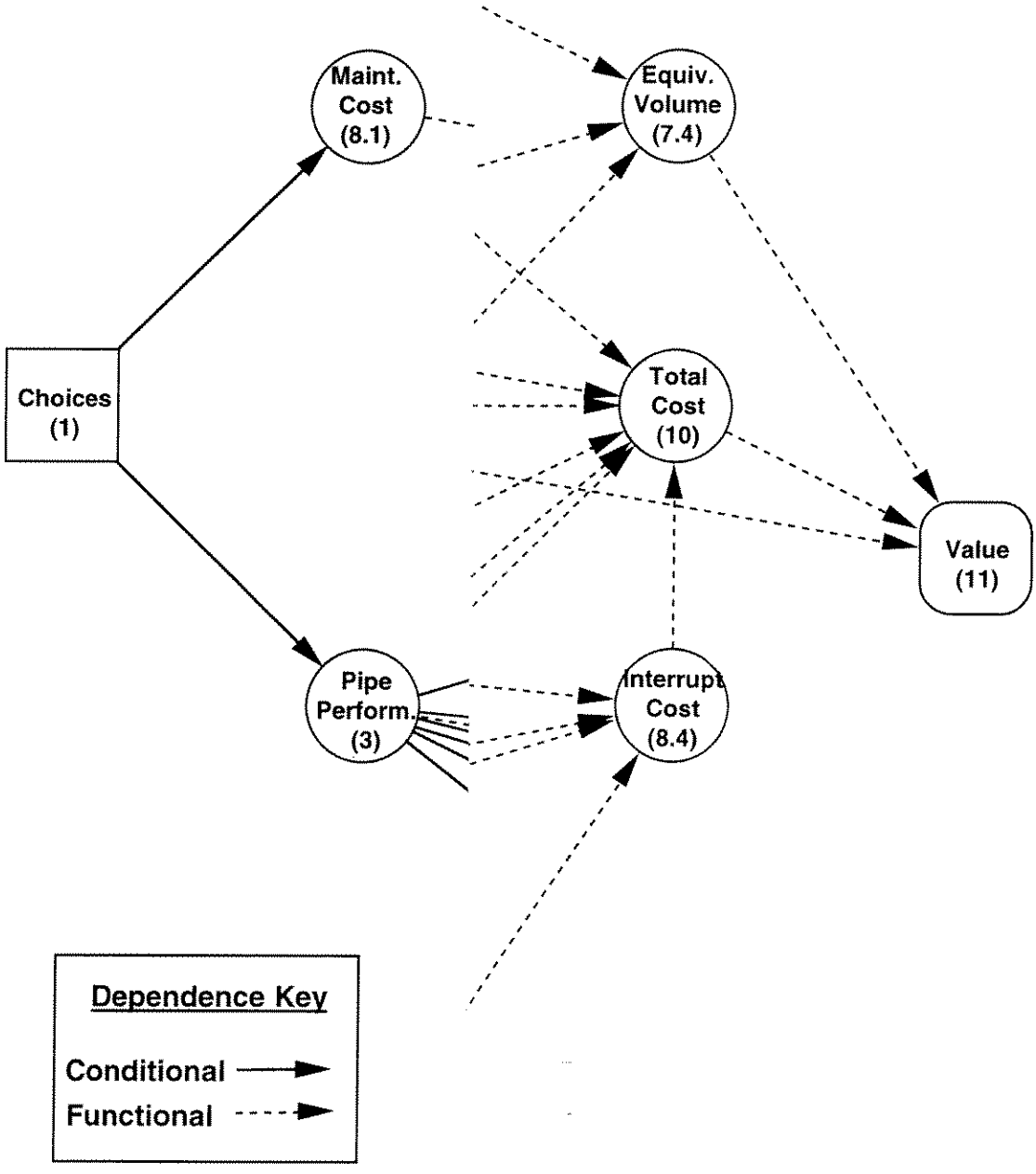
Maint.
Cost
(8.1)
Equiv.
Volume
(7.4)
Choices
(1)
Total
Cost
(10)
Value
(11)
Pipe
Perform.
(3)
Interrupt
Cost
(8.4)
Dependence Key
Conditional
Functional

et al. 1996)

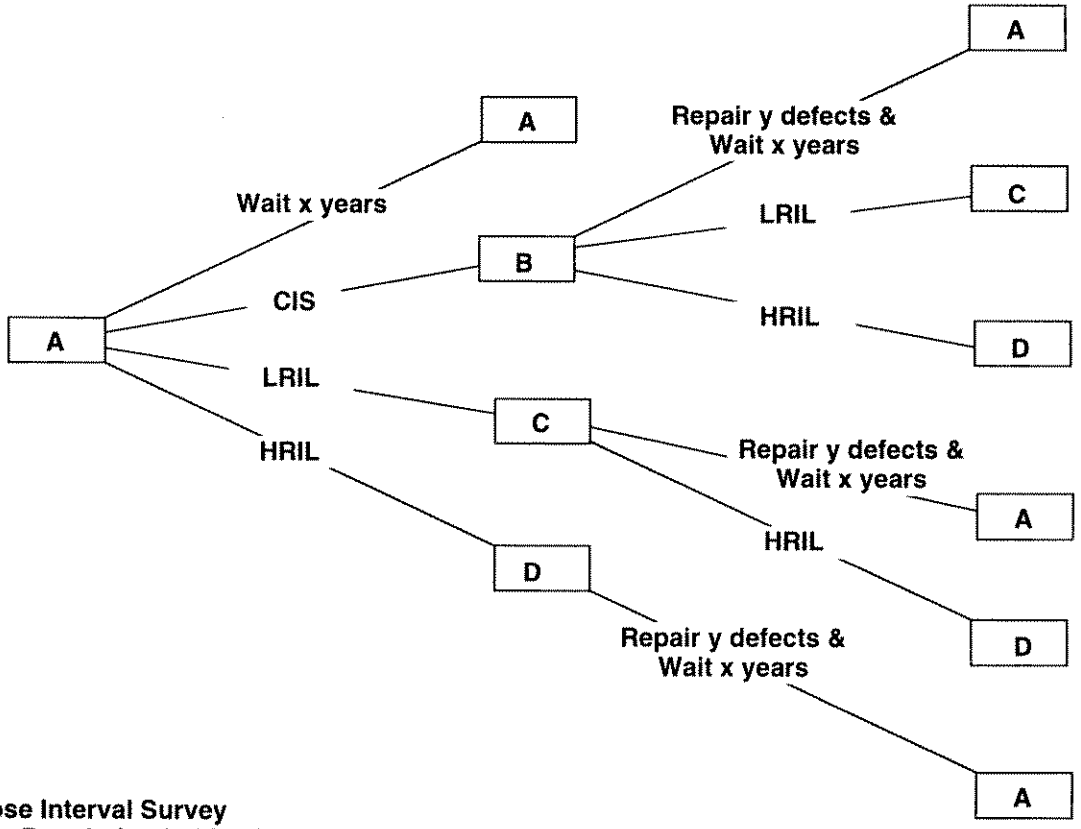

Figure 2.5 Decision-making sequence for corrosion inspection and repair

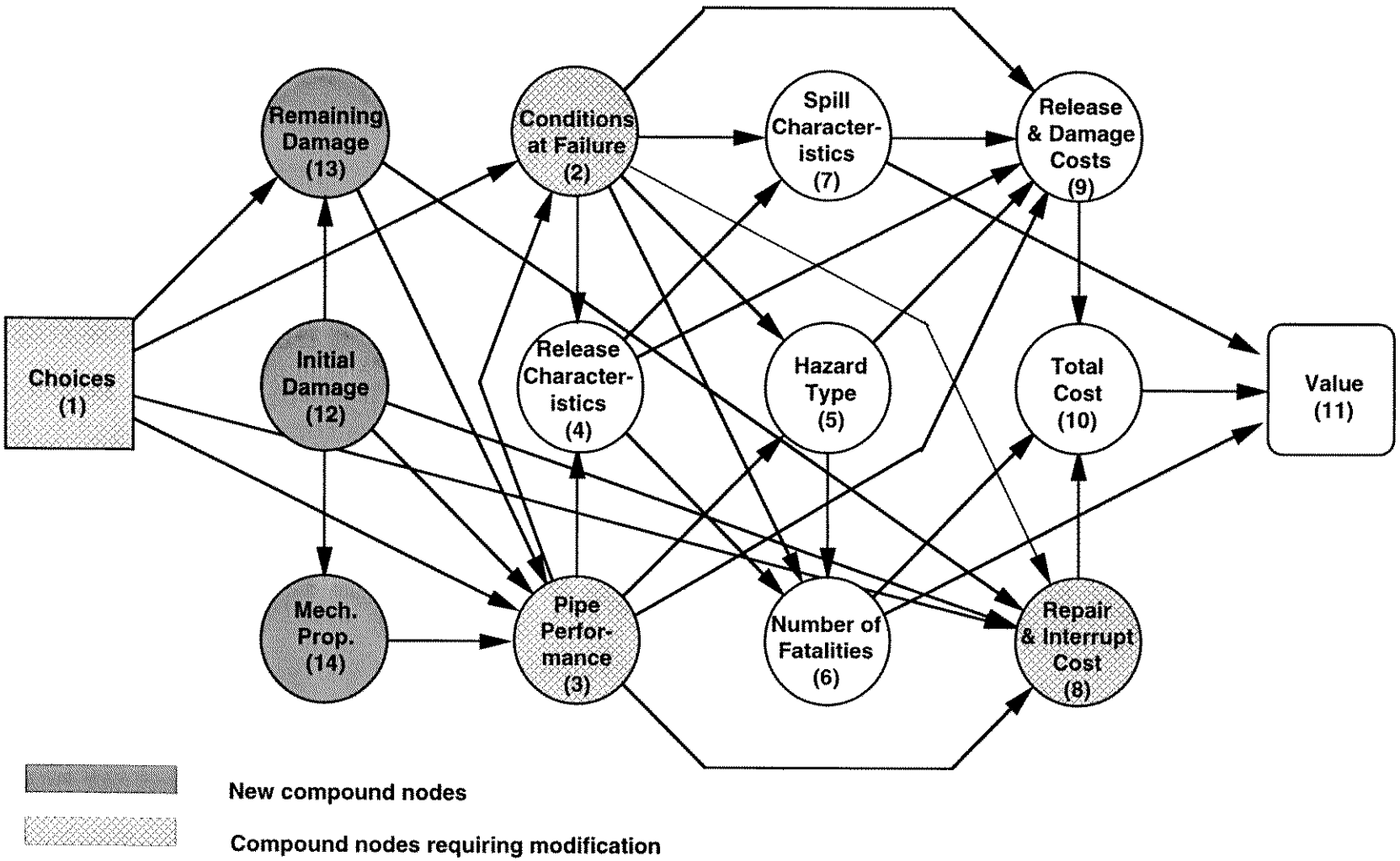

Figure 2.6 Compact influence diagram for corrosion maintenance optimization

3.0 CHOICES

3.1 Overview

The Choices node group (group 1) is highlighted in the version of the compound influence diagram shown in Figure 3.1. This node group includes basic nodes that represent the corrosion maintenance decisions considered by PIRAMID. These include the inspection method (or tool), the defect excavation and repair criteria, and the time interval between maintenance events. The basic nodes representing the individual choices associated with corrosion maintenance are highlighted in the version of the basic node corrosion influence diagram shown in Figure 3.2. These basic nodes are discussed in the following sections.

3.2 Inspection Method

3.2.1 Node Parameter

The Inspection Method node (node 1.1) is highlighted in the version of the basic node corrosion influence diagram shown in Figure 3.2. The specific decision parameter of this node is the inspection method/tool used to determine the degree of corrosion damage in the line. Options are classified into three major categories, namely coating surveys, in-line inspection using a low resolution tool, and in-line inspection using a high resolution tool.

3.2.2 List of Possible Choices

As mentioned in Section 3.2.1, three categories of inspection methods are considered, namely coating damage surveys, low resolution in-line inspection and high resolution in-line inspection. Several tools within each category may be considered in any given run, with each tool defined by a specific label.

The inspection tool options defined by the user are used by the program to develop a list of possible choices. For a pre-inspection run (program operation mode I as defined in Section 2.3.2), it is assumed that the user is making a decision regarding whether an immediate inspection is needed and if so, what inspection tool is optimal. The list of options in this case consists of the following:

1. no inspection;
2. in-line inspection using tool 1;
3. in-line inspection using tool 2; and so on for all inspection tools considered.

Choices

The "no inspection" option is added by default, and the inspection tool options are listed in order of increasing accuracy. For this purpose it is assumed that coating damage surveys are least accurate, followed by low resolution in-line inspections, and that high resolution in-line inspections are most accurate. Within each category it is left up to the user to list the different tools being considered in order of increasing accuracy.

For a post-inspection run (program operation mode II as defined in Section 2.3.2), it is assumed that the user is making a decision on whether to make repairs based on the available inspection results, or carry out another inspection using a more accurate tool. Assuming that the tool just used is tool i on the increasingly accurate list of tools, the decision options will consist of the following:

1. repair;
2. in-line inspection using tool i+1;
3. in-line inspection using tool i+2; and so on for all inspection tools considered.

The "repair" option is included by default in this case and the inspection tools considered are assumed to have greater accuracy than the tool already used to obtain the available inspection results.

3.2.3 Characteristics of Inspection Methods

3.2.3.1 Modelling the Effectiveness of Inspection

In addition to the name of each inspection tool, this node requires the user to define some characteristics related to the type of measurements made, the probability that the method will detect an existing defect, the frequency of false indications, and the accuracy limits associated with the measurement provided. It is also necessary to define the criterion used to excavate portions of the pipeline for further investigation and possible repair based on the inspection data. The general models used to characterize the efficiency and accuracy of different inspection methods are described in this section. Specific implementations of these models for different inspection methods are discussed in Section 3.2.3.2.

1. *Probability of false indication.* This is defined as the probability that an indication of corrosion damage reported by the inspection tool does not correspond to an actual defect.
2. *Probability of detection.* This accounts for the possibility that the inspection method/tool will fail to detect some of the existing defects. The probability of detection is characterized as a function of defect size; the larger the defect the higher the probability that it will be detected. For corrosion defects Rodriguez and Provan (1989) suggested an exponential detection curve of the form

Choices

$$p_{dis} = 1 - e^{-qs} \quad [3.1]$$

where p_{dis} is the probability of detection for a defect of size s, and q is a constant that determines the overall detection power of the tool. According to this relationship the detection probability starts at zero for very small defects and approaches 1 for large defects. In PIRAMID, the constant q is calculated from a single user-defined point on the detection curve. This point is defined by asking the user to enter the probability of detection for a defect with a specified size. Sample detection probability curves, given as a function of defect depth, are shown in Figure 3.4.

3. *Measurement errors* are included to account for tool accuracy limitations with respect to defect sizing. Measurement errors are characterized by the lower and upper bounds of an error band (E_{min} and E_{max}) and the probability (p) that the error will fall within this band. Depth measurement error for example, may be defined as falling between -10% and +10% of the pipe wall thickness, with a probability of 0.90. It is noted that measurement error need not be symmetric around the measured value (*e.g.*, E_{min} = -10% and E_{max} = +15%). The error bounds and associated probability is used to calculate the mean value (μ_E) and standard deviation (σ_E) of the measurement error (E). Assuming that E has a normal distribution (Dally *et al.* 1983), the mean and standard deviation of E can be calculated from the specified error range and corresponding probability using the following equations (see Figure 3.5):

$$\mu_E = (E_{\min} + E_{\max}) / 2 \quad [3.2a]$$

$$\sigma_E = (E_{\max} - \mu_E) / [\Phi^{-1}(\frac{1+p}{2})] \quad [3.2b]$$

where Φ^{-1} is the inverse standard normal distribution function (obtained from normal distribution tables). The mean and standard deviation of E are calculated for use in subsequent nodes as will be demonstrated in the remainder of this report.

4. *Excavation threshold.* Associated with each inspection tool is a threshold defining defects that will be excavated for further investigation and possible repair. For example, the excavation threshold associated with a low resolution in-line inspection tool would be defined in terms of the measured wall thickness loss (*e.g.*, > 50%). It is noted that the excavation threshold is not treated as a decision parameter in the present version of PIRAMID.

3.2.3.2 Characterization of Different Inspection Methods

3.2.3.2.1 Introduction

The inspection accuracy characterization models described in Section 3.2.3.1 take a different form for each inspection method, depending on the corrosion size indications provided by the method. This section describes the specific implementations of the probability of detection, the

measurement error and the excavation threshold for the three inspection methods considered by PIRAMID.

3.2.3.2.2 High Resolution In-line Inspection

A high resolution in-line inspection tool provides information on the number, location and geometry of defects. Defect geometry characterization includes estimates of defect depth, length and width. Since presently available failure pressure estimation models are independent of defect width (see Section 7.2.4), defect size is characterized only by length and depth. Depending on the tool used, defect depth may be characterized by the *maximum* depth, defined as the depth perpendicular to the pipe wall at the deepest point of the defect; or the *average* depth, defined as the mean of depth measurements taken along the deepest route through the defect (see Figure 3.3). Defect length is defined as the maximum length of the defect measured along the pipe axis (see Figure 3.3). The characterization of high resolution tools in PIRAMID is described in the following.

1. The *probability of false indication* for high resolution tools is generally associated with signal distortion due to non-defect features such as misalignment at connections, pipe supports, past repairs or metal objects buried adjacent to the pipe (Shannon 1986). This probability (p_{fi}) can be estimated from verification excavations using:

$$p_{fi} = \frac{n_{fi}}{n_t} \qquad [3.3]$$

   where n_{fi} is the number of false indications and n_t is the total number of excavations. It is likely that inspection vendors can provide this probability from their own data bases on previous performance of the tool.

2. As mentioned in Section 3.2.3.1, the *probability of detection* is generally a function of defect size. Tool specifications provided by vendors will typically give a minimum detectable defect depth, which may be dependent on the areal extent of the defect (*e.g.*, minimum detectable depth is 0.1 wt (wall thickness) if defect diameter is > 3 wt, and 0.2 wt if diameter is between 2 wt and 3 wt, where wt is the wall thickness). There are however exceptions to these specifications. For example, the probability of detection for magnetic flux tools depends on the rate of wall thickness change; a defect with a significant maximum depth could be missed if its length is large and the change in wall thickness is very gradual. Further, the orientation of small defects may affect detection by magnetic flux tools, which tend to detect circumferentially oriented defects much better than axially oriented defects.

   A detection model that accounts for all of these aspects would involve a level of complexity that is not justified in the context of the present project. Instead, the basic assumption of an exponential increase in detection probability with defect size (as explained in Section 2.3.3.1) was considered adequate. Furthermore, the probability of detection was assumed to be a function of the defect depth only (*i.e.*, independent of defect length and width), which is an appropriate assumption for defects with a diameter larger than 2 or 3 wt. Using this assumption for all defects is justified by the fact that longer defects have the most significant

Choices

impact on pipeline reliability because they are the only ones likely to fail by ruptures or large leaks. Based on these assumptions, the information required to characterize the probability of detection relationship in Equation [3.1] for high resolution in-line inspection tools consists of the probability of detection for one specific value of the defect depth (taken as 10% wt in PIRAMID). This probability (p_d) can be estimated from

$$p_d = \frac{n_d}{n_t} \qquad [3.4]$$

where n_d is the number of defects with a depth of 10% wt that were correctly reported by the tool and n_t is the total number of defects with the same depth that were found in the verification excavation. The value of p_d can also be obtained directly from inspection vendors. It is noted that the defect depth of 10% wt is defined for this purpose in terms of average depth or maximum depth depending on the output of the inspection tool (*i.e.*, define the probability of detection for a defect of a maximum depth of 10% if the tool provides a maximum depth estimate, and the probability of detection for a defect with an average depth of 10% if the tool provides an average depth measurement).

3. For high resolution inspection tools, *measurement error* characterizations (according to the model described in Section 3.2.3.1) are required for both depth and length. Consistent with common practice, the defect depth measurement error is defined as a percentage of pipe wall thickness and the defect length measurement error is defined as an absolute value. As in 2) above, the depth measurement error is defined in terms of average or maximum depth values depending on the type of inspection tool. The required information can be obtained from vendor specifications or from verification excavations. If verification data are used, the required parameters can be defined by calculating the error for all available measurements using

$$e_i = m_i - a_i \qquad [3.5]$$

where e is the error, m is the measured value obtained from the inspection tool, a is the actual value obtained from an in situ measurement after excavation, and i is an index indicating that this is to be done for all defects in the verification data base. The mean value of the measurement error is estimated by the average of all e_i values obtained from Equation [3.4]. The next step is to select a reasonable error range (E_{min} to E_{max}). Note that this range must be symmetric around the mean value of the measurement error. The probability of being within the error range (p in Equation [3.2]) can be estimated by the ratio between the number of e_i values falling within the range and the total number of e_i values.

4. The *excavation threshold* for high resolution inspection is defined as a multiple of the repair threshold. Since the repair threshold is defined in terms of a minimum pressure resistance (measured in multiples of MAOP as described in Section 3.3), the excavation threshold also represents a minimum allowable pressure resistance. This is possible in the case of high resolution inspection because the inspection tool provides sufficient information on defect dimensions to calculate the failure pressure before the excavation is carried out. The excavation threshold, t_e, is therefore defined as follows:

$$t_e = r_e / r_r \qquad [3.6]$$

Choices

where r_e is the minimum resistance for excavation and r_r is the minimum resistance for repair (both in multiples of MAOP). It is noted that the resistance calculated from inspection data (and used to make excavation decisions) is affected by measurement uncertainties that do not affect the resistance calculated from in situ measurements after excavation (and used in making repair decisions). Without this additional uncertainty it would be reasonable to use the same values for r_r and r_e (*i.e.*, t_e would be 1.0), which means that since defect dimensions are known with absolute accuracy before excavation, one need only excavate defects that need repair. In reality however measurement errors lead to the possibility of underestimating the size of critical defects. It is therefore prudent to use a more stringent criterion for excavation than for repair in order to ensure that defects that may have been critical for repair but undersized by the tool are ultimately repaired. This implies that the excavation criterion t_e as defined in Equation [3.5] should be greater than 1.0. The actual magnitude of t_e depends on the measurement accuracy of the inspection tool (higher values for less accurate tools).

3.2.3.2.3 Low Resolution In-line Inspection

Low resolution in-line inspection tools are similar to high resolution ones except that they have fewer sensors and are therefore less accurate. Low resolution in-line inspections generally provide the location of metal loss corrosion defects and an indication of the maximum defect depth. The depth is typically defined by a number of coarse categories (*e.g.*, < 30%, 30-50% and >50% wt). The information and procedures required to characterize the probability of false indication, the probability of detection and defect depth measurement error is identical to that for high resolution in-line inspection tools (see Section 3.2.3.2.2). The excavation threshold cannot be defined in terms of pressure resistance as low resolution inspection tools do not normally provide an estimate of defect length. The excavation threshold is therefore defined as a maximum allowable defect depth.

Some inspection vendors offer the option of carrying out more analyses to provide an information upgrade that includes length estimates and more accurate depth values for selected defects. In such cases, the information upgrade can be treated as a high resolution inspection option.

3.2.3.2.4 Coating Damage Surveys

Existing coating damage survey methods include Pearson surveys, current attenuation surveys, Close Interval Potential Surveys (CIPS) and the D.C. Voltage Gradient surveys (DCVG) technique. All of these methods detect coating damage and provide an indication of the severity (or size) of damage. On the other hand, there are significant differences between these methods with respect to the physical principles used, and the type of information and interpretation required. In addition, some of these methods produce additional information (beyond coating damage indications) that is relevant to corrosion. CIPS for example, determines the effectiveness of cathodic protection, whereas DCVG surveys provide an indication of whether or not corrosion is active at a given location. Table 3.1 (from Harvey 1994) gives a summary of the capabilities and limitations of different coating damage survey methods.

Choices

The intent of this project was to develop a single model to quantify the impact of different coating damage survey methods on pipeline reliability. The approach adopted was to model aspects that are common to all survey methods, while allowing for differences between the methods to be addressed by varying model input parameters. The assumptions made in developing the model are as follows:

1. All survey methods are capable of detecting and locating coating damage.

2. Coating damage has a general association with external corrosion; however, it is neither a necessary nor sufficient condition for corrosion to occur. For example, coating damage will not lead to corrosion if cathodic protection is adequate. On the other hand, corrosion may occur due to disbonded coating without significant detectable coating damage.

3. All survey methods provide an indication of the size of coating damage based on the intensity of a measurable signal.

Based on these assumptions, the parameters characterizing coating survey methods are defined as follows:

1. The *probability of false indication* in this case refers to the capability of the method and any subsequent analysis to identify actual *corrosion defects* as opposed to just identifying coating damage features. In other words, a correctly detected coating damage feature that does not involve any corrosion should be counted as a false indication for the purpose of corrosion maintenance. In this regard, DCVG surveys may have a lower probability of giving false indications because they also give an indication of whether or not corrosion is active. Similarly, CIPS have an advantage in this regard because they provide an indication of the effectiveness of cathodic protection. Pearson surveys, on the other hand, are likely to have a high probability of false indications because they only provide information on coating defects and are not able to distinguish between coating defects and metal objects near the pipe.

2. The *probability of detection* refers to detection of corrosion defects rather than coating damage features. This means that definition of this parameter must account for corrosion defects that are not associated with detectable coating damage. For example, corrosion associated with disbonded coating is not detectable by most coating survey methods. Therefore, the probability of detection using these methods should be assigned a low value for pipelines that are suspected of having disbonded coating problems. It is noted that the probability of detection is defined by a single value which is assumed to be independent of corrosion defect size. Although the probability of detection is likely to be correlated to coating damage size, it is not necessarily correlated to corrosion defect size since the exposed pipe steel will not necessarily corrode as a single defect.

3. *Measurement error* is not a consideration for coating damage surveys since they do not provide any direct information on corrosion defect sizes. It is recognized that there may be an indirect relationship between the size of coating damage (which can be inferred from the strength of the signal obtained from the survey) and the size of corrosion defect since a large coating holiday creates an opportunity for a large corrosion defect. This relationship however was considered too fuzzy to provide a method for sizing corrosion defects on the basis of coating damage survey results.

Choices

4. The *excavation threshold* for coating damage surveys will be based on an interpretation of the survey results. This interpretation will involve inferences regarding the size of coating damage as indicated by the strength of the signal as well as other factors that depend on the survey method used (*e.g.*, the level of cathodic protection for CIPS or the presence of active corrosion for DCVG). To accommodate the diversity of different methods in this regard, PIRAMID requires direct input of the ratio of defects that are expected to be excavated based on a given survey method.

3.3 Repair Criterion

The Repair Criterion node (node 1.2) is highlighted in the version of the basic node corrosion influence diagram shown in Figure 3.2. The parameter of this node is the *repair criterion* defined as the minimum calculated pressure resistance at a given defect, below which the defect must be repaired. The repair threshold is defined as a multiple of the Maximum Allowable Operating Pressure (MAOP) for the pipeline section containing the defect. For example, a repair criterion of 1.25 MAOP means that any defect leading to a calculated pressure resistance below 125% MAOP must be repaired.

The pressure resistance at a given defect can be calculated as a function of the defect depth, defect length, specified minimum yield strength of the pipe steel, pipe diameter, and pipe wall thickness. This calculation can be based for example, on the ASME-B31G (1991) Standard titled the Remaining Strength of Corroded Pipe. The B31G criterion is based on a fracture mechanics model developed in the early 1970's (Kiefner *et al.* 1973 and Shannon 1974). Since the initial development of this model, different improvements have been made to its accuracy, resulting in several variations on the original model. The specific model used in this work (Brown *et al.* 1995) is described in detail in Section 7.0. It is noted that definition of the repair criterion in terms of the calculated pressure resistance is possible because the defect will first be excavated, allowing accurate measurement of its depth and length before the final repair decision is made.

3.4 Inspection Interval

The Inspection Interval node (node 1.3) is highlighted in the version of the basic node corrosion influence diagram shown in Figure 3.2. The parameter of this node represents the time interval (in years) between the present inspection and the point in time at which another inspection is considered. In the special case where the "no inspection" option is optimal, the inspection interval represents the time between completion of the analysis and time at which another inspection is considered. The inspection interval is input to the program as a number of discrete choices listed in increasing order (*e.g.*, 2, 5, 10, 20 years). it is noted that the inspection intervals considered need not be equally spaced in time.

Figures and Tables

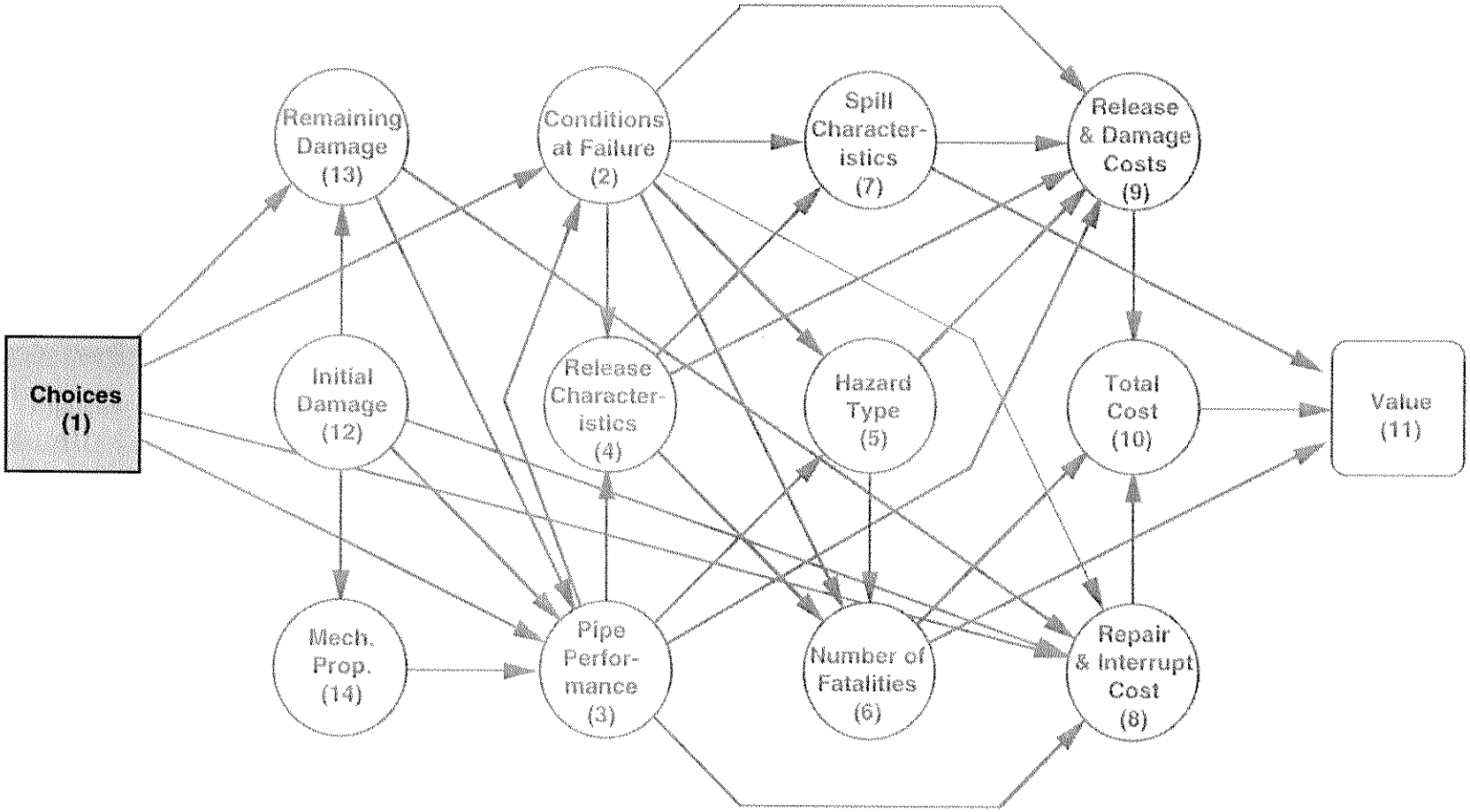

Figure 3.1 Compound node influence diagram highlighting Choices node group

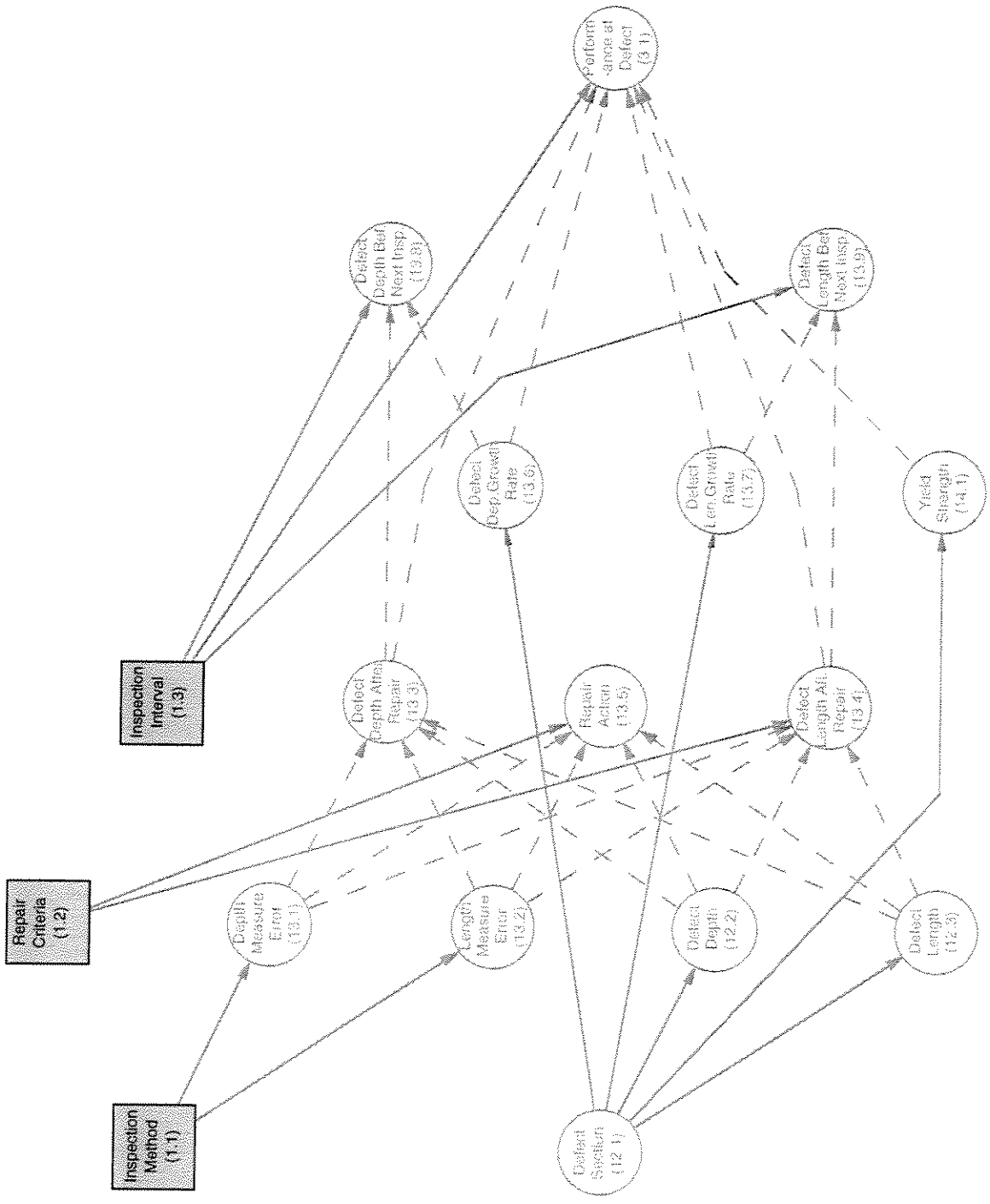

Figure 3.2 Basic node corrosion influence diagram highlighting Choices nodes

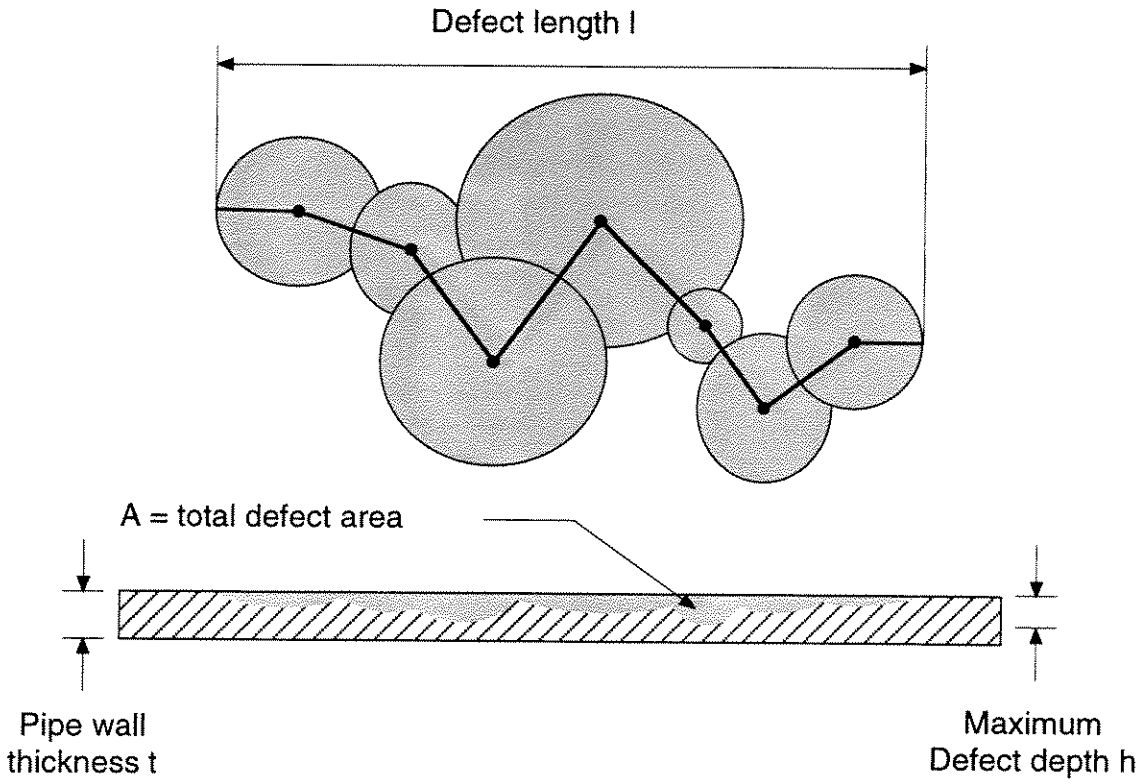

Figure 3.3 Geometry of corrosion defect

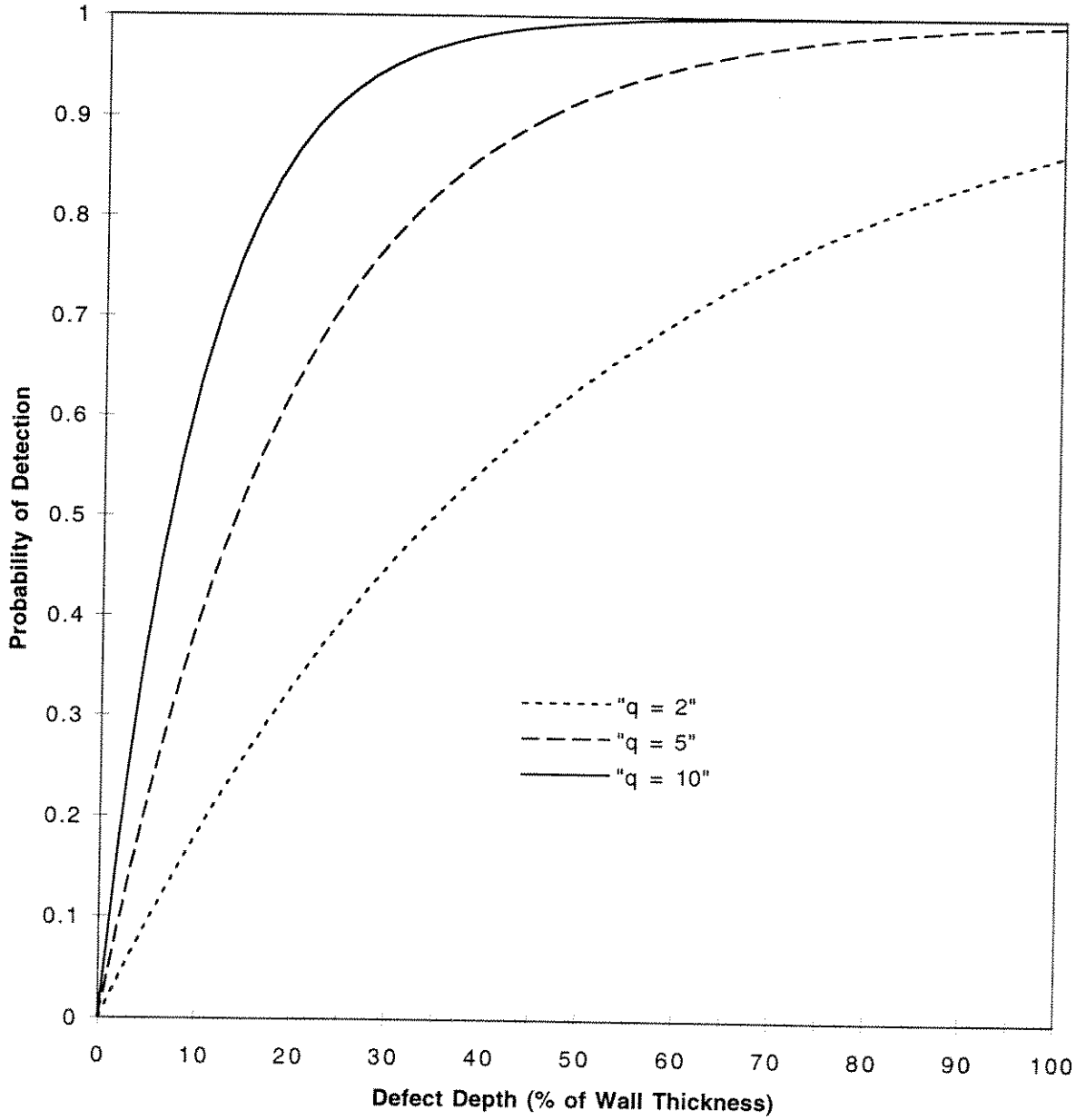

Figure 3.4 Probability of detection as a function of defect depth

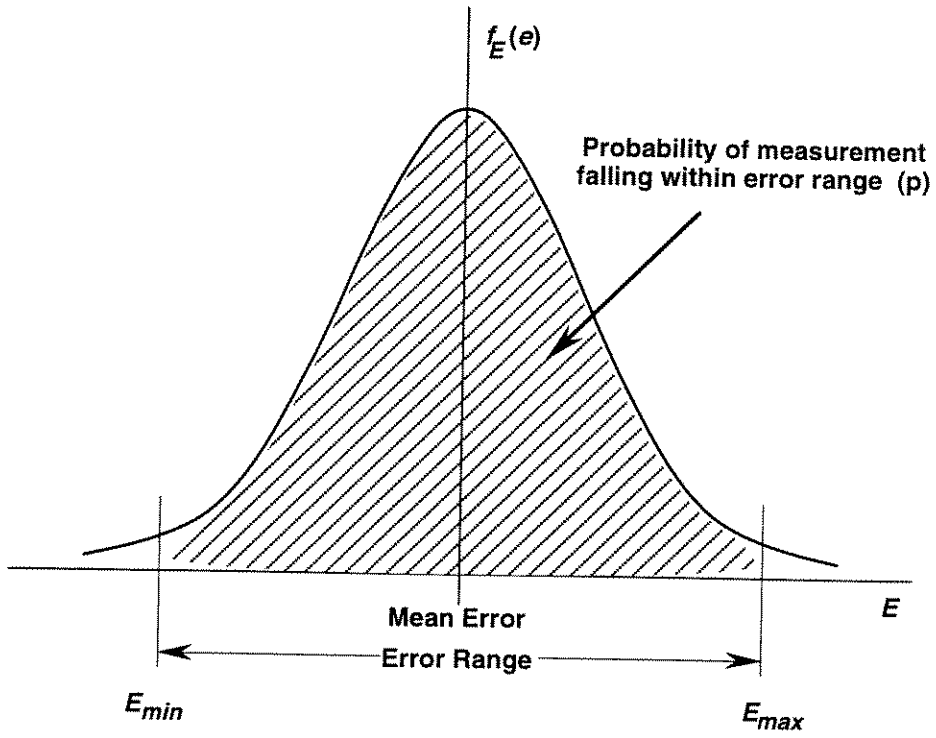

Figure 3.5 Illustration of the probability distribution of actual defect size given the measured size

Survey Techniques	Detection Capability	Advantages	Disadvantages
Pearson survey	Coating defects Extraneous metal	Locates all defects and metal objects Requires full line walk If recorded, provides an indication of fault severity	Requires full line walk Does not distinguish between coating defect and close extraneous metal objects Does not indicate effectiveness of CP Unlikely to indicate disbonded coating Does not indicate extent of corrosion
Current attenuation survey	Coating defects	Does not require full line walk Locates low-resistance faults Can be used in paved areas Indicates severity of fault Repeat survey comparison	Does not locate high-resistance faults Does not locate metal objects Does not indicate effectiveness of CP Unlikely to indicate disbonded coating Does not indicate extent of corrosion
Close-interval polarized potential survey	Coating defects CP effectiveness	Locates unprotected areas Locates coating defects Indicates severity of fault	Requires full line walk May not indicate disbonded coating Does not indicate extent of corrosion
DC voltage gradient survey	Coating defects	Requires full line walk Locates all defects Indicates severity of fault Indicates if corrosion is active Not subject to AC interference	Requires full line walk Does not indicate effectiveness of CP Unlikely to indicate disbonded coating Does not indicate extent of corrosion No permanent record of defect location

Table 3.1 Characteristics of coating damage survey methods

4.0 INITIAL DAMAGE

4.1 Overview

The Initial Damage node group (group 12) is highlighted in the version of the compound influence diagram in Figure 4.1. This node group includes parameters describing the extent of corrosion damage present in the pipeline at the time of inspection. The individual parameters associated with the Initial Damage node group are highlighted in the version of the basic node corrosion influence diagram shown in Figure 4.2. The parameters of these nodes are discussed in the Section 4.2.

The parameters required to define initial damage include the number of corrosion defects per unit length, the defect depth and the defect length. In a post-inspection analysis, these parameters will be available from the inspection results. In a pre-inspection run, they must be defined directly by the user. Since no inspection data are available for the specific line being considered, definition of these parameters must be based on correlation with relevant pipeline attributes, inspection data from similar lines or subjective judgment. An approach has been defined to derive default values of the corrosion frequency and dimensions from such line attributes as age, coating condition and soil corrosivity. This approach is described in Section 4.3.

4.2 Initial Damage Node Paramters

4.2.1 Defect Section

4.2.1.1 Node Parameter

The Defect Section node (basic node 12.2) is highlighted in the version of the basic node corrosion influence diagram in Figure 4.2. This node has no other predecessor nodes and is therefore not dependent on any other parameters or conditions. The Defect Section is represented by a discrete parameter defining the section within the pipeline segment that contains a randomly selected corrosion defect.

4.2.1.2 Division of Pipeline Segment Into Sections

The number of values that may be assumed by the Defect Section node parameter are equal to the number of distinct sections within the pipeline segment being considered. A section is defined as a length of pipeline over which the system attributes relevant to corrosion are constant. Definition of the node parameter therefore requires the specification of all relevant pipeline

system attributes along the entire length of the pipeline segment. From this information the pipeline segment is sub-divided into distinct sections, each section having a common set of attribute values.

4.2.1.3 Defect Density

The program requires that the *defect density*, ρ_i (defined as the number of defects per unit length) be defined for each section. For a pre-inspection run, this value represents the user's best estimate of defect density (default values are provided by the program as described in Section 4.3). For a post inspection run, the program expects the user to input the density of defects detected by the inspection, ρ_d. The estimated actual defect frequency, $\rho_{a\,i}$ and the density of detected defects are related by the following equation:

$$\rho_a = \frac{\rho_d (1 - p_{fi})}{p_d} \qquad [4.1]$$

where p_{fi} is the probability that a given defect indication is false, and p_d is the probability of detecting a randomly selected defect.

4.2.1.4 Coating Damage Density

If the inspection methods considered include coating damage surveys, the program also requires definition of the density of coating damage features (defined a the average number of coating damage feature per unit length). This parameter is included to account for the fact that the density of coating damage could be different from the density of corrosion defects because some coating damage features may not include any corrosion defects whereas others may include multiple corrosion defects. Similar to defect density, coating damage density is a user estimate for a pre-inspection run. For a post inspection run, the actual density of coating damage features detected by the inspection should be entered. In the latter case, the program derives the actual number of defects from the number of observed indications using Equation [4.1].

4.2.1.5 Probability Distribution of Defect Section

The probability that a randomly selected defect will fall within a given section is proportional to the number of defects in the section, which equals the product of the defect density (ρ_i) and the section length (l_i). Based on this, the probability of a given section can be calculated as the number of defects in the section divided by the total number of defects in the whole pipeline segment. This can be expressed as:

Initial Damage

$$p_i = \frac{\rho_i l_i}{\sum_{all\,i} (\rho_i l_i)} \qquad [4.2]$$

The set of line attributes that must be specified to define a defect section are listed in Table 4.1. The table contains a complete list of line attributes that have an impact on the probability of pipeline failure due to corrosion. It is noted that subdivision of the pipeline segment into defect sections with consistent corrosion-related attributes is done independently of subdivision into failure sections with consistent consequence-related attributes. Attributes that affect both corrosion and consequences (as indicated in Table 4.1) are used independently in the two cases.

4.2.2 Defect Depth

4.2.2.1 Node Parameter

The Defect Depth node (basic node 12.2) and its direct predecessor node are highlighted in the version of the basic node corrosion influence diagram in Figure 4.2. The parameter of this node represents the average depth of a randomly selected defect (H). The average defect depth is defined as the total defect area projected on a plane parallel to the pipeline axis and through its centre, divided by the maximum defect length along the pipeline (see Figure 3.3). The influence diagram indicates that the Defect Depth node is conditionally dependent on the Defect Section node, which means that a separate Defect Depth probability distribution is required for each Defect Section. The Defect Depth is defined by a continuous probability distribution.

The *average depth*, instead of the maximum depth, is selected as the parameter characterizing Defect Depth because it better correlated to pressure resistance (see Section 7.2.4.2). Some inspection tools provide a direct estimate of the average defect depth, whereas other tools provide only the maximum defect depth. To address this, a relationship was developed between the maximum and average depth of a corrosion defect. This relationship is used to calculate the average defect depth from the maximum defect depth in cases where the inspection tool provides maximum depth measurements. This relationship is based on an analysis of the average depth against the maximum depth for 86 corrosion defects that were profiled in detail from pipe taken out of service (Kiefner and Vieth 1989). The resulting relationship is

$$H_{ave} = c\, H_{\max} \qquad [4.3]$$

where H_{ave} is the average defect depth, H_{max}, and c is the regression coefficient (c = 0.5464). Figure 4.3 shows the data and regression line. The data scatter can be taken into account by defining a regression error E_c. The data indicate that E_c can be modelled by a normal distribution with a mean of μ_{ec} = 0.0 and a standard deviation of σ_{ec} = 0.12 wt, where wt is the pipe wall thickness. Equation [4.3] and the associated uncertainty is used in PIRAMID as a basis for converting a maximum defect depth measurement into an estimate of the average defect depth.

Initial Damage

4.2.2.2 Calculation of Defect Depth

For a pre-inspection analysis, or a post-inspection analysis where the inspection was method used is a coating damage survey, the probability distribution of H is defined by direct user input since no data on defect depth would be available. In this case PIRAMID will provide default inputs that are derived from corrosion-related segment attributes (see Section 4.3 for a description of the method used in deriving the default values).

For a post-inspection analysis where the inspection involved running an in-line tool, defect depth data will be available from the inspection. In this case the input required by PIRAMID consists of the probability distribution of the *measured defect depth* (for detected defects only) as obtained directly from the inspection. This distribution can be defined by grouping the depth data for all corrosion defects observed on a given pipeline section into a histogram, and using a probability fitting technique to select the best fit probability distribution. There are standard software tools to carry out this fitting analysis. A sample result of a fitting analysis of corrosion defect depth using C-FER's software C-FIT (1995) is shown in Figure 4.4. Depending on the type of inspection tool used, the measured defect depth may represent the average defect depth or the maximum defect depth. If the input represents a maximum defect depth distribution, Equation [3.4] is used to convert the input into an average depth distribution (which is the actual node parameter). This conversion results in the same probability distribution type for average depth as for maximum depth, with the mean (μ) and standard deviation (σ) defined as follows:

$$\mu_{Have} = c\,\mu_{H\max} \qquad [4.4a]$$

$$\sigma_{Have} = c\,\sigma_{H\max} \qquad [4.4b]$$

It is noted that the probability distribution of the measured defect depth is not exactly the same as the distribution of actual defect depth. The difference is partly caused by the possibility that some defects will be missed by the inspection tool. These defects belong to the distribution of actual defects but are not included in the distribution of measured defects. The difference is also contributed to by measurement error (see Section 3.2.3). A model was developed to derive the probability distribution of the actual defect depth from the probability distribution of the measured defect depth, taking into account detection uncertainties and measurement errors. For the post-inspection (using an in-line tool) analysis mode, this model is used to derive the probability distribution of the actual defect depth (which is the parameter of this node) from the probability distribution of the measured defect depth. The model is described in detail in Appendix A.

Initial Damage

4.2.3 Defect Length

4.2.3.1 Node Parameter

The Defect Length node (basic node 12.3) and its direct predecessor node are highlighted in the version of the basic node corrosion influence diagram in Figure 4.2. The parameter of this node represents the maximum length of the corrosion defect along the pipe axis (L). The influence diagram indicates that the Defect Length node is conditionally dependent on the Defect Section node, which means that a separate Defect Length probability distribution is required for each Defect Section. The Defect Length is defined by a continuous probability distribution.

The influence diagram model assumes that Defect Length (L) is independent of Defect Depth (H). This assumption was supported by the results of a correlation analysis between H and L using the same corrosion defect data mentioned in Section 4.3 (from Kiefner and Vieth 1989). The correlation coefficient was found to be 0.006. A similar analysis on a set of 63 external corrosion defects provided by one of the project participants had a correlation coefficient of 0.08. These figures are sufficiently small to substantiate lack of correlation.

4.2.3.2 Calculation of Defect Length

As for the Defect Depth, the probability distribution of L is defined by direct user input for a pre-inspection analysis or a post inspection analysis for which the inspection tool used does not provide an estimate of defect length (*i.e.*, coating damage survey or low resolution in-line inspection).

For a post-inspection analysis involving a high resolution in-line tool, defect length data would be available from the inspection. As in the case of defect depth (see Section 4.2.2), a best fit probability distribution of the *measured defect length* is required as input to PIRAMID. Also, as in the case of defect depth, PIRAMID will derive the probability distribution of the actual defect length from the probability distribution of the measured defect length using the model described in Appendix A.

4.3 Default Values for Initial Damage

4.3.1 Approach

As mentioned in Section 4.2, probabilistic characterizations of defect frequency, depth and length are required to initiate the corrosion maintenance analysis in cases where line-specific data regarding corrosion defects are not available. This information can be defined directly by the user based on experience and observations related to similar pipeline segments. However, it was

recognized during the development of PIRAMID that sufficient information to defined these parameters explicitly may not be available. To address this situation, an approach was developed to derive the required default values from the corrosion-related line attributes.

The parameters for which default values are required include: 1) the defect density, 2) the probability distribution of the average defect depth (mean value standard deviation and distribution type), and 3) the probability distribution of the maximum defect length (mean value, standard deviation and distribution type). In principle, such default values could be defined on the basis of inspection information from pipelines with attributes matching the pipeline being considered. This however, would require a large data base that is not available at present. To overcome this problem a limited amount of inspection data was collected from member companies and supplemented by some analysis to derive reasonable estimates of the required default values. The data consisted of high resolution inspection logs for six pipeline segments with varying attributes. The inspection data and corresponding line attributes are summarized in Table 4.2.

The approach adopted in deriving default values was to find a corrosion defect population that satisfies the following conditions:

1. The probability of failure calculated from the defect population should be consistent with the value predicted from line attributes. The prediction of a failure probability from line attributes was based on the model developed by Stephens *et al.* (1996) as part of the PIRAMID prioritization module.

2. The relative frequencies of small leaks versus large leaks and ruptures calculated from the defect population should be consistent with historical data, which indicate that approximately 85% of all failures are small leaks and 15% are large leaks and ruptures combined.

3. The default defect population should have statistical characteristics that are consistent with those of the in-line inspection data.

Effectively, this approach utilizes information on corrosion-related failure rates and the corresponding relative frequency of different failure modes to supplement the limited amount of inspection information given in Table 4.2.

It is recognized that the proposed approach is based on a very limited data sample and that improvements can be made if more data are obtained. What is important to note, however is that the results are not intended as a definitive description of the defect population in the line. Rather they are intended as reasonable default values that are consistent with the reliability of the line as determined from its attributes. As for all other defaults these values can be over written by the user if more specific information is available.

Initial Damage

4.3.2 Results

4.3.2.1 Defect Density

Table 4.2 shows the defect density (number of defects per unit length) for 5 pipeline segments as obtained from a number of project participants. The minimum observed defect density in this data set is 0.12 defects per km for a pipeline with above average coating in soil with low corrosivity, and the maximum density is 81.9 defects per km for a pipeline with below average coating condition in highly corrosive soil. Based on the data in Table 4.2 it was felt reasonable to assume that the defect density is primarily a function of coating type, coating condition and soil corrosivity. The rationale for this is that coating damage provides the opportunity for corrosion to take place, while soil corrosivity determines how much corrosion is likely to occur at a specific location where the coating has broken down.

PIRAMID Technical Reference Manual 4.1 (Stephens 1996) defines three factors characterizing coating type, coating condition and soil corrosivity (denoted F_{CT}, F_{CC}, and F_{SC}, respectively. The combined impact of these three parameters can be represented by the product of the three factors, $F = F_{CT} \times F_{CC} \times F_{SC}$. Based on this, defect density is assumed to be a function of F.

It is also assumed based on the data that a defect density range of 0.1 and 10 defects per km is representative. This ignores the line with 81.9 defects per km in Table 4.2, since it was felt that this represents an extreme case that is not representative of the majority of pipelines. A corrosion density of 0.1 defects per km was assumed to correspond to the best possible value of F, whereas a density of 10 defects per km was assumed to correspond to the worst possible value. The defect density for any given pipeline is obtained by linear interpolation in this range based on the corresponding value of F. This leads to the following relationship:

$$n_d = 0.188\,F - 0.08, \qquad 0.0825 < F < 52.8 \qquad [4.5]$$

4.3.2.2 Defect Depth and Length Distributions

Assuming that failures at individual defects are independent events, the probability of failure at a single randomly selected corrosion defect, p_{fd}, can be calculated as follows:

$$p_{fd} = p_f / n_d \qquad [4.6]$$

where p_f is the probability of failure per unit length.year for the pipeline and n_d is the number of defects per unit length. As mentioned earlier in Section 4.3.1, one of the criteria used to define the default defect population is that the total probability of failure calculated from the population should be equal to the probability of failure calculated from the pipeline attributes (see Stephens 1996). Given the value of n_d (see Section 4.3.2.1) and of p_f (as calculated from the line

attributes), this condition would be satisfied if the probability of failure per defect p_{fd} matches the value calculated from Equation [4.6].

To define the distributions of defect depth and defect length, fitting analyses were carried out on the data given in Table 4.2. These analyses showed that the best fit distribution varies for the different data sets, but that the lognormal and Weibull provide the best fit for most cases, with the lognormal fitting more cases than the Weibull. Based on this the lognormal distribution was selected as a default distribution type for both defect depth and defect length. In addition, Table 4.2 shows that the coefficient of variation of defect length varies over a fairly small range. If segment No. 3 is ignored (because it represents a very small number of defects, namely 0.12 x 41 = 5 defects), it can be seen that the coefficient of variation of defect length varies between 0.43 and 0.63. Based on this a fixed value of 0.5 was used for the coefficient of variation of defect length.

Given the above, the remaining information required to fully specify the required distributions of defect length and depth consists of the mean defect depth, the standard deviation of defect depth and the mean defect length. These parameters were obtained using an optimization procedure that ensures that the set of parameters chosen satisfies (with the least possible error) the two remaining conditions, namely that the probability of failure per defect matches the value calculated from line attributes and that 85% of failures are small leaks and 15% are large leaks and ruptures. The failure conditions used to define failures and classify them into leaks and ruptures are described in Section 7.2.4.

The above calculations were carried out for a range of failure probabilities and the results were used to develop a set of empirical relationships defining the average defect depth μ_H, the standard deviation of defect depth σ_H, and the mean defect length μ_L. These relationships are as follows:

$$\mu_H = t[0.123\Phi^{-1}(p_{fd}) + 0.562], \qquad \mu_H > 0.05t \qquad [4.7]$$

$$\sigma_H = t[-0.0363\{\Phi^{-1}(p_{fd})\}^2 - 0.1135\Phi^{-1}(p_{fd}) + 0.0673], \qquad \sigma_H \geq 0.2\mu_H \qquad [4.8]$$

$$\mu_L = 31.98\Phi^{-1}(p_{fd}) + 122.3, \qquad \mu_L > 10mm \qquad [4.9]$$

where t is the pipe wall thickness and Φ is the cumulative normal distribution function.

Figures and Tables

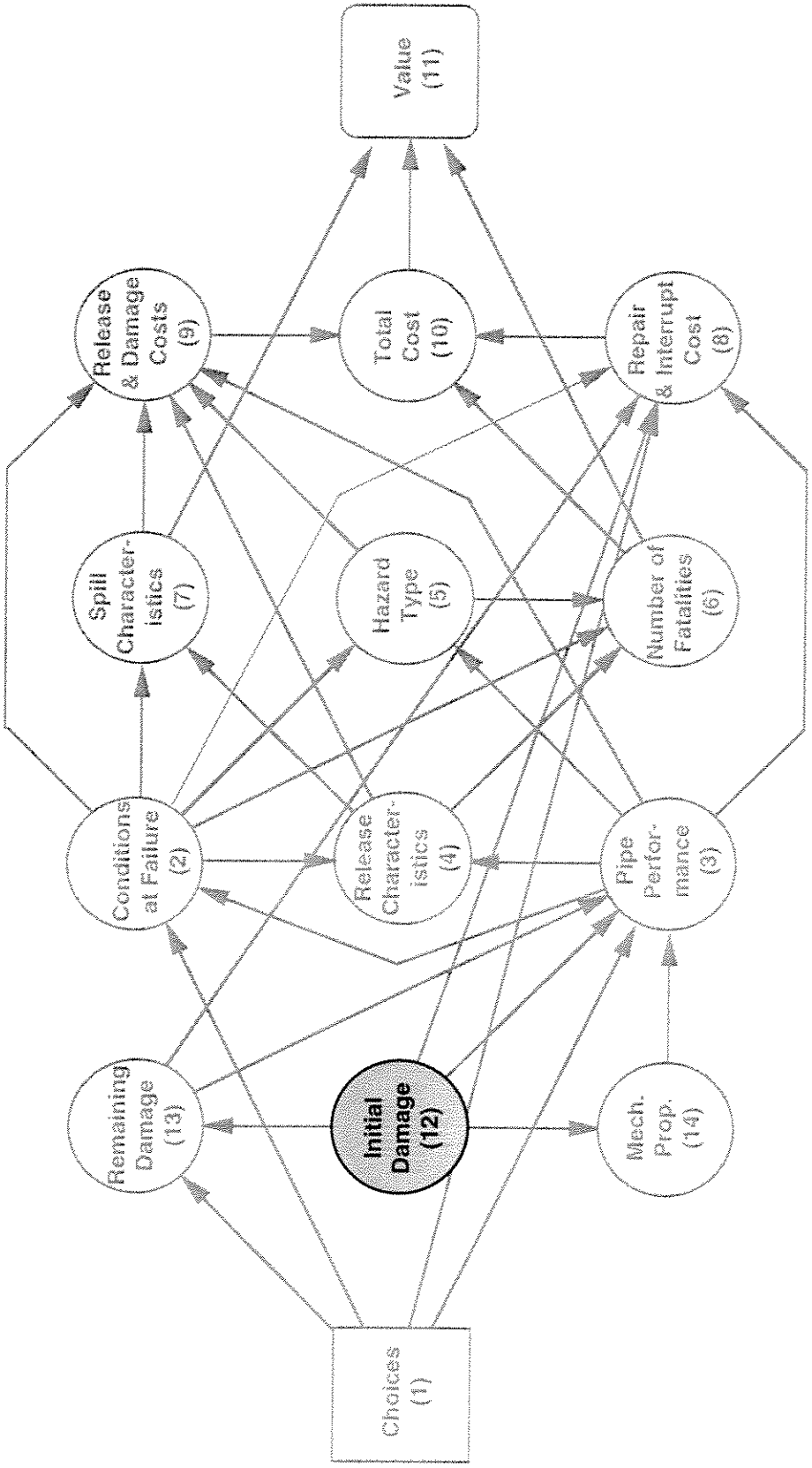

Figure 4.1 Compound node influence diagram highlighting Initial Damage node group

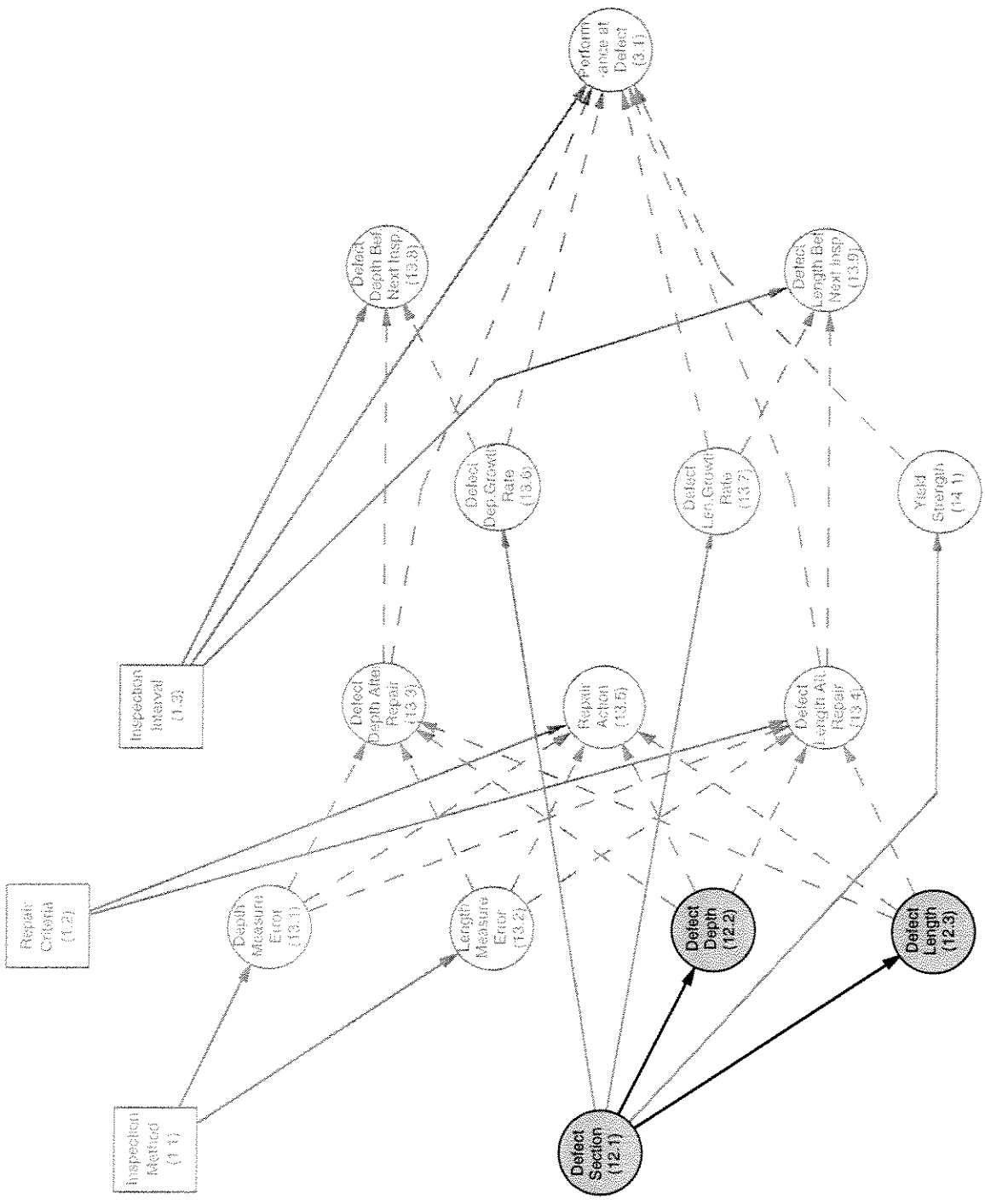

Figure 4.2 Basic node corrosion influence diagram highlighting Initial Damage nodes

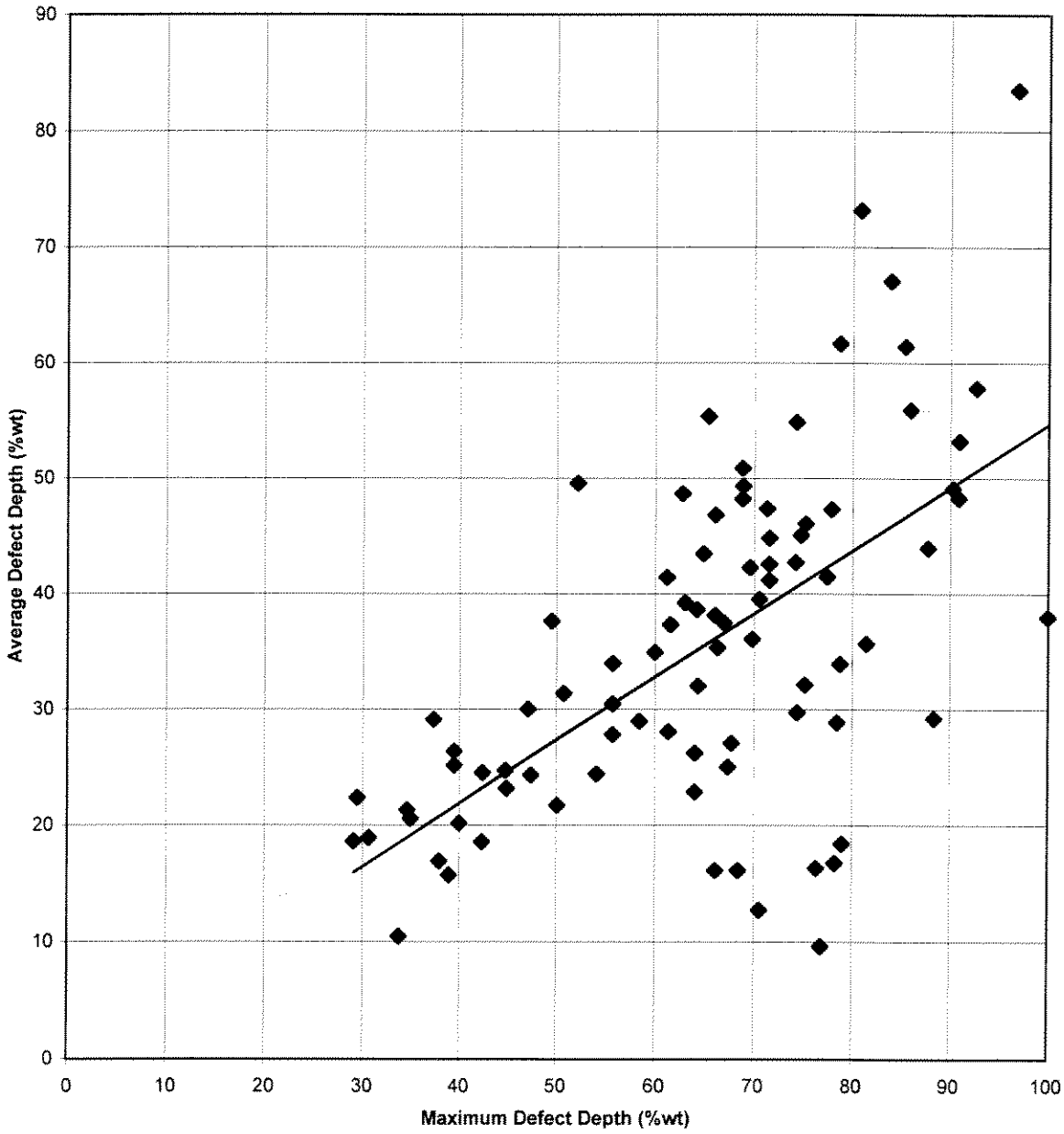

Figure 4.3 Maximum versus average defect depth (data and derived relationship)

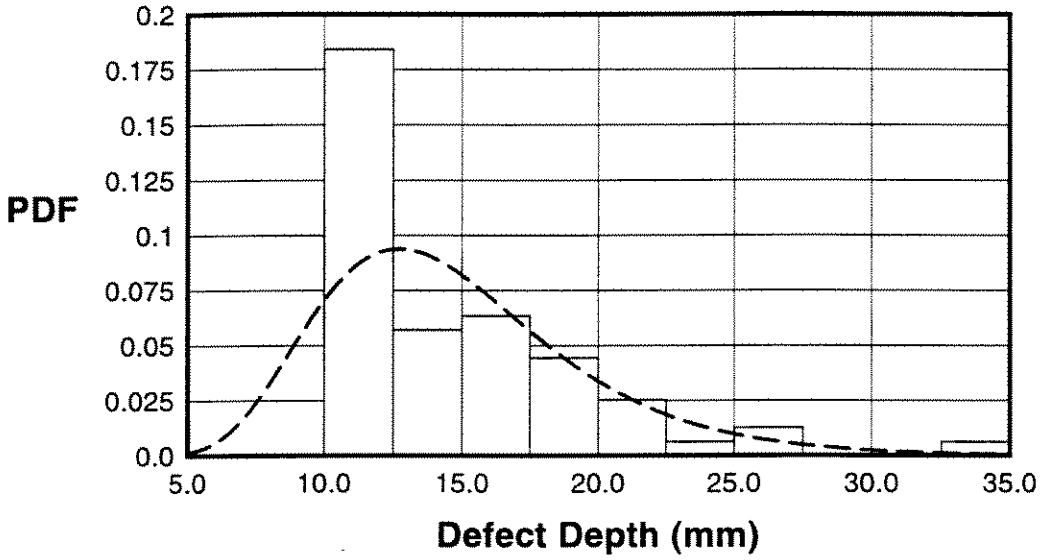

a) Probability density function

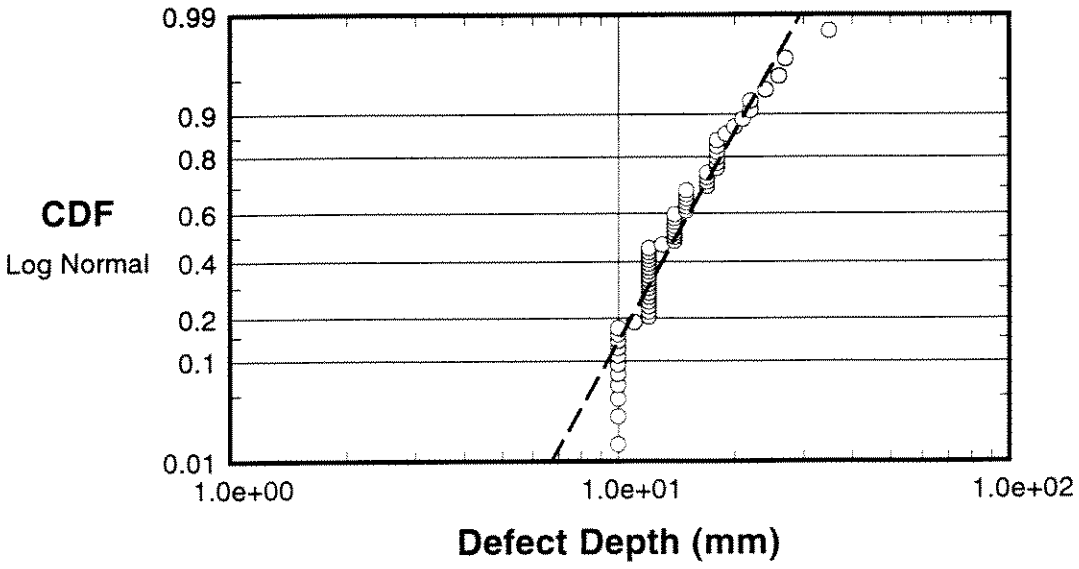

b) Cumulative probability on lognormal probability paper

Figure 4.4 Defect depth data and best fit lognormal distribution - a sample output of the fitting program C-FIT (1995)

Attribute	Definition	Affects Consequences? Yes / No
Pipe Wall Thickness (mm)	Numeric value	Yes
Operating Pressure (kPa)	Numeric value	Yes
Operating Temperature (°C)	Numeric value	Yes
Line Age (years)	Numeric value	No
General Soil Corrosivity	low Resistivity (ohm/cm) > 10,000	No
	below average 10,000< Resistivity (ohm/cm) < 5,000	
	average 5,000< Resistivity (ohm/cm) < 2,000	
	above average 2,000< Resistivity (ohm/cm) < 1,000	
	high Resistivity (ohm/cm) < 1,000	
External Pipe Coating Type	polyethylene / epoxy	No
	coal tar	
	Asphalt	
	tape coat	
	none (bare pipe)	
External Pipe Coating Condition	above average	No
	average	
	below average	
Cathodic Protection Level	above average (adequate voltage, uniform level)	No
	average (adequate average voltage, some variability)	
	below average (inadequate voltage and/or high variability)	
	no cathodic protection	
Presence of Coating Shielding	Yes	No
	No	
Presence of Electrical Interference or Casing Short	Yes	No
	No	

Table 4.1 Segment attributes affecting the probability of line failure due to corrosion

Segment No.	Segment Length (km)	Number of Defects/km	Defect Depth (%WT)			Defect Length (mm)			Line Attributes							
			Mean	Std. Dev.	COV	Mean	Std. Dev.	COV	Temp Deg C	Age Years	Soil Corrosivity	Coating Type	Coating Condition	Cathodic Protection	Coating Shielding	Electrical Interference
1	46.6	1.25	14.7*	4.8*	0.32	27	17	0.62	8 - 17	15	-	Tape	Average	Average	Yes	No
2	22.4	0.89	12.7**	8**	0.62	37	16	0.43	5 - 15	20	Low	Tape	Above Av.	Above Av.	Yes	No
3	41	0.12	21**	8.5**	0.41	62	21	0.35	5 - 15	20	Low	Tape	Above Av.	Above Av.	Yes	No
4	42.9	1.75	15.6**	11.1**	0.71	42	26	0.63	5 - 15	20	Average	Tape	Average	Above Av.	Yes	No
5	36.2	5.3	16	8.3**	0.52	36	19	0.54	5 - 15	20	High	Tape	Average	Above Av.	Yes	No
6	39.3	81.9	15.5**	8.3**	0.53	43	22	0.52	5 - 15	25	Very High	Tape	Above Av.	Above Av.	Yes	No

* Maximum defect depth
** Average defect depth

Table 4.2 External corrosion data for six line segments with various attributes

5.0 REMAINING DAMAGE

5.1 Overview

The Remaining Damage node group (group 13) is highlighted in the version of the compound influence diagram in Figure 5.1. This node group includes parameters describing the extent of corrosion damage remaining after the maintenance event is complete. Some damage will remain in the line after maintenance because the inspection is imperfect and may therefore fail to detect some of the existing defects. In addition, some of the defects that are detected will be too small to require repair. The population of remaining defects will therefore consist of defects that are not detected and defects that are detected but not repaired. Remaining defects are used to quantify the residual probability of failure after maintenance.

The individual parameters associated with the Remaining Damage node group are highlighted in the version of the basic node corrosion influence diagram shown in Figure 5.2. These nodes are discussed in the following sections.

5.2 Depth Measurement Error

The Depth Measurement Error node (node 13.1) and its direct predecessor node are highlighted in the version of the basic node corrosion influence diagram shown in Figure 5.2. The parameter of this node (denoted E_h) represents the measurement error associated with the value of the average defect depth as estimated from the inspection. For high and low resolution in-line inspection tools, defect depth measurement error is defined as a percentage of the pipe wall thickness. This parameter is not required for coating damage surveys as they do not provide any information on defect depth.

The Depth Measurement Error node is conditional on the inspection tool, which implies that a separate probability distribution of E_h is required for each tool. A normal distribution is typically used for measurement error (*e.g.*, Dally *et al.* 1983) and this assumption is adopted in PIRAMID. The mean and standard deviation of E_h are calculated from the tool accuracy specifications which are defined as part of the user input for the Inspection Method node (node 1.1), using the calculation procedure explained in Section 3.2.3.

As mentioned in Sections 3.2.3.1 and 3.2.3.2 the input for depth measurement error is assumed to match the tool measurement for user convenience (*i.e.*, in terms of average depth for a tool that measures average and maximum depth for a tool that measures maximum). Since the node parameter itself is defined in terms of the error corresponding to average depth, the conversion of Equations [4.3 and 4.4] is applied to measurement error for tools that measure maximum depth. In this case, the conversion error associated with Equation [4.3] is also added to the measurement error since the average defect depth estimate used is affected by both errors combined.

Remaining Damage

5.3 Length Measurement Error

The Length Measurement Error node (node 13.2) and its direct predecessor node are highlighted in the version of the basic node corrosion influence diagram shown in Figure 5.2. The parameter of this node represents the measurement error associated with the value of the defect length provided by the inspection tool, and is denoted E_l. Defect length measurement error is defined in units of length. It is noted that this parameter is defined only for high resolution in-line inspection tools since low resolution in-line tools and coating damage surveys do no provide any information on defect length.

The Length Measurement Error node is conditional on the inspection tool, which implies that a separate probability distribution of E_l is required for each tool. Similar to the Depth Measurement Error, a normal distribution is used for the Length Measurement Error. The mean and standard deviation of E_l are calculated from the tool accuracy specifications which are defined as part of the user input for the Inspection Method node (node 1.1), using the calculation procedure explained in Section 3.2.3.

5.4 Defect Depth After Repair

5.4.1 Node Parameter

The Defect Depth After Repair node (node 13.3) and its direct predecessor nodes are highlighted in the version of the basic node corrosion influence diagram shown in Figure 5.2. The node parameter represents the mean depth of a randomly selected defect after the maintenance event is complete. As indicated in Figure 5.2, this is a functional node for which the probability distribution can be calculated from the distributions of the direct predecessor nodes.

Figure 5.3 illustrates the steps involved in the calculation of the node parameter. These steps are described conceptually in Sections 5.4.2 to 5.4.6. Details of the mathematical models used are given in Appendix B. It is noted that Figure 5.3 is based on a high resolution in-line inspection, which is the most general case with respect to distribution updating because it provides information on the largest number of parameters (*i.e.*, number of defects, defect depth and defect length). Low resolution in-line inspection and coating damage surveys are treated as special cases or simplifications of the high resolution case. These simplifications will be discussed throughout Sections 5.4.2 and 5.4.6 and in Appendix B.

It is also worth noting that all the models described in Sections 5.4.1 through 5.4.6 calculate the mean and standard deviation (not the full distribution) of the parameters involved. The distribution types for all defect sub-populations are assumed to be the same as the user-defined distribution type for the original defect population. For example, if a Weibull distribution is selected by the user for defect depth, then the probability distributions of detected defects, undetected defects, remaining defects after repair are all assumed to be Weibull. These Weibull

distributions are then fitted to the parameter based on the calculated mean and standard deviation of each sub-population. Although this approach is not strictly correct from an analytical point of view, it was adopted to ensure that the computation time remains within practical limits.

5.4.2 Depth Distributions of Detected and Undetected Defects

It is assumed that the probability distribution of the depth of initial defects is defined from node 12.2 (see Figure 5.3). Once an inspection is carried out, the population of initial defects is divided into two separate sub-populations. The first sub-population includes *defects that are detected*, and the second includes *defects that are not detected.* The models used to calculate these distributions for the different inspection methods are as follows:

1. *High and Low resolution In-line Tools.* The probability of detection for in-line inspection tools is defined as a function of the defect depth such that deeper defects are more likely to be detected (see Section 3.2.3). It can be expected therefore that the distribution of detected defects will have a higher mean depth than the distribution of undetected defects. The model used to calculate the depth distributions for detected and undetected defects is a "filter" that separates initial defects into detected and undetected sub-populations based on the probability of detection as a function of defect depth. Figure 5.4 illustrates the model by showing a plot of the probability distributions of defect sizes for original, detected and undetected defects, assuming a detection probability curve with $q = 5$ (where q is a constant defining the detection efficiency of the tool as described in Section 3.2.3). This figure shows that, as mentioned earlier, the size distribution of detected defects is shifted to the right (higher values), whereas the size of undetected defects is shifted to the left (lower values).

2. *Coating Damage Surveys.* Because this class of survey methods detect coating damage rather than actual corrosion defects, the probability of detecting a specific corrosion defect (through identifying damage in the coating) is independent of the defect depth. This means that detection does not provide any information regarding defect depth, and consequently that the probability distributions of both detected and undetected defect depths are identical to the probability distribution of depth for all defects.

5.4.3 Measured Defect Depth Distribution

The next step in Figure 5.3 is to estimate the probability distribution of the *measured depth of detected defects*. This step is not applicable to coating damage surveys as they do not provide a defect depth measurement. For in-line inspection tools (both high and low resolution), the measured depth is different from the actual depth because of measurement error. The measured depth, H_m, can be calculated from

$$H_m = H + E_h \qquad [5.1]$$

where H is the actual defect size and E_h is the measurement error. Given the probability distributions of H, and E_h, the distribution of H_m can be estimated using standard probabilistic

methods. Figure 5.5 illustrates this step for the initial defect distribution used in Figure 5.4 and a measurement error with a mean value of 0 and a standard deviation of 5.5% the pipe wall thickness. Note that the size distribution of measured defects is "flatter" than that of the initial defects because of the additional uncertainty associated with the measurement.

5.4.4 Excavated and Unexcavated Defect Depth Distributions

The next step in the model is to separate the distribution of detected defects into two populations, the first including defects that will be excavated for more accurate sizing and potential repair, and the second including defects that will not be excavated (see Figure 5.3). The model used to calculate the probability distributions of defect depth for *excavated* and *unexcavated* defects is a truncation model, in which detected defects that meet the excavation criterion belong to the excavated population, and defects that do not meet the criterion belong to the unexcavated population. The excavation criteria for the different inspection methods are as follows:

1. *High resolution in-line tools.* In this case, a pressure-based criterion is used to make excavation decisions and as a basis for the filtering model. The criterion is expressed as a minimum ratio between the calculated pressure resistance and the Maximum Allowable Operating Pressure (MAOP), such that any defect that has a ratio less than the minimum value should be excavated. The model used to calculate the pressure resistance is explained in detail in Section 7.2.4.2. Using this model the excavation criterion can be expressed as follows:

$$\left[\mu_C \frac{2.3 t_n}{d_n} s_n \left(\frac{1-h_m/t_n}{1-h_m/m t_n}\right)\right] / MAOP \leq t_e\, r_r \qquad [5.2a]$$

where m is the Folias factor given by

$$m = \sqrt{1+0.6275\frac{l_m^{\,2}}{d_n t_n} - 0.003375\frac{l_m^{\,4}}{d_n^{\,2} t_n^{\,2}}} \quad \text{for} \quad \frac{l_m^{\,2}}{d_n t_n} \leq 50, \text{ and} \qquad [5.2b]$$

$$m = 0.032\frac{l_m^{\,2}}{d_n t_n} + 3.3 \quad \text{for} \quad \frac{l_m^{\,2}}{d_n t_n} > 50, \text{ and} \qquad [5.2c]$$

and

μ_c is the mean model error (equals 1.16 as explained in Section 7.2.4.2);

t_n is the nominal wall thickness;

d_n is the nominal pipe diameter;

s_n is the (nominal) specified minimum yield strength;

MAOP is the maximum allowable operating pressure;

l_m is the measured defect length;

h_m is the average defect depth estimated from the inspection. (If the inspection tool provides the maximum defect depth, Equation [4.3] should be used to convert the maximum depth values into average depth, which amounts to using 0.5464 h_m in Equation [5.2a]);

t_e is the excavation threshold defined as a multiple of the repair threshold (see Section 3.2.3.2.2); and

r_r is the repair resistance threshold defined as a multiple of MAOP (see Section 3.3).

2. *Low resolution in-line tools.* The excavation threshold is defined in terms of a maximum allowable defect depth. A defect is therefore excavated if

$$h_m \geq h_e \qquad [5.3]$$

where h_m is the measured defect depth and h_e is the excavation threshold depth value. The filtering in this case is based only on defect depth. If the inspection tool provides the maximum defect depth, Equation [4.3] should be used to convert the maximum depth values into average depth, which amounts to using 0.5464 h_m in Equation [5.3].

3. *Coating damage surveys.* Excavations based on coating damage surveys are decided on the basis of the size of coating damage rather than the size of the corrosion defect. It is therefore assumed that the percentage of indications that will be excavated is a direct user input. Since excavation decisions are independent of defect depth, the depth distributions for both excavated and unexcavated defects are identical to the depth distribution of original defects.

5.4.5 Repaired and Unrepaired Defect Depth Distributions

The next step in the analysis is to determine which of the excavated defects will be repaired (see Figure 5.3). The repair criterion is based on pressure resistance for all inspection methods because the excavated defects will be measured in situ before a repair decision is made. Furthermore, the pressure resistance estimate used to decide on repair is calculated from the *actual* rather than the measured defect dimensions because once a defect is excavated, its actual dimensions can be determined accurately from an in situ measurement. It is noted that in the present context, repair refers to work carried out on the pipe body to eliminate the section with reduced pressure resistance (*e.g.*, sleeving or cut-out replacement). It is recognized that pipe cleaning and coating repairs will be carried out for all defects that are excavated, even if in situ measurements show that they do not require pipe body repair, to ensure that further growth of the defect will not occur. Coating repairs are therefore treated as an integral part of defect excavation activities. This has implications with respect to definition of the costs of excavation and repair as will be discussed in Section 9.2.

The actual pressure resistance, r_a, as calculated from actual defect depth and length is calculated from (see Section 7.2.4.2):

$$\left[\mu_C \frac{2.3t_n}{d_n} s_n \left(\frac{1-h/t_n}{1-h/mt_n}\right)\right] / MAOP \leq r_r \qquad [5.4a]$$

Remaining Damage

where m is the Folias factor given by

$$m = \sqrt{1 + 0.6275\frac{l^2}{d_n t_n} - 0.003375\frac{l^4}{d_n^2 t_n^2}} \quad \text{for} \quad \frac{l^2}{d_n t_n} \leq 50, \text{ and} \qquad [5.4b]$$

$$m = 0.032\frac{l^2}{d_n t_n} + 3.3 \quad \text{for} \quad \frac{l^2}{d_n t_n} > 50, \text{ and} \qquad [5.4c]$$

and

μ_c is the mean model error (equals 1.16 as explained in Section 7.2.4.2);

t_n is the nominal wall thickness;

d_n is the nominal pipe diameter;

s_n is the (nominal) specified minimum yield strength;

MAOP is the maximum allowable operating pressure;

l is the actual defect length from in situ measurement;

h is the average defect depth from in situ measurement;

r_r is the repair resistance threshold defined as a multiple of MAOP (see Section 3.3).

PIRAMID assumes that defects that do not meet the condition in Equations [5.4] will be repaired. Similar to the previous section, a truncation model is used to calculated the probability distributions of depth for repaired and unrepaired defect. The model identifies defects that meet the condition in Equations [5.4] as belonging to the repaired population and defects that do not meet the condition as belonging to the unrepaired population.

5.4.6 Remaining Defect Depth Distribution

The final step in the analysis is to derive the probability distribution of the Defect Depth After Repair (which is the parameter of node 13.3) by combining the depth distributions of undetected, unexcavated and unrepaired defects (see Figure 3.5). The model used for this is based on a weighted sum of the three sub-populations. Figure 5.6 shows results corresponding to a simplified example case, in which it is assumed that all excavated defects are repaired. The figure shows the defect depth distributions for all detected defects and for defects that remain after repair. The remaining defect depth distributions are given for two repair criteria based on 1.25 MAOP and 1.5 MAOP. The figure illustrates the total impact of inspection and repair on the defect size population, which is represented by a shift of the size distribution toward the left (lower values). A more stringent repair criterion results in higher reductions in the defect size.

Remaining Damage

5.5 Defect Length After Repair

The Defect Length After Repair node (node 13.4) and its direct predecessor nodes are highlighted in the version of the basic node corrosion influence diagram shown in Figure 5.2. The parameter of this node represents the maximum axial length of a randomly selected defect after the maintenance event is complete. This is a functional node for which the probability distribution can be calculated from the distributions of the direct predecessor nodes.

The calculation procedure for this node is similar to the Defect Depth After Repair node, with one exception relating to the probability distributions of the length of detected and undetected defects (see Figure 5.3). While defect depth distributions for detected and undetected defects were different in the case of in-line inspection tools because the probability of detection is dependent on the defect depth, the distributions of defect length are the same for detected and undetected defects. This is because the probability of detection is assumed to be independent of the defect length, and therefore detection does not change one's mind about the probability distribution of defect length. This implies that the probability distributions of defect length for both detected and undetected defects are the same as the distribution for initial defects. Apart from this exception, all other calculations are the same for defect length as for defect depth.

5.6 Repair Action

The Repair Action node (node 13.5) and its direct predecessor nodes are highlighted in the version of the basic node corrosion influence diagram shown in Figure 5.2. The parameter of this node represents the action taken to repair a defect that is randomly selected from the population of defects. Recall that repair actions include excavation of the defect, repair of the coating and, if necessary, repair of the pipe body. Repair Action is a discrete parameter that may take one of three values defined as follows:

- *No action.* This occurs if the defect is not detected or if the calculated pressure resistance is greater than the excavation threshold. The probability of no action can therefore be calculated as the sum of two probabilities

$$p_{na} = p_{nd} + p_{ne\backslash d}\, p_d \qquad [5.5]$$

  where p_{nd} is the probability that the defect is not detected, $p_{ne\backslash d}$ is the probability of no excavation for a detected defect, and p_d is the probability of defect detection. For in-line inspection tools, the probability of detection (p_d) can be obtained as the sum of the probability of detection for different defect sizes, each weighted by the probability of that size occurring. The probability of non detection is calculated by subtracting the probability of detection from 1. Finally, $p_{ne\backslash d}$ can be calculated based on Equations [5.2 or 5.3] as the probability that the pressure resistance is higher than the excavation threshold.

- *Excavation and coating repair (no pipe body repair).* The probability of this event is equal to the joint probability that 1) the defect meets the excavation threshold and is thus excavated, and 2) the defect is found not to require repair (*i.e.*, the pressure resistance based on actual in situ measurements of defect dimensions is higher than the repair threshold). It is assumed

however that a coating repair will be carried out to ensure that the defect does not grow to critical size in the future.

- *Excavation with pipe body and coating repairs.* The probability of this event is equal to the joint probability that 1) the defect meets the excavation threshold and is thus excavated, and 2) the defect is found to require repair (*i.e.*, the pressure resistance based on actual in situ measurements of defect dimensions is lower than the repair threshold).

Details of the calculations involved in the above are given in Appendix C.

5.7 Defect Depth Growth Rate

The Defect Depth Growth Rate node (node 13.6) and its direct predecessor node are highlighted in the version of the basic node corrosion influence diagram shown in Figure 5.2. The parameter of this node represents the growth rate of the average defect depth in unit length/year. The node is conditional on the Defect Section node, implying that the probability distribution of defect depth growth rate can be varied from one defect section to the next.

The probability distribution of this node parameter is defined by direct user input. A literature review revealed a small amount of experimental data relating corrosion growth rates for buried pipelines to soil corrosivity (see Table 5.1). The information in the table is based on the weight loss rate of cathodically unprotected pipe buried in soils with different corrosivity levels. Because it is based on weight loss, the data gives a suitable representation of the average corrosion growth rate for a given defect. Since the data were collected for pipes that were not cathodically protected, the numbers are likely to be on the conservative side.

Using this information, a relationship between the mean corrosion growth rate, G_h, and soil corrosivity index (F_{SC} as defined by Stephens 1996) was developed in the form:

$$G_h = 0.078\, F_{SC} \quad (mm / year) \qquad [5.6]$$

The only information found regarding the coefficient of variation and distribution type of corrosion growth rate was for water injection pipeline systems (Sheikh *et al.* 1990). This indicates that the growth rate has a Weibull distribution with a coefficient of variation of approximately 60%. These values were adopted as defaults in PIRAMID.

5.8 Defect Length Growth Rate

The Defect Length Growth Rate node (node 13.7) and its direct predecessor node are highlighted in the version of the basic node corrosion influence diagram shown in Figure 5.2. The parameter of this node represents the growth rate of the maximum axial defect length in unit length/year. The node is conditional on the Defect Section node, implying that the probability distribution of the defect length growth rate can be varied from one section to the next. The probability

distribution of this node parameter is defined by direct user input. No information was found in the open literature on typical values of corrosion length growth rates, and therefore PIRAMID does not define default values for this parameter.

5.9 Defect Depth Before Next Inspection

The Defect Depth Before Next Inspection node (node 13.8) and its direct predecessor nodes are highlighted in the version of the basic node corrosion influence diagram shown in Figure 5.2. The parameter of this node represents the average depth of a randomly selected defect before the next maintenance event. Defect depth before the next maintenance event (H_τ) is calculated from the Defect Depth After Repair (H_0) for the current maintenance event, the Defect Depth Growth Rate (G_h), and the time interval to next maintenance event τ using the following equation

$$H_\tau = H_0 + \tau G_h \qquad [5.7]$$

Figure 5.2 shows that the Defect Depth Before Next Inspection is an end node. It does not have any successor nodes in the influence diagram and is therefore not used in further analysis. It is only included to provide information to the user regarding the likely condition of the pipeline before the next maintenance event. This information can be used as input to the program for runs aimed at planning future maintenance events.

5.10 Defect Length Before Next Inspection

The Defect Length Before Next Inspection node (node 13.9) and its direct predecessor nodes are highlighted in the version of the basic node corrosion influence diagram shown in Figure 5.2. The parameter of this node represents the maximum axial length of a randomly selected defect before the next maintenance event. Defect length before the next maintenance event (L_τ) is calculated from the Defect Length After Repair (L_0) for the current maintenance event, the Defect Length Growth Rate (G_l), and the time interval to next maintenance event τ using the following equation

$$L_\tau = L_0 + \tau G_h \qquad [5.8]$$

Figure 5.2 shows that the Defect Length Before Next Inspection is an end node. It does not have any successor nodes in the influence diagram and is therefore not used in further analysis. It is only included to provide information to the user regarding the likely condition of the pipeline before the next maintenance event. This information can be used as input to the program for runs aimed at planning future maintenance events.

Figures and Tables

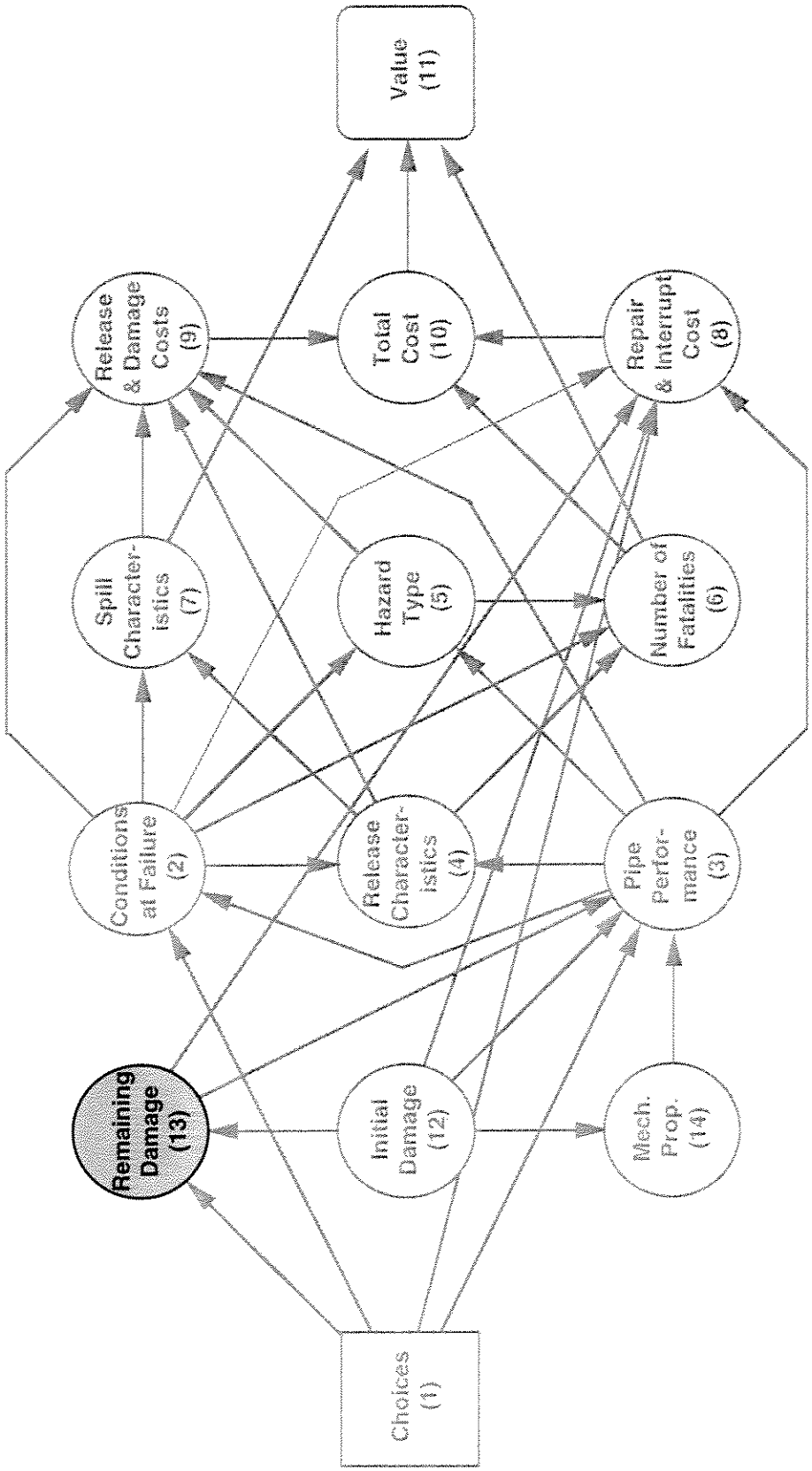

Figure 5.1 Compound node influence diagram highlighting Remaining Damage node group

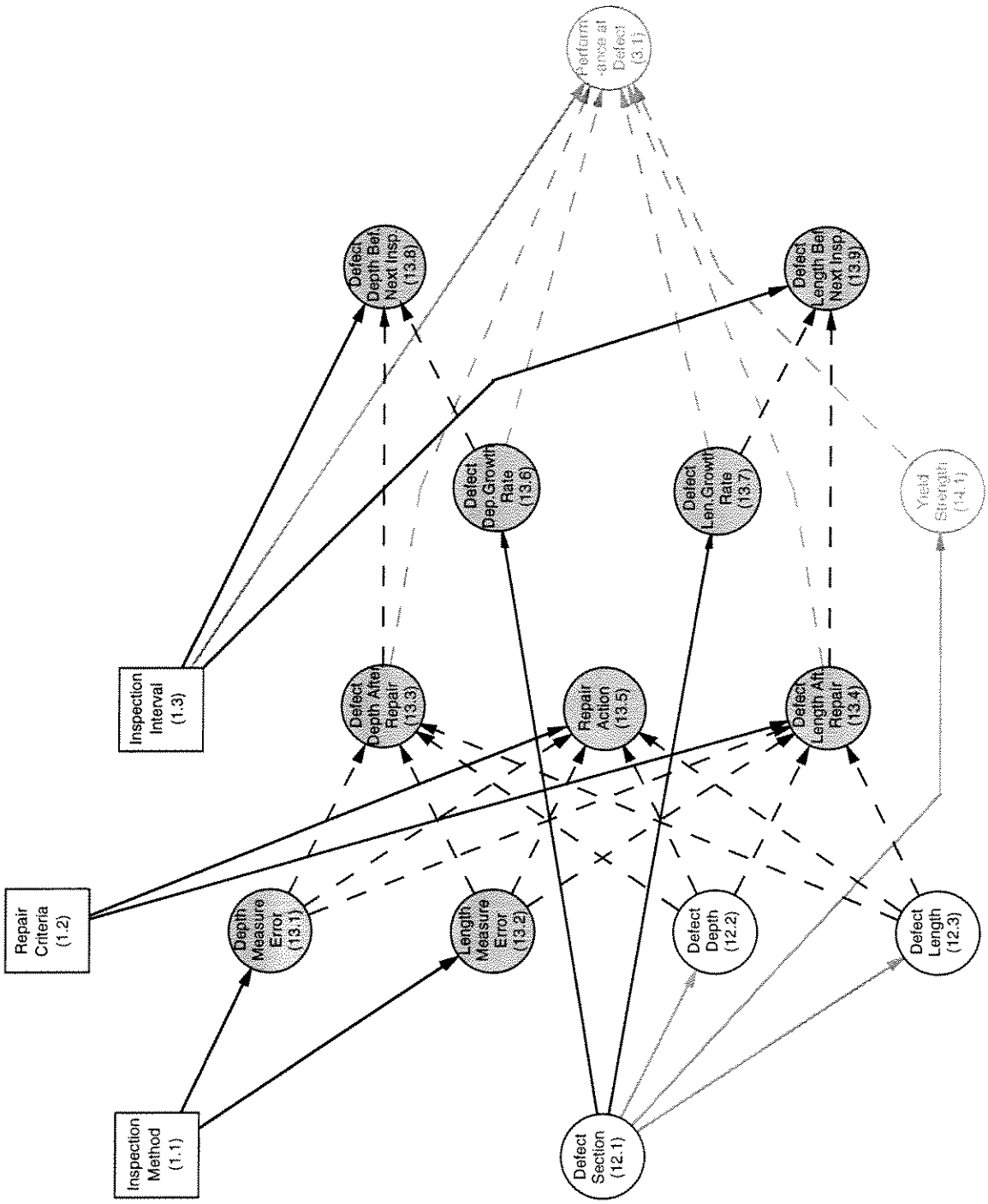

Figure 5.2 Basic node corrosion influence diagram highlighting Remaining Damage nodes and associated immediate predecessor nodes

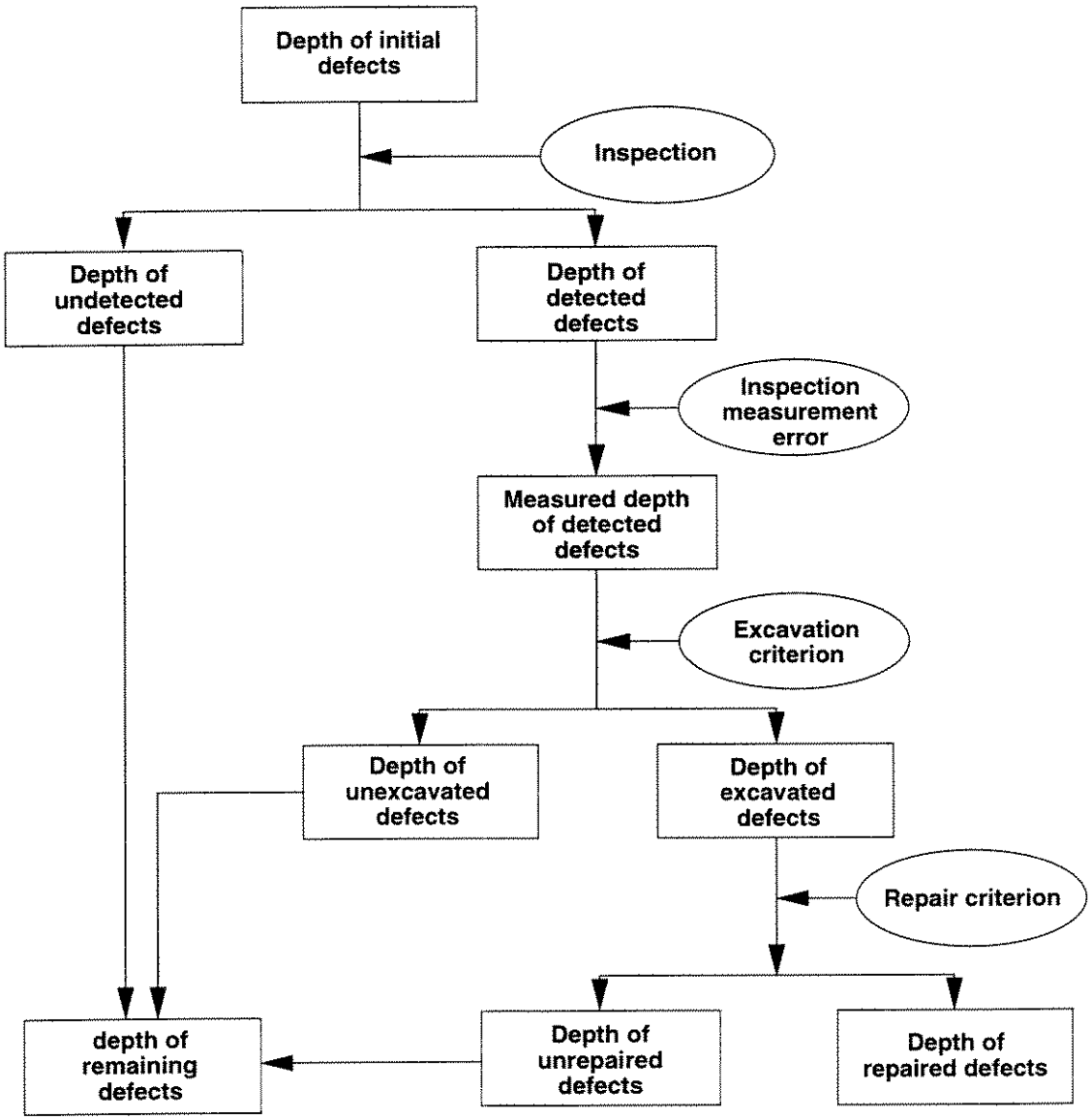

Figure 5.3 Illustration of the procedure used to calculate the size of defects remaining after inpsection and repair

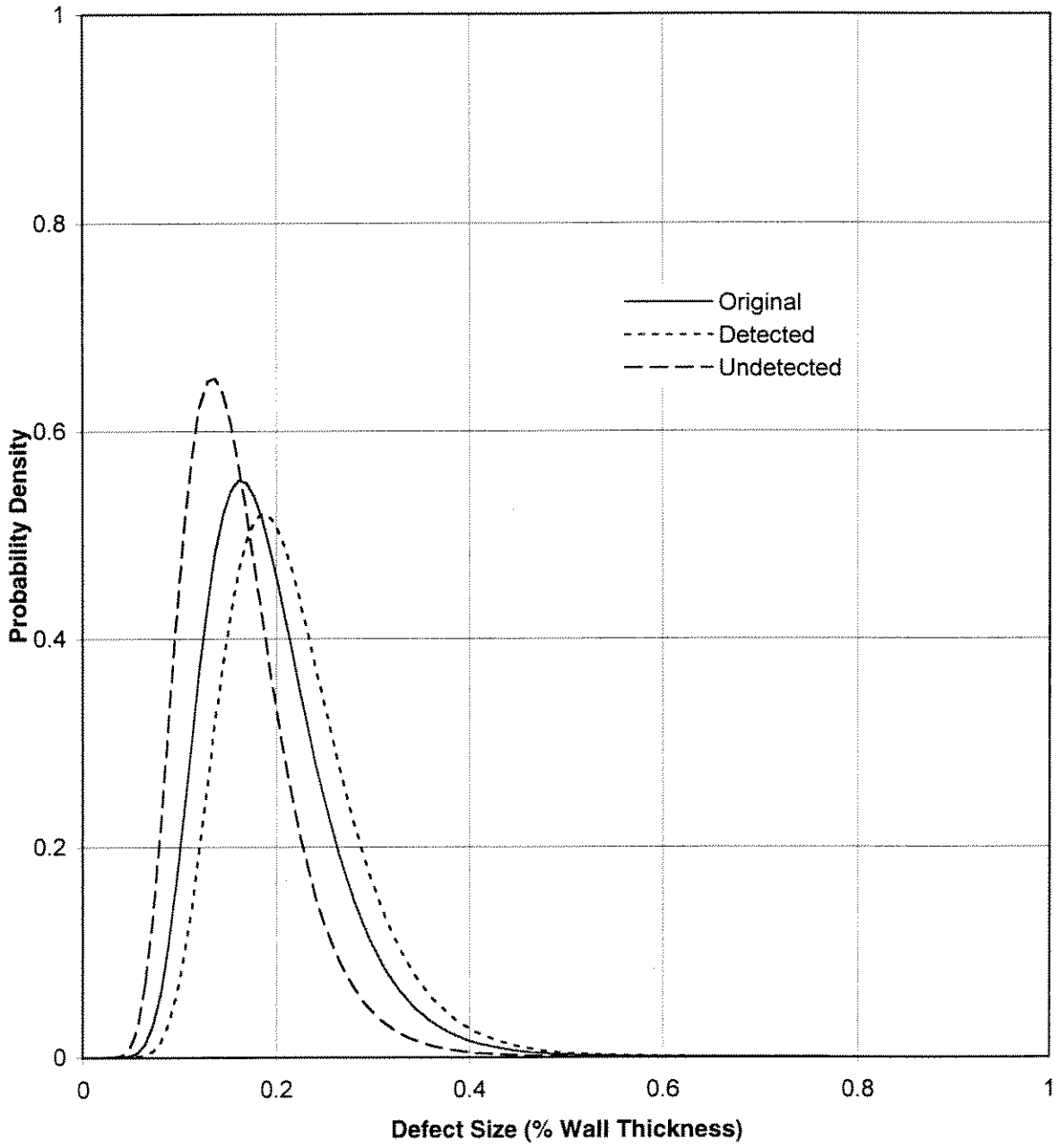

Figure 5.4 Probability distributions of the defect sizes for initial, detected and undetected defects

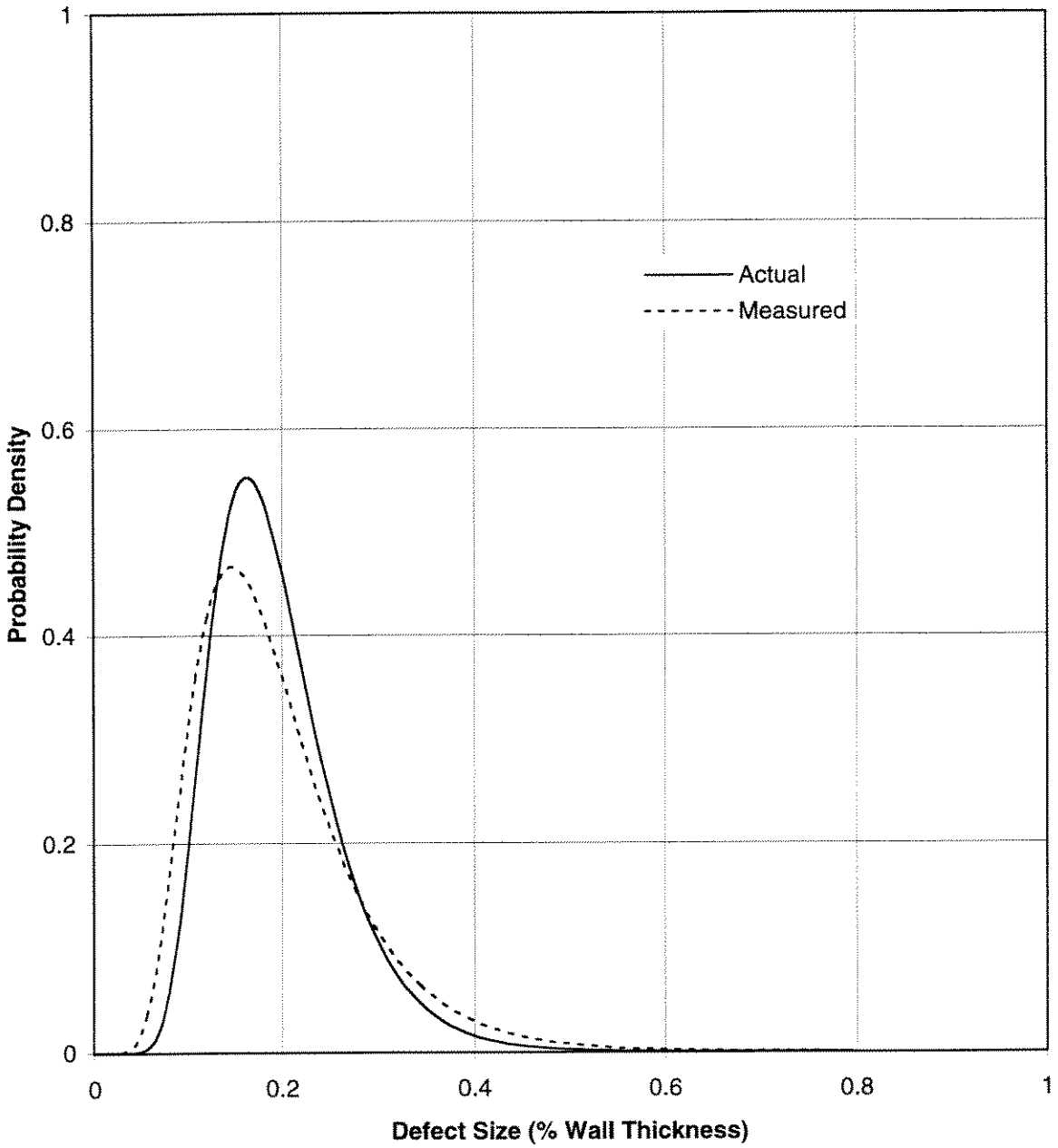

Figure 5.5 Probability distributions of the actual and measured defect size

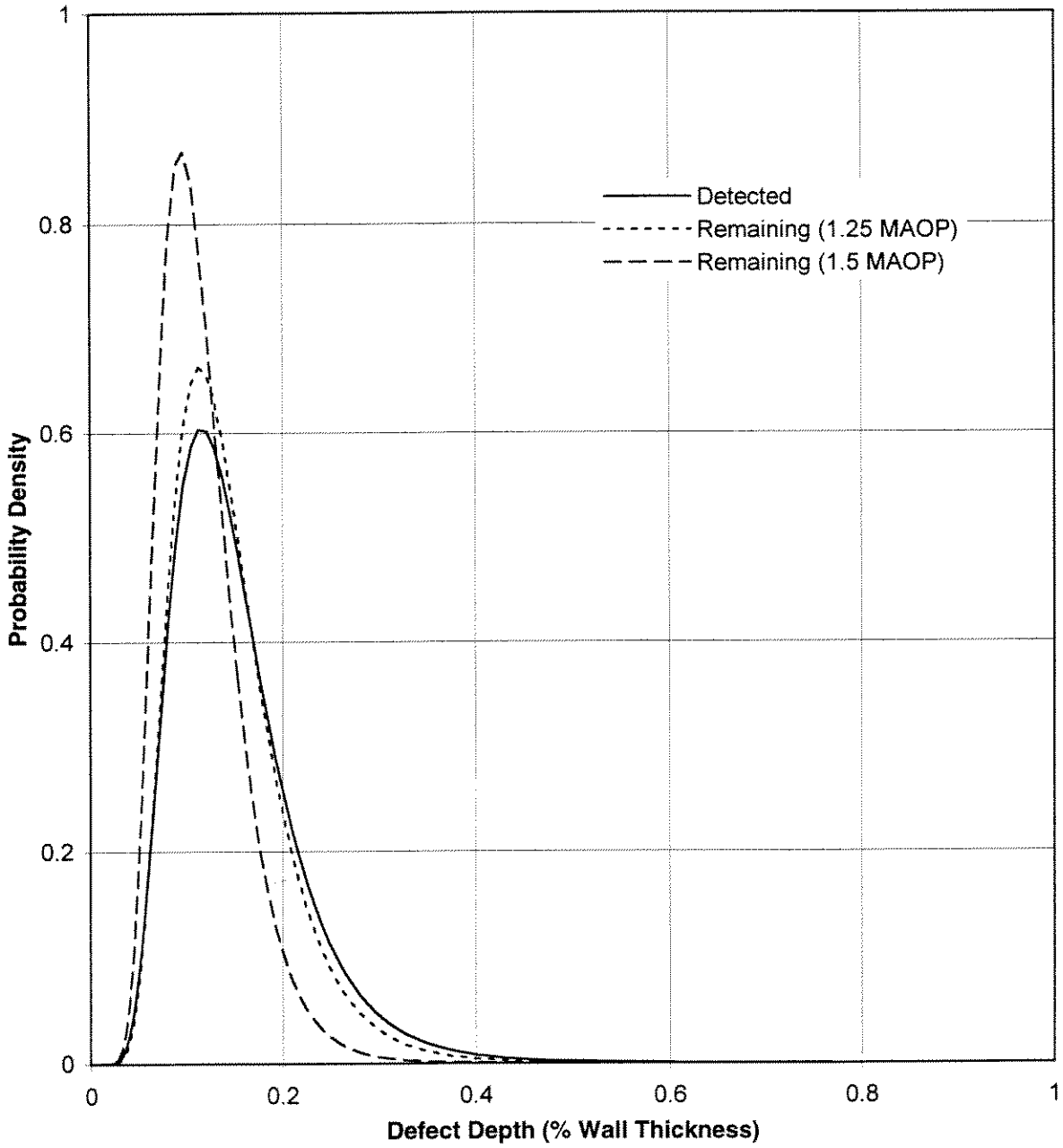

Figure 5.6 Probability distributions of the defect size for detected defects before repair, and remaining defects after repair based on 1.25 and 1.5 MAOP

Soil Corrosivity	Average Growth Rate (mm/year)
Low	0.0837
Low	0.0677
Below Average	0.1634
High	0.4681

Table 5.1 Average corrosion growth rates for pipelines in soils with different corrosivity

6.0 MECHANICAL PROPERTIES

6.1 Overview

The Mechanical Properties node group (group 14) is highlighted in the version of the compound node influence diagram in Figure 6.1. This node group includes parameters describing the pipe mechanical properties that are required to calculate its probability of failure. For the corrosion analysis influence diagram, this node group contains only one node representing the yield strength of the pipe steel. The parameter of this node is described in Section 6.2 below.

6.2 Yield Strength

The Yield Strength node (node 14.1) and its direct predecessor node are highlighted in the version of the basic node corrosion influence diagram shown in Figure 6.2. The node parameter represents the actual yield strength of the pipe steel at the location of a randomly selected corrosion defect. As indicated in Figure 6.2, this is a conditional node for which the probability distribution must be defined by the user for each possible value of its predecessor node. Since the predecessor node represents the section of pipeline at which the defect is located, the yield strength distribution must be defined for each pipeline section defined at the Defect Section node.

Randomness in the yield strength results from variabilities in the manufacturing process. Because of these variabilities, the yield strength at different locations of the pipe body will vary. An analysis of existing data indicates that the probability distribution of the actual yield strength can be derived from the nominal (or specified minimum) value of the yield strength. This relationship is derived from the information in Table 6.1, which was collected directly from different Canadian pipe manufacturers or found in the literature. The table gives the mean to nominal ratio, γ, and the coefficient of variation (defined as the standard deviation divided by the mean value), v, of the yield strength data obtained from a number of sources. The value of γ is always greater than 1.0 because the nominal yield strength is treated as a minimum allowable value. Pipe manufacturers design their product to have a higher average yield strength than the minimum allowable in order to minimize the chance of producing steel that does not meet specifications. The data in the table indicate that representative values of γ and v are 1.1 and 3.5%, respectively. It is noted that these default values represent recent pipe manufacturing standards and that they may be different for older pipe.

PIRAMID uses the above-mentioned values of γ and v to derive default values for the mean and standard deviation of the yield strength from the specified (or nominal) value, s_n, which is defined by the user as part of the segment attributes. PIRAMID calculates the mean, μ_s, and standard deviation, σ_s, from the following relationships:

$$\mu_S = \gamma s_n \qquad [6.1a]$$

Mechanical Properties

$$\sigma_S = v\,\mu_s \qquad [6.1b]$$

The aforementioned data sources indicate that the yield strength can be represented by either the normal or lognormal distribution. The normal distribution was selected as the default type in PIRAMID. All default values are presented to the user for modification as required.

Figures and Tables

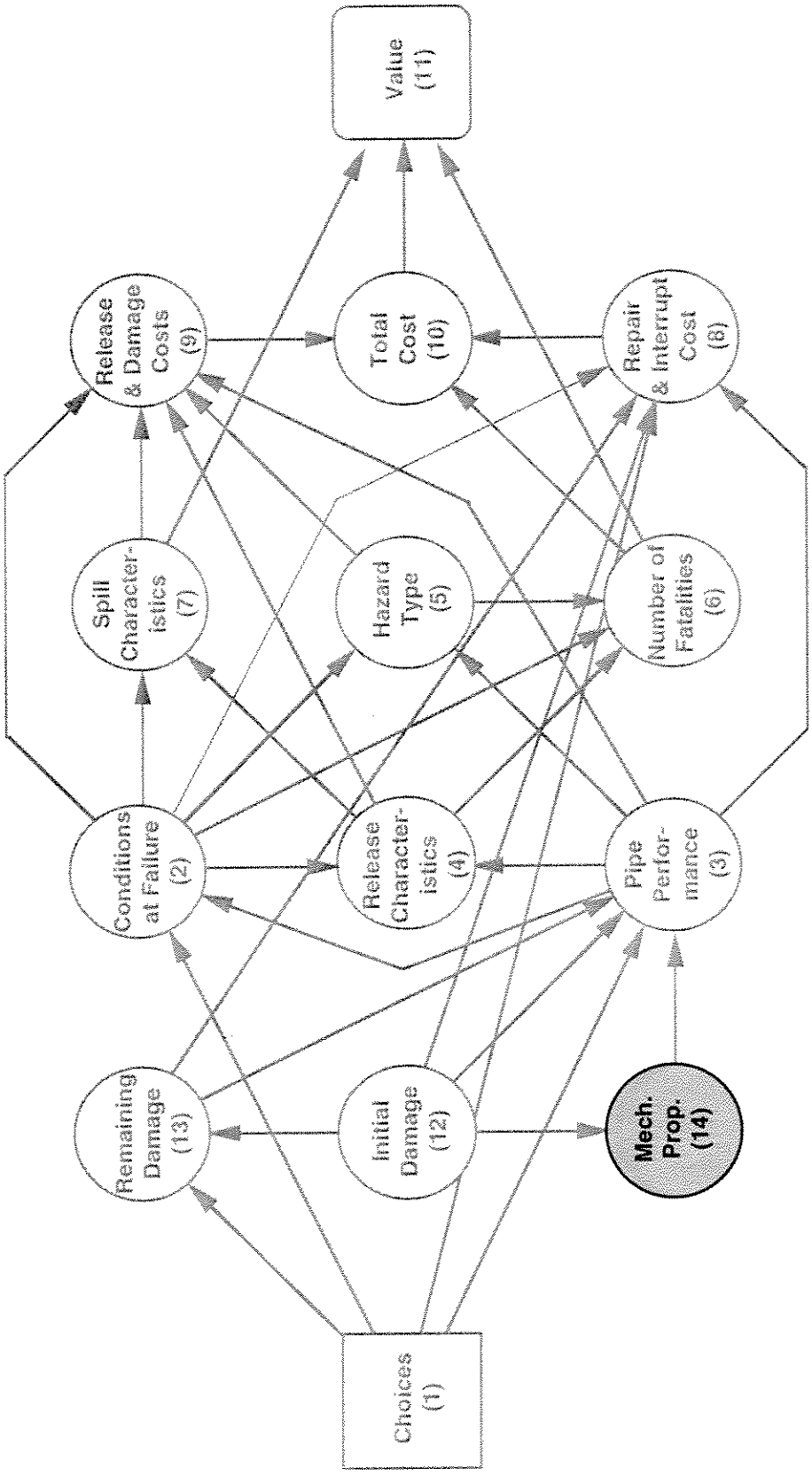

Figure 6.1 Compound node influence diagram highlighting Mechanical Properties node group

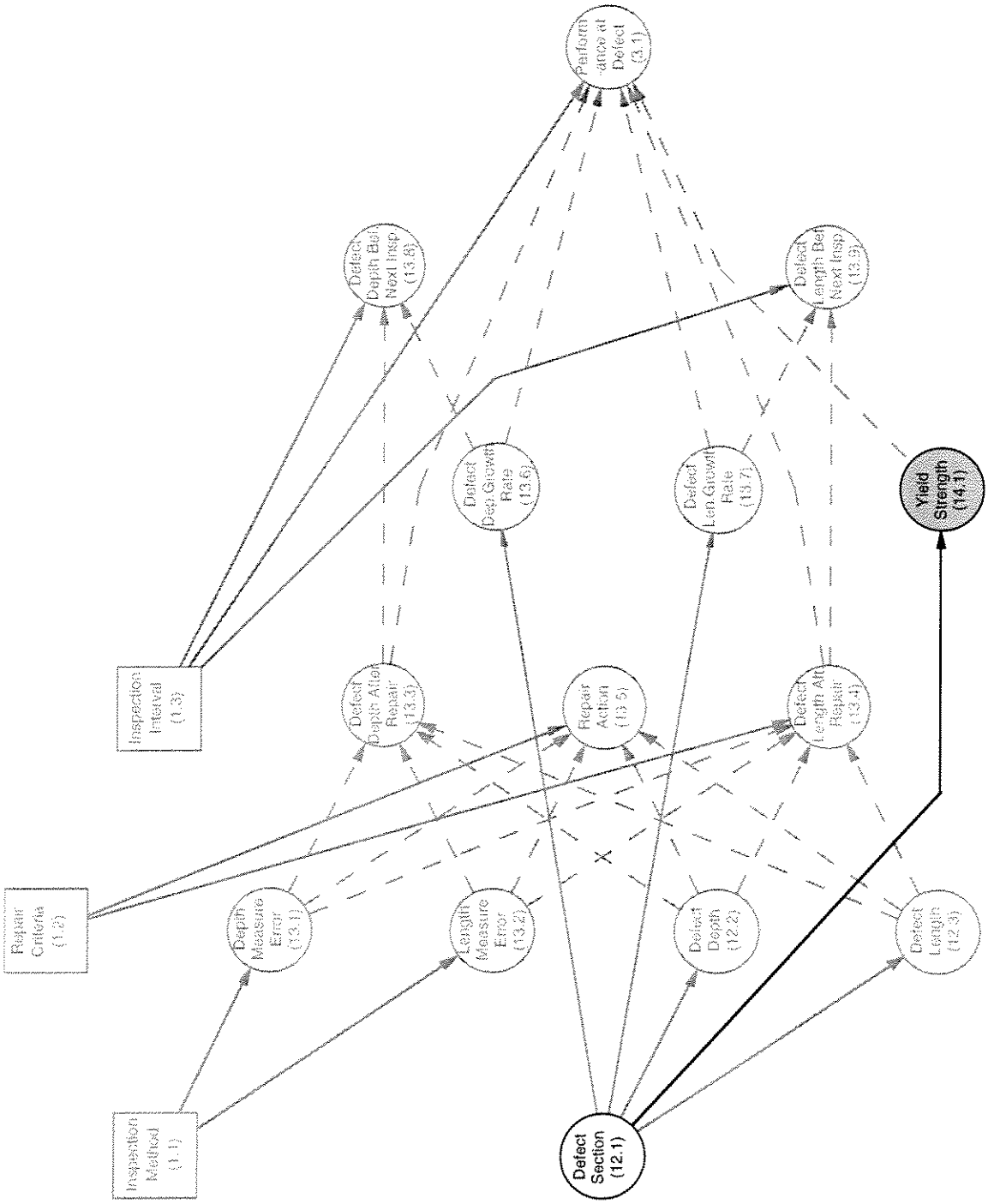

Figure 6.2 Basic node corrosion influence diagram highlighting Mechanical Properties node and associated immediate predecessor node

Data Source	Pipe Information	Mean / Nominal	StDev / Nominal	COV (%)	Distribution Type
Mill data	spiral pipe, X60	1.11	0.0370	3.3	–
Mill data	spiral pipe, X65	1.09	0.0359	3.3	–
Mill data	spiral pipe, X70	1.06	0.0317	3.0	–
Mill data	U&O pipe, X70	1.15	0.0419	3.6	normal
Jiao *et al.* 1992	offshore pipelines	1.07	0.0428	4.0	lognormal
Abrams and Hansen 1984	U&O pipe, X70	1.09	0.0440	4.0	normal

Table 6.1 Pipe yield strength data

7.0 PERFORMANCE

7.1 Overview

The Performance node group (group 3) is highlighted in the version of the compound influence diagram in Figure 7.1. This node group includes parameters describing the pipe performance during the time period between completion of the current and next maintenance events. The node group includes two individual nodes. The first node (Performance at Defect - node 3.1) represents the performance at a single randomly selected corrosion defect. Its probability distribution is evaluated from the corrosion analysis portion of the influence diagram (Figure 7.2). The second node (Segment Performance - node 3.2) represents the performance of a whole segment of pipe. It's probability distribution is evaluated from the distribution of the Performance at Defect node (3.1) and the frequency of corrosion defects in the segment (from node 12.1 representing Defect Section). It is then used in the consequence analysis portion of the influence diagram (Figure 7.3) as described in PIRAMID Technical Reference Manual No. 3.2 (Stephens *et al.* 1996).

7.2 Performance at Defect

7.2.1 Node Parameter

The Performance at Defect and its direct predecessor nodes are highlighted in the version of the corrosion analysis influence diagram shown in Figure 7.2. The specific node parameter is defined as the performance of the pipeline at a randomly selected single corrosion defect during the inspection interval (defined as the time between the current maintenance event and the next maintenance event). As indicated in Figure 7.2, the performance is defined as a function of the defect depth and length after repairs have been carried out, the defect depth and length growth rates, the inspection interval and the yield strength of the pipe.

The node parameter is a discrete random variable that can assume one of four possible values or states:

- safe;
- small leak;
- large leak; and
- rupture.

Performance

A small leak corresponds to a small pin-hole and a slow product release rate that does not result in a significant hazard. A large leak, involving a hole size of tens of millimeters, or a rupture involving a hole size on the order of the pipe diameter are assumed to result in high release rates and the potential for significant hazard to people and property.

The probability distribution of this node consists of estimates of the probabilities associated with each of the possible states of the node parameter (safe, small leak, large leak or rupture). Calculation of these probabilities involves the use of the probability distributions of corrosion defect sizes, corrosion growth rates and material properties in deterministic response models that define the conditions leading to the different possible failure modes. Two issues that have not arisen in previous PIRAMID probability calculations need to be considered for this node:

- *Time dependence.* Because of the gradual growth of defect sizes, pipe resistance will decrease with time causing the probability of failure to increase with time. Since PIRAMID evaluates consequences on an annual basis, a special modelling approach is required to convert the time-dependent probabilities of failure into annual probabilities that are suitable for use in the PIRAMID optimization analysis. This modelling approach is discussed in Section 7.2.2.

- *Simultaneous consideration of multiple response functions.* To evaluate the probabilities of different failure modes, the different criteria governing these failures must be considered simultaneously at this node. This implies that the standard probabilistic models that are used in PIRAMID to calculate the probability distributions associated with functional nodes (Nessim and Hong 1995) are not directly applicable. The models developed to address this are described in Section 7.2.3.

After dealing with the above-mentioned aspects, the deterministic models used to predict leaks and ruptures from defect sizes and material properties are described in Section 7.2.4.

7.2.2 Annual Failure Probabilities for a Time-Dependent Problem

This section describes the approach used to calculate the annual probabilities of failure due to corrosion considering the associated time dependence mentioned in Section 7.2.1. For the purposes of this sub-section, the total probability of failure, p_f, is used without distinction between the different failure modes. This distinction is addressed in Section 7.2.3.

It is assumed for the purpose of corrosion analysis that internal pressure is a fixed sustained load. This is a simplifying assumption since the operating pressure will typically vary with time. In principle, the model can be extended to account for these variations. It is suggested, however, that a preliminary assessment of the magnitude of variability in the maximum operating pressure should be undertaken to determine the significance of this factor before this level of complexity is added to the model. The necessary data for this assessment could not be obtained for this study.

Performance

Based on the fixed pressure assumption, Figure 7.4 illustrates the model used to calculate the failure probability at a given corrosion defect. As indicated in the figure, failure occurs at any corrosion defect when sufficient time has elapsed for the pressure resistance at the defect to drop below the applied pressure. The probability of failure occurring before time τ has elapsed, $p_f(\tau)$, can be expressed as

$$p_f(\tau) = p[P > R(\tau)] = p[R(\tau) < 0] \qquad [7.1]$$

where P is the pressure load and $R(\tau)$ is the pressure resistance at time τ. Equation [7.1] states that the probability of failure on or before time τ is equal to the probability that damage growth during that period will be sufficient to causes the resistance, $R_r(\tau)$, to drop below the load, P.

Equation [7.1] gives the probability that failure will occur at any time before the time interval τ has elapsed. If that time interval is 10 years for example, then $p_f(10)$ is the probability that failure will occur at any point in time between initial construction and the end of that 10 year period. As will be shown in the remainder of this section, $p_f(\tau)$, is the basic quantity used in calculating cumulative and annual failure probabilities. Calculation of $p_f(\tau)$ itself is described in Section 7.2.3 for different failure modes.

The probability of failure before time τ, $p_f(\tau)$, can be used to calculate the probability of failure during a specific time interval (τ_1 to τ_2) using the following relationship (Madsen *et al.* 1986, pp. 287):

$$p_f(\tau_1 < \tau < \tau_2) = \frac{p_f(\tau_2) - p_f(\tau_1)}{1 - p_f(\tau_1)} \qquad [7.2]$$

This equation states that the probability of failure during a given time interval is equal to the probability of failure before the end of the interval less the probability of failure before the beginning of the interval, all divided by the probability that failure will not occur before the interval begins.

Equation [7.2] can be used to calculate the required node probabilities. These include the following:

1) Probability of failure before time τ, taking into account the fact that the pipeline is safe at present. This can be obtained by setting $\tau_1 = 0$ and $\tau_2 = \tau'$, in Equation [7.2] leading to

$$p_f(0 < \tau < \tau') = \frac{p_f(\tau') - p_f(0)}{1 - p_f(0)} \qquad [7.3]$$

2) Annual probability of failure as a function of time. This can be calculated by substituting the beginning and end of each year for τ_1 and τ_2 in Equation [7.2]. For example, the annual probability of failure during the n^{th} year can be obtained by substituting $\tau_1 = n-1$ and $\tau_2 = n$ in Equation [7.2], leading to

Performance

$$p_f(n) = \frac{p_f(n) - p_f(n-1)}{1 - p_f(n-1)} \qquad [7.4]$$

Finally, it is noted that the probabilities associated with this node are all defined as yearly average values for the time interval between inspections. This allows comparison of options involving different inspection intervals on an equal basis. The average annual probability of failure, for example, is calculated from

$$p_f = [\sum_{i=1,n} p_f(i)] / n \qquad [7.5]$$

where n is the number of years to the next inspection. The use of the average probability of failure is justified on the basis that failure costs are all defined in terms of present worth currency, so that the actual cost of failure is the same for all years. Under these conditions, the average cost of failure over a given interval of time is equal to the cost of failure multiplied by the average probability of failure.

After calculating the probability of failure from the foregoing procedure, the probability of safe performance can simply be calculated from

$$p_s = 1 - p_f \qquad [7.6]$$

7.2.3 Probabilities of Different Failure Modes as Functions of Time

Section 7.2.2 indicates that the basic quantities required to calculate the probability distribution of the node parameter are the probabilities of failure before time τ has elapsed (defined as functions of time) for the three different failure modes. These probabilities are denoted $p_r(\tau)$ for rupture, $p_{ll}(\tau)$ for large leaks, and $p_{sl}(\tau)$ for small leaks. Given these quantities, Equations [7.2] to [7.6] can be used to calculate all probabilities associated with the node. This section explains how $p_r(\tau)$, $p_{ll}(\tau)$, $p_{sl}(\tau)$ are calculated in the corrosion analysis influence diagram.

The basic model used for this calculation involves defining deterministic failure conditions that relate the events of small leak, large leak or rupture to the parameters of the predecessor nodes, and then using the FORM algorithm to determine the probability that the parameters of the predecessor nodes will assume a set of values that correspond to each of these events. In general, a failure condition can be developed by defining a safety margin, $g(\tau)$, characterizing the excess resistance over the applied pressure load. According to this definition

$$g(\tau) = R(\tau) - P \qquad [7.7]$$

Failure occurs if the safety margin is less than zero and the pipeline is safe if the safety margin is greater than zero. The probability of failure can therefore be calculated from

Performance

$$p_f(\tau) = p[g(\tau) = R(\tau) - P < 0] \quad [7.8]$$

Pipe resistance to corrosion failures is dependent on the parameters of the predecessor nodes to the Performance at Defect node as seen from Figure 7.2. Specifically, these parameters are

- average defect depth, H;
- total defect length, L;
- defect depth growth rate, G_h;
- defect length growth rate, G_l;
- yield strength, S; and
- time, τ.

Based on this, Equation [7.9] can then be re-written as

$$p_f(\tau) = p[g(P, H, L, G_h, G_l, S, \tau) < 0] \quad [7.9]$$

The probability of failure is therefore equal to the probability of occurrence of all combinations of $P, H, L, G_h, G_l, S, \tau$ that cause g to be less than zero. To illustrate the calculation of this probability, consider a failure condition that is defined as a function of only two random parameters, namely the defect depth and length, H and L. In this case, g can be plotted in a two-dimensional space as shown in Figure 7.5. The function g divides the H-L plane into two domains, one containing combinations leading to failure and the other containing safe combinations. The probability of failure in this case is calculated as the probability or occurrence of all H-L combinations on the failure side of the response function.

Application of the basic approach to the Performance at Defect node, requires the definition of a number of failure conditions corresponding to ruptures, large leaks and small leaks. These conditions are described in detail in Section 7.2.4. To continue with the discussion in this section regarding the probabilistic model, the purpose and format of each of these models are outlined. They are as follows:

1. *Condition for pipe body failure (leaks and large ruptures).* Ruptures and large leaks are defined as events involving a pressure-induced failure of the pipe body around the corrosion defect. Models are available that can be used to formulate a failure condition for this scenario in the form

$$g_1(P, H, L, G_h, G_l, S, \tau) = 0 \quad [7.10]$$

such that a pipe body failure (*i.e.*, leak or rupture) occurs if $g_1 < 0$ and does not occur if $g_1 > 0$.

2. *Distinction between large leaks and ruptures.* Within the category of pipe body failures, distinction is made between large leaks and ruptures. Large leaks are assumed to correspond

to a "stable" failure involving flow of the pipe material and leading to a hole of significant size. Ruptures on the other hand are assumed to involve propagation of the defect after the initial failure to a size that is potentially large enough to cause unconstrained release of product. The ratio of large leaks to ruptures was defined on the basis of a conservative interpretation of a small amount of historical data suggesting that for wall thicknesses typical of transmission lines (EGIG 1993)

$$p_{sl} = 3p_r \qquad [7.11]$$

3. *Condition for occurrence of small leaks.* Small leaks are assumed to occur when a defect corrodes through the pipe wall without causing a pipe body failure. The criterion for through wall thickness corrosion can be written as

$$g_2(H, G_h, \tau) = 0 \qquad [7.12]$$

This condition is independent of defect length, yield strength and pressure, since it represents through wall corrosion growth without pipe body failure. Equation [7.12] is assumed to be formatted such that $g_2 < 0$ corresponds to a failure by small leak.

The two failure conditions given in Equations [7.10] and [7.12] are illustrated graphically in two-dimensional space of *H-L* in Figure 7.6. Note that the area corresponding to small leaks is bounded by the small leak criterion g_2 and the pipe body failure criterion, such that it is on the failure side of the small leak condition and the safe side of the pipe body failure condition. This reflects the assumption that a small leak will only occur if the defect geometry is such that it will not fail before its depth reaches the pipe wall thickness. Since the chance of a pipe body failure is higher for longer corrosion defects, it can be expected that shorter defects are likely to corrode through the wall causing small leaks.

The total failure probability before a given time τ is calculated as the probability associated with the combined failure domain (see Appendix D for details). Dividing the total failure probability into probabilities of small leak and pipe body failure (large leak or rupture) at any point in time is done using a probabilistic model that was developed under the PIRAMID corrosion research project. This model acknowledges that failure occurs as corrosion defects cross the boundary between the safe domain and the failure domain shown in Figure 7.6 due to corrosion growth with time. The probability of a small leak or pipe body failure at a given point in time, is therefore equal to the probability that the crossing will occur through the corresponding portion of the failure condition (see Figure 7.6). Details of this model are given in Appendix D.

Given the annual probability of failure, $p_f(n)$, (Equation [7.5]) and the relative probabilities of rupture, large leak and small leak as a function of time [denoted $f_r(n)$, $f_{ll}(n)$, and $f_{sl}(n)$], the probability of rupture before time τ can be calculated by a summation over time

$$p_r(\tau) = \sum_{i=0,n} p_f(n).f_r(n) \qquad [7.13]$$

Performance

The probabilities of large leak and small leak can be calculated from equations analogous to†[7.13].

7.2.4 Deterministic Pipe Performance Models

7.2.4.1 General

Section 7.2.3 described the models used to calculate the probabilities that a corrosion defect will fail by rupture, large leak or small leak. It was shown in that discussion that calculation of these probabilities requires deterministic models defining the conditions leading to occurrence of the different failure modes. As mentioned in Section 7.2.3, three models are required:

1. pipe body failure model; and
2. small leak model for pipes that do not fail according to model 1.

This following sub-sections describe these models as implemented in PIRAMID.

7.2.4.2 Pipe Body Failure Model

7.2.4.2.1 Model Selection

The hoop stress at failure for a ductile pipe with a longitudinally oriented metal loss defect can be estimated using a semi-empirical model that was developed by Battelle (Kiefner 1969). Since its development, this model has been widely used as a basis for estimating the remaining strength of corroded pipe (ASME-B31G 1991). Although the basic format of the model has not changed, there have been attempts to redefine some of the input parameters in order to achieve better accuracy (*e.g.*, Kiefner and Vieth 1989, and Bubenik *et al.* 1992). The model used in PIRAMID was developed as an improvement over the original semi-empirical model. This model was developed by C-FER for a different study and was subsequently published by Brown *et al.* (1995).

The model was developed using a data set obtained from 69 burst tests carried out on corroded segments of pipe that have been removed from service (Kiefner and Vieth 1989). These data points are tabulated in Appendix E. There are reports of other burst test data for pipe with machined defects (*e.g.*, Kiefner *et al.* 1973 Shannon 1974 and Mok *et al.* 1990), however, these were not used in model development because machined defects do not represent the geometric randomness observed in actual defects.

Performance

The basic model employed calculates the pressure resistance of a pipe with a specific corrosion feature using an equation of the following general format (Shannon 1974 and ASME-B31G 1991):

$$r = \frac{2t}{d} s_f \left(\frac{1 - a/a_0}{1 - a/ma_0} \right) \qquad [7.14]$$

where r is the pressure resistance, t is the pipe wall thickness, s_f is the flow stress, d is the pipe diameter, a is the longitudinal area of the corrosion feature, a_0 is the original area before corrosion, and m is the Folias factor (Folias 1964).

Different implementations of this model have been suggested based on different definitions of the corroded area, flow stress, yield stress and Folias factor. Table 7.1 summarizes the definitions considered in developing the present model. In the table, 'parabolic area' refers to the assumption that the corroded area has a parabolic shape with a maximum depth equal to the maximum measured depth of the corrosion feature. The 'effective area' is defined as the corrosion area corresponding to the lowest pressure resistance of the values calculated by taking each possible subset of the corrosion length and treating the corresponding feature as if it were the total corrosion feature (Kiefner and Vieth 1989).

Different combinations of the parameter definitions in Table 7.1 were examined in order to select the set leading to the most accurate results. The approach used for this was to select one combination of parameter definitions, calculate the error ratio c of the measured to predicted pressure resistance for each data point, and then evaluate the mean and standard deviation of c for all data points. The mean value of c is an indication of model bias and the standard deviation is an indication of model scatter. An accurate model would have a mean of c close to 1.0 and standard deviation of c close to 0.0. The most accurate results corresponded to $s_f = 1.15\ s$ (where s is the yield strength), a = the total area calculated as hl (where h is the average defect depth and l is the axial defect length), and the Folias factor m given by the three-term relationship in Table 7.1. The final model obtained by substituting these values into Equation [7.14] is

$$r = \frac{2.3ts}{d} \left(\frac{1 - h/t}{1 - h/mt} \right) \qquad [7.15]$$

where m is given by the three-term relationship defined in Table 7.1.

The definition of the corroded area was found to be the most significant factor influencing model prediction accuracy. To demonstrate this, the mean and standard deviation of c obtained by using different definitions of the corroded area in Equation [7.14] are shown in Table 7.2. This shows that the parabolic area assumption used in ASME-B31G is more conservative and has a higher scatter than the effective area or total area methods. The table also shows that the total area and effective area methods give similar accuracy with the total area giving a lower bias but a slightly higher scatter. Calculation of the effective area requires a complete longitudinal profile

of the corrosion feature and some tedious calculations. The total area was therefore selected because it is much simpler to calculate and gives similar accuracy to the effective area method.

7.2.4.2.2 Model Uncertainty

Having selected the model in Equation [7.15], it is necessary to characterize the uncertainty associated with using it in estimating the pressure resistance of a given corroded pipe. This uncertainty, combined with the uncertainties associated with the input parameters determine the final uncertainty in pressure resistance. Model uncertainties arise from the limitations of model assumptions and idealizations. For example, Equation [7.15] does not take into account the corrosion shape or its circumferential extent.

A model uncertainty analysis was carried out for Equation [7.15] using the 69 burst test data points given in Appendix E. The approach used in this analysis was to treat the model error parameter, defined as the ratio between actual and calculated pressures as a random variable (C). The burst test data and corresponding model predictions were then used to calculate the value of C for the 69 data points. The resulting values were then analyzed statistically to determine the mean, standard deviation and distribution type of C. This analysis showed that C can be modelled by a normal distribution with a mean of 1.16 and a standard deviation of 0.191.

Adding the model error factor to Equation [7.15] gives

$$r = C\frac{2.3\ ts}{d}\left(\frac{1-h/t}{1-h/mt}\right) \qquad [7.16]$$

Figure 7.7a provides a comparison between the model in Equation [7.16] and the burst data used in developing it. The model falls in the middle of the data points thus providing a mean estimate of the resistance. The error bands in the figure correspond to one standard deviation of C on either side of the mean. They represent the degree of uncertainty associated with the model.

For comparison, a model uncertainty analysis was carried out on the ASME-B31G (1991) criterion. The results of this analysis are shown in Figure 7.7b. The figure shows that the B31G criterion is much more conservative and has a higher degree of uncertainty than the model used in this work.

7.2.4.2.3 Final Model for Resistance as Function of Time

In PIRAMID the resistance of the pipe at a given defect is calculated as a function of time to account for defect growth. In addition, all the input parameters (such as defect dimensions, growth rates and yield strength) are treated as random variables. (Recall that standard probability

notation calls for using upper case letters to denote random variables). Considering randomness and defect growth with time, defect depth and length can be expressed as:

$$H(\tau) = H_0 + \tau G_h \qquad [7.17a]$$

$$L(\tau) = L_0 + \tau G_l \qquad [7.17b]$$

where τ is time elapsed, $H(\tau)$ and $L(\tau)$ are the average defect depth and maximum axial defect length at time τ, H_0 and L_0 are the initial average defect depth and maximum axial length, and G_h and G_l are the growth rates for the average defect depth and maximum axial defect length. Substituting [7.17] into [7.16] leads to

$$R(\tau) = C\frac{2.3tS}{d}\left[\frac{1-(H_0+\tau G_h)/t}{1-(H_0+\tau G_h)/(M(\tau)t)}\right] \qquad [7.18a]$$

where d is the pipe diameter and t is the wall thickness. These two parameters are treated as deterministic because the uncertainties associated with them are very small compared to other parameters. M is the Folias factor given by

$$M(\tau) = \sqrt{1+0.6275\frac{(L_0+\tau G_l)^2}{dt} - 0.003375\frac{(L_0+\tau G_l)^4}{d^2t^2}} \quad \text{for} \quad \frac{(L_0+\tau G_l)^2}{dt} \le 50 \qquad [7.18b]$$

$$M(\tau) = 0.032\frac{(L_0+\tau G_l)^2}{dt} + 3.3 \quad \text{for} \quad \frac{(L_0+\tau G_l)^2}{dt} > 50 \qquad [7.18c]$$

Finally the failure condition in Equation [7.10] can be defined by subtracting the applied pressure, P, from the resistance defined in Equation [7.18a], leading to

$$g_1 = R(\tau) - P = C\frac{2.3tS}{d}\left[\frac{1-(H_0+\tau G_h)/t}{1-(H_0+\tau G_h)/(M(\tau)t)}\right] - P \qquad [7.19]$$

It is noted that the model represented by Equations [7.18] is also used in PIRAMID to define excavation and repair thresholds as discussed in Sections 5.4.4 and 5.4.5. It was favoured over the standard ASME-B31G criterion because, as shown in this section, it is more accurate and less conservative. This allows the user to build appropriate conservatism explicitly into the definition of repair thresholds. For example, if the user considers repairing all defects with a pressure resistance lower than 1.25 MAOP, then the resistance would be calculated accurately and an actual safety factor of 1.25 would be realized. This approach provides a realistic estimate of the degree of conservatism built into the repair criteria considered.

Performance

7.2.4.3 Small Leak Model

The small leak model is based on the assumption that a small leak occurs if the defect depth exceeds the pipe wall thickness before failure of the pipe body occurs. The condition corresponding to the defect depth exceeding the wall thickness can be written as

$$g_2 = t - (H_0 + \tau G_h) / c \qquad [7.20]$$

where t, H_0, τ, and G_h are as defined before and c is the maximum depth to average depth conversion factor in Equation [4.3]. Equation [7.20] is defined such that $g_3 < 0.0$ represents a small leak and $g_3 > 0.0$ represents no leak. It simply states that the leak will occur when the maximum defect depth has grown to a depth in excess of the pipe wall thickness.

7.2.5 Example Application

To demonstrate the model used to calculate the probability distribution of the Performance at Defect and the resulting outputs, an example calculation is presented. The example corresponds to a pipeline with a diameter of 914 mm, wall thickness of 8.75 mm and a maximum pressure of 7500 kPa. The specified minimum yield strength of the pipe steel was assumed to be 414 MPa. The probability distributions of the random input parameters used in the calculation are shown in Table 7.3. The corresponding probabilities of failure are plotted in Figures 7.8 and 7.9. Figure 7.8 shows the total probability of failure before a certain time elapses, whereas Figure 7.9 gives the annual probability of failure as a function of time.

The input parameter distributions were selected to give failure probabilities that are in the same order of magnitude as those observed from historical failure data. For example, the annual probability of failure at a randomly selected defect in the fifth year is 2.5×10^{-4}. The inputs were also selected to provide approximately the same relative frequency of small leaks, versus large leaks and ruptures. In the fifth year, the relative frequencies are 83% small leaks, 17% large leaks and ruptures, compared to the historical relative frequencies of approximately 85% and 15%, respectively. These results show that reasonable input parameters lead to results that are consistent with observations, this providing some evidence to the validity of the model.

Figures 7.8 and 7.9 may be used as decision making tools, without completing the consequence analysis part of the influence diagram. An operator may, for example, define a maximum allowable annual probability of failure due to corrosion. Figure 7.9 may then be used to determine the time at which this condition would be violated, thus defining the maximum allowable time interval to the next inspection.

Performance

7.3 Segment Performance

7.3.1 Node Parameter

The Segment Performance node and its direct predecessor node are highlighted in the version of the consequence analysis influence diagram shown in Figure 7.10. The specific node parameter is defined as the performance of the pipeline segment during the inspection interval. As discussed in Section 2.3, this node also requires information from two nodes in the corrosion analysis influence diagram, namely the probability of failure for a single defect from node 3.1 and the defect density from node 12.1.

The node parameter is a discrete random variable that can assume one of four possible values or states:

- safe;
- small leak;
- large leak; and
- rupture.

A small leak corresponds to a small hole and a slow product release rate that does not result in a significant hazard. A large leak, involving a hole of significant size, or a rupture are assumed to result in high release rates and the potential for significant hazard to people and property.

7.3.2 Calculation of Node Probability Distribution

Calculation of the probabilities of failure for the pipeline segment is based on the assumption that failures at different corrosion defects are independent events. This assumption implies that all the random variable affecting failure at a given defect (*e.g.*, yield strength, defect dimensions and growth rates) are independent from one defect to the next. This assumption is not strictly valid because some correlations between the values of such parameters can be expected. For example, correlations would exist between the yield strength values at corrosion defects located within the same pipe joint. In absence of sufficient information to characterize these correlations, the conservative assumption of independence was adopted.

Segment probability of failure due to corrosion can be calculated by multiplying the probability of failure at a single defect by the number of defects in the segment. Observing that the segment will consist of different defect sections, i, each potentially having a different corrosion defect density, ρ_i, the segment failure probability due to corrosion, pcs_j (where the subscript j represents the failure mode) can be calculated from

Performance

$$pcs_j = \sum_i pcd_{ij} \rho_i l_i \qquad [7.21]$$

where pcd_{ij} is the probability of failure in the j^{th} failure mode for a single defect in the i^{th} defect section, and l_i is the length of the i^{th} defect section. Equation [7.21] can be used to calculate both cumulative and annual probabilities of failure as a function of time, as well as the average annual probability of failure during the time period between inspections.

In order to solve the consequence analysis influence diagram, the probabilities of failure due to other causes must be added to the probabilities of failure due to corrosion at this node. This ensures that maintenance decisions are based on the total risk associated with the line segment, not just the risk due to corrosion. In order to achieve this, the node requires definition of the probabilities of failure due to other causes. The required information includes

- the failure rate per unit length.year, λ_k, for each major failure cause, k, other than corrosion; and
- the relative frequency q_{jk} of different failure modes, j, for each failure cause, k.

The total annual probability of failure for the segment, ps_j, for each cause j can be calculated using

$$ps_j = pcs_j + l \sum_k \lambda_k q_{jk} \qquad [7.22]$$

where pcs_j is the average annual probability of failure mode j for the segment due to corrosion and l is the total length of the segment. Equation [7.22] assumes that failure rates due to all causes other than corrosion are uniform along the segment. The probability of safe performance for the segment can be calculated by subtracting the total segment failure probabilities due to all causes from 1.

It is noted that estimating the total annual probability of failure as the failure rate times the segment length is a valid approximation provided that the annual probability of more than one failure on the line segment is small (*i.e.*, less than 0.1).This condition is satisfied if the total failure probability from Equation [7.22] is less than 0.5. If this condition can is not satisfied the pipeline can be analyzed in smaller segments.

7.3.3 Failure Rate Estimates for Other Causes

A review of historical pipeline failure rates was carried out as part of another project within the PIRAMID development program (PIRAMID Technical Reference Manual No. 4.1 - Stephens 1996). This review produced baseline failure rates representing natural gas and hydrocarbon liquids pipelines that are considered to be average with respect to construction, operation and

maintenance practices. These rates are given in Table 7.4 and are included in the program as default failure probabilities that can be used in the absence of more line-specific data.

Note that it is not necessary to define the failure rates by failure cause as indicated in Table 7.4, since only the total failure rate per failure mode is used in the calculation. The input format in Table 7.4 is selected because it was believed that it is easier to define the relative frequency of different failure modes separately for different failure causes. An equivalent input would consist of the total failure rate due to all causes other than corrosion and the corresponding relative frequencies of different failure modes, defined in any row of Table 7.4, with zero inputs in all other rows.

Figures and Tables

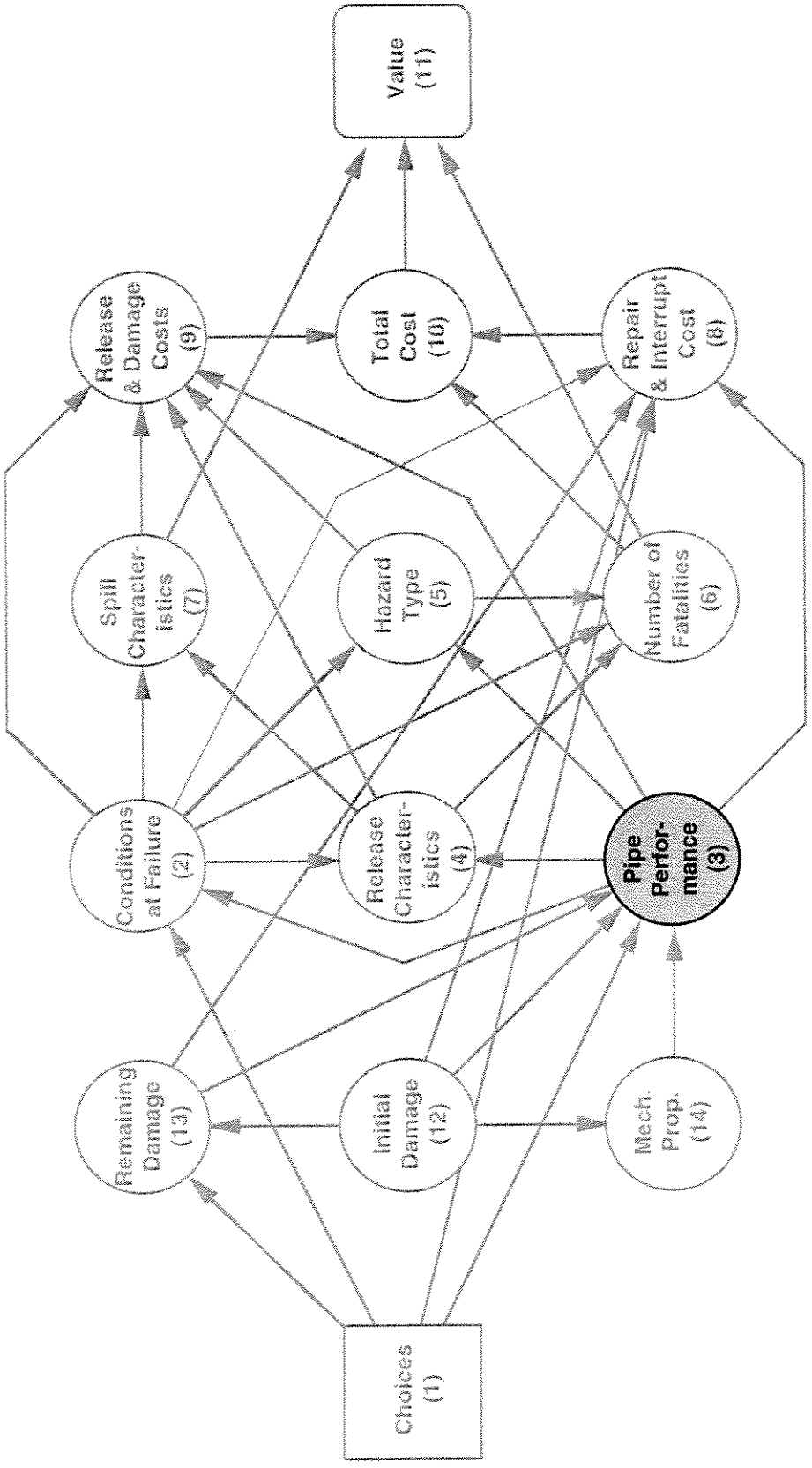

Figure 7.1 Compound node influence diagram highlighting Pipe Performance node group

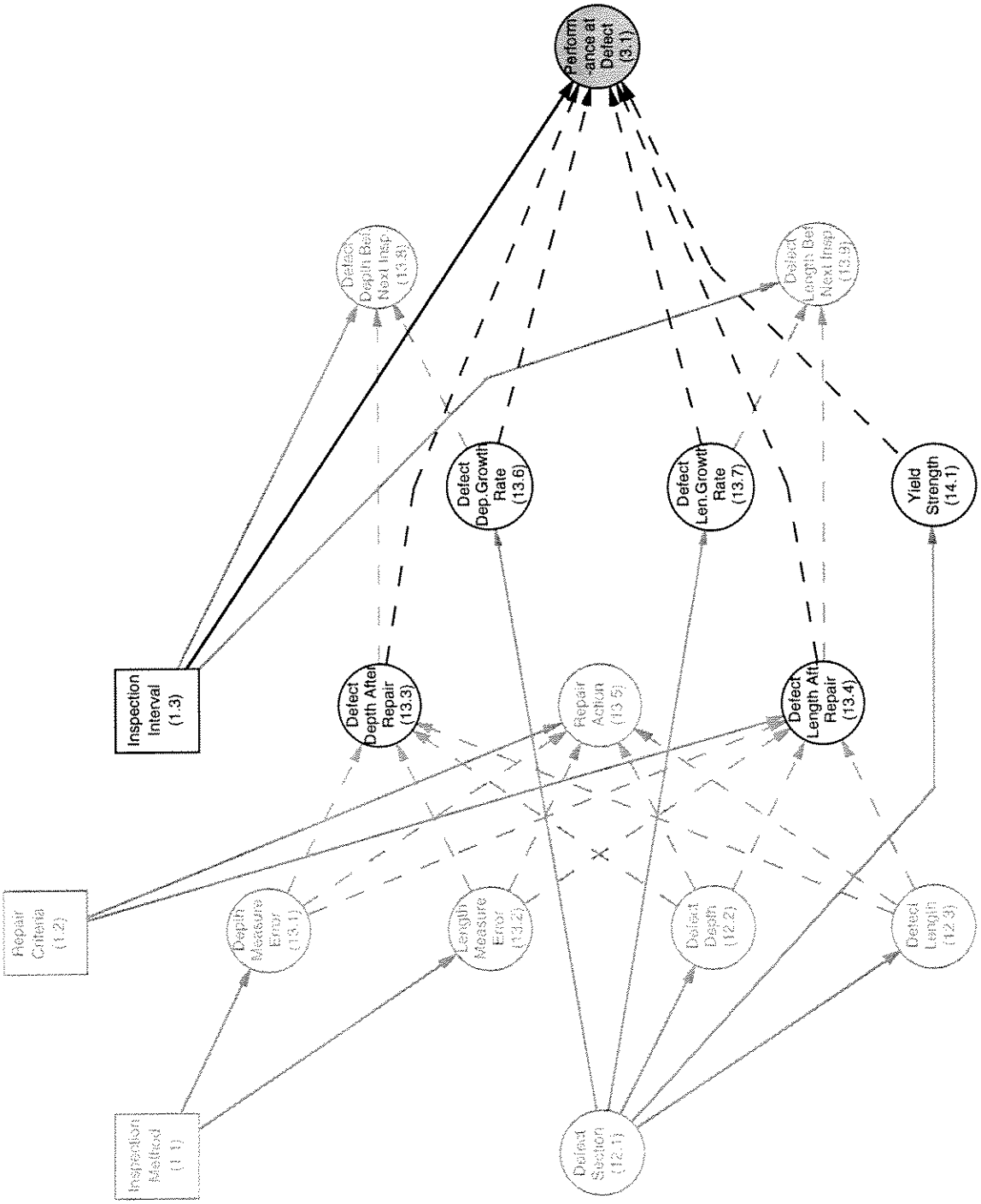

Figure 7.2 Basic node corrosion influence diagram highlighting Pipe Performance node and associated immediate predecessor nodes

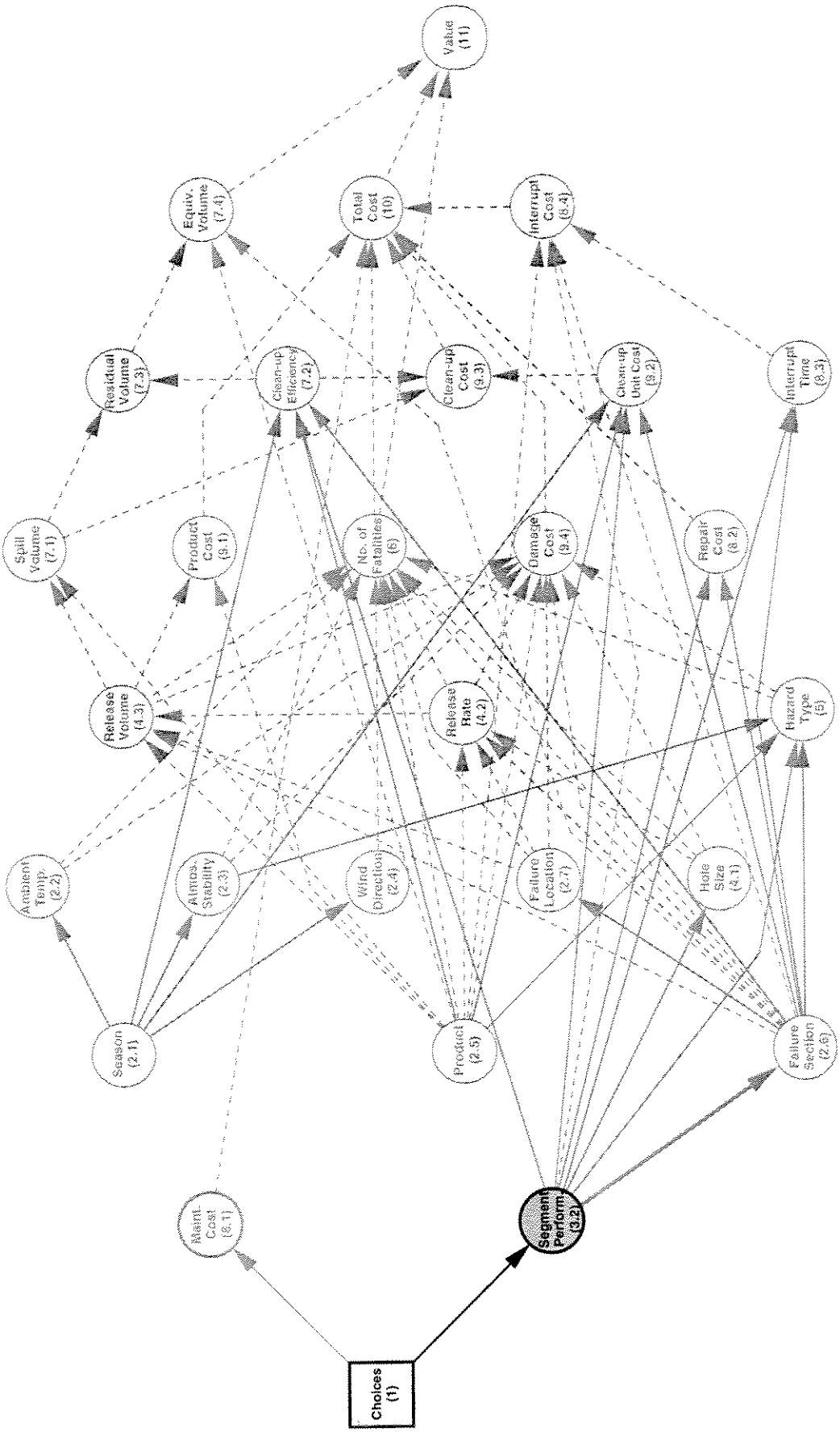

Figure 7.3 Basic node consequence influence diagram highlighting Segment Performance node and associated immediate predecessor node

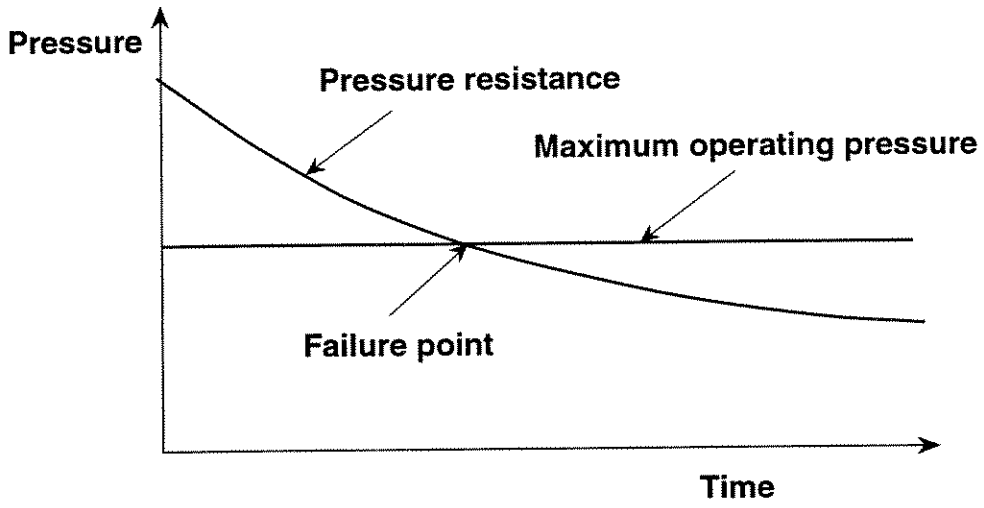

Figure 7.4 Illustration of the failure condition for failures caused by corrosion damage

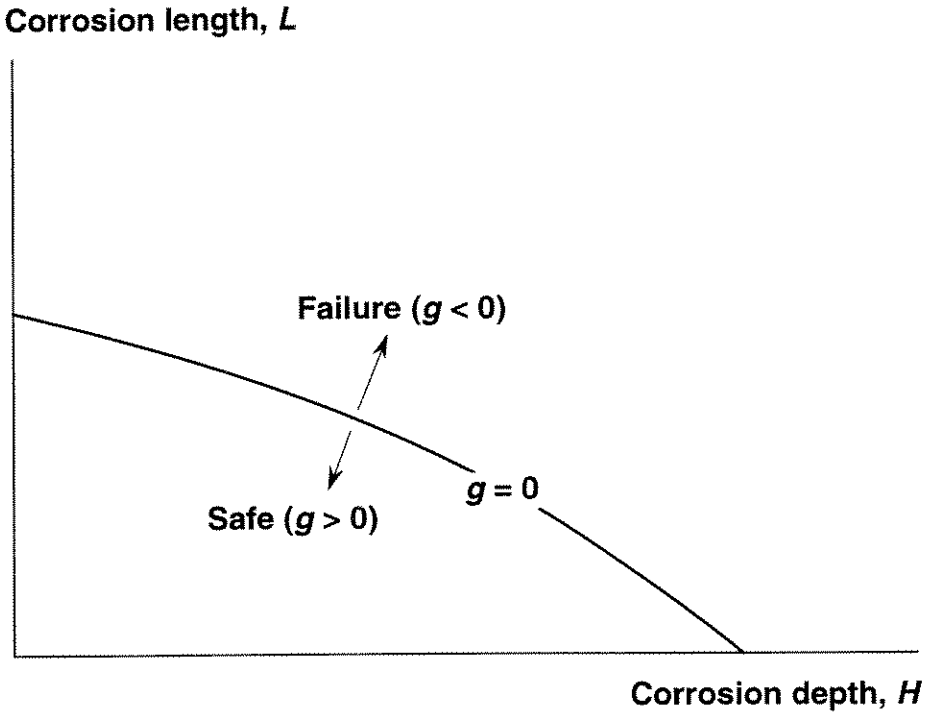

Figure 7.5 Illustration of the calculation of the failure probability

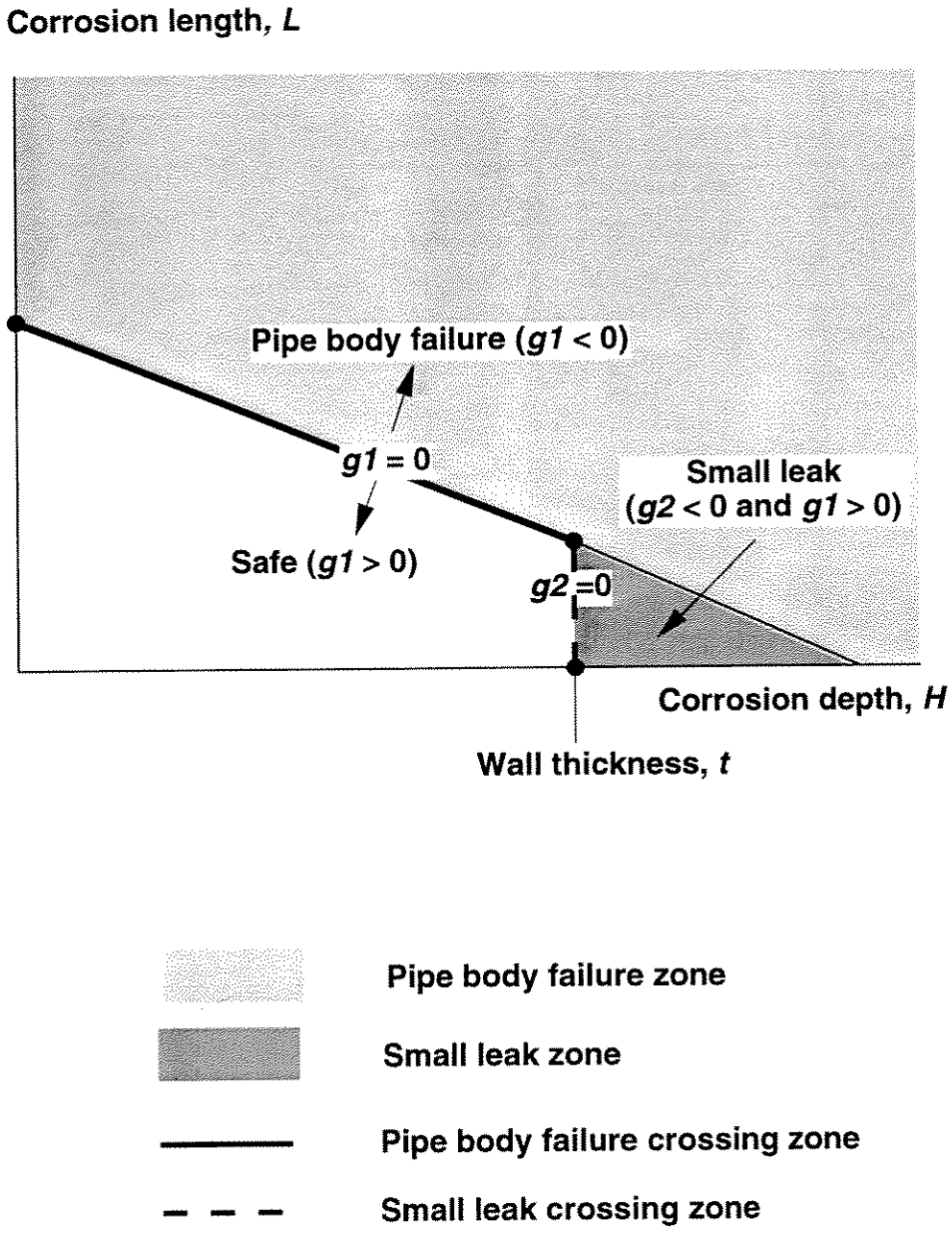

Figure 7.6 Illustration of the calculation of Failures and Small leaks

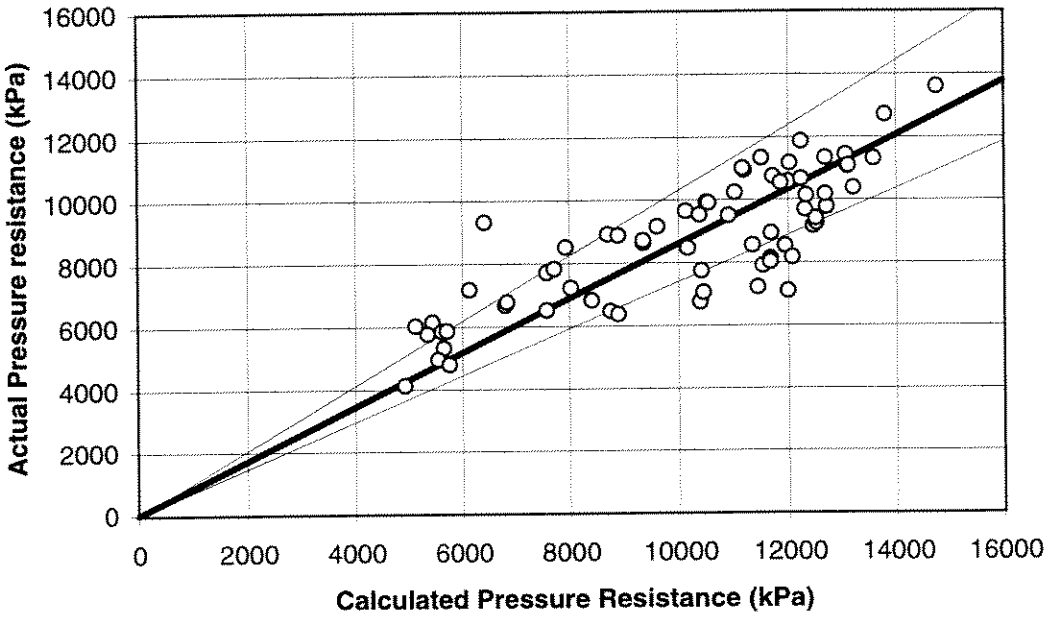

a) Model Used in PIRAMID

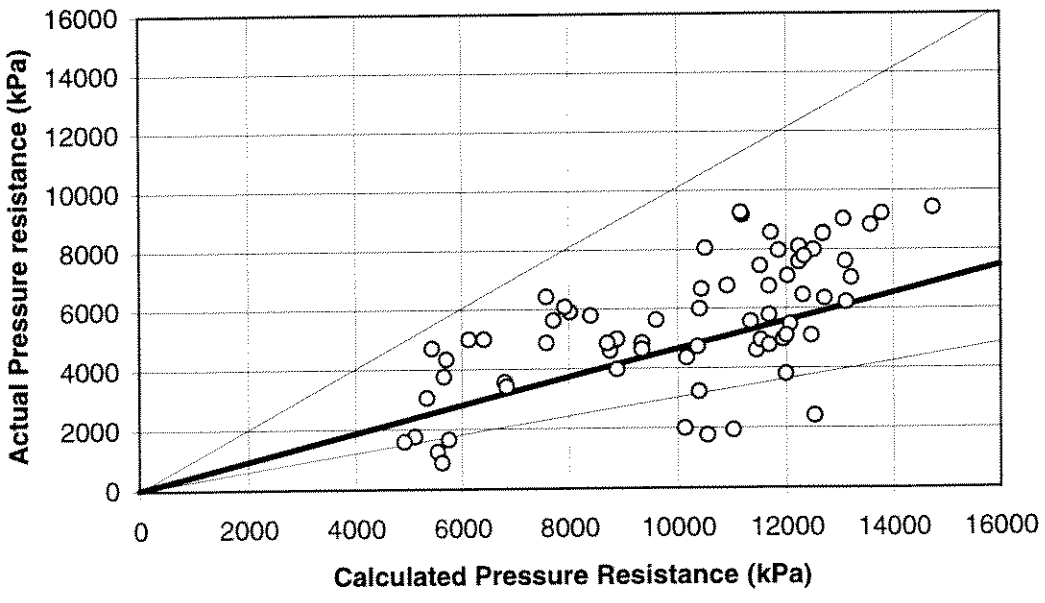

b) ASME-B31G criterion

Figure 7.7 Comparison between actual and calculated pressure resistance of corroded pipe

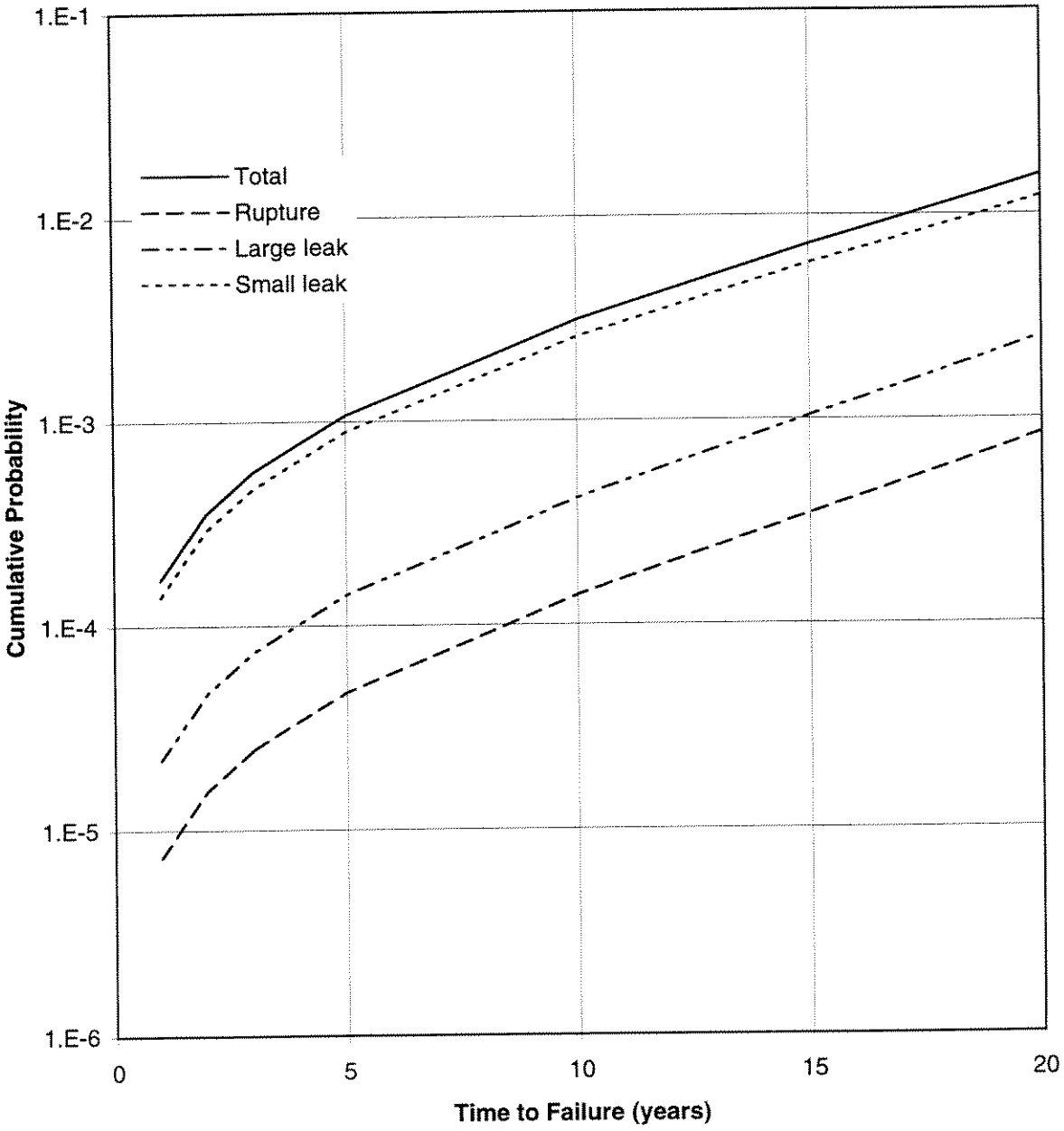

Figure 7.8 Cumulative probability distribution of the time to failure

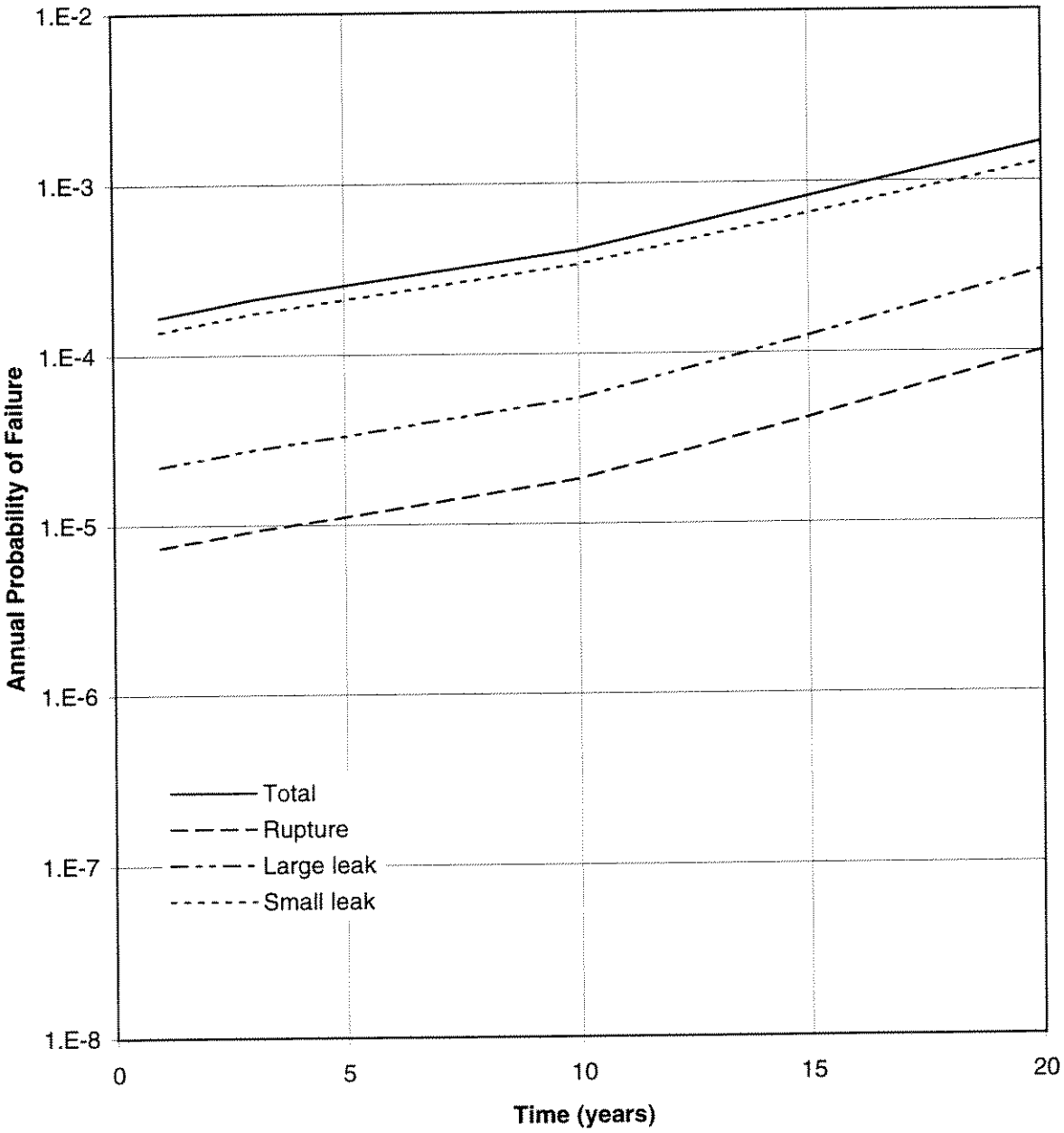

Figure 7.9 Annual probability of failure as a function of time

Yield Stress (s)	Flow Stress (s_f)	Corroded Area (a)	Folias Factor (m)
• Stress at 0.5% Strain • Specified Minimum Yield Strength	• $s_f = cs$ where c = 1.0 to 1.25 • $s_f = s + c$ where c = 0 to 20 ksi	• Total area $a = hl$ [1,2] • Parabolic area $a = 2/3\ h_{max}\ l$ [3] • a = Effective Area	• Three term[4] • Two term[5]

(1) h = average depth of corrosion feature

(2) l = total axial length of corrosion feature

(3) h_{max} = maximum depth of corroded feature

(4) $$m = \sqrt{1 + 0.6275\frac{l^2}{dt} - 0.003375\frac{l^4}{d^2t^2}} \quad \text{for} \quad \frac{l^2}{dt} \leq 50$$

$$m = 0.032\frac{l^2}{dt} + 3.3 \quad \text{for} \quad \frac{l^2}{dt} > 50$$

where l is the axial length of the corrosion feature, d is the pipe diameter and t is the pipe wall thickness (Kiefner and Veith 1989).

(5) $$m = \sqrt{1 + \frac{0.8l^2}{dt}}$$

where l, d and t are as defined in (4).

Table 7.1 Different definitions of the input parameters attempted in Equation [2.1]

No.	Definition of Area	Mean of c	Standard Deviation of c
1	Total area	1.16	0.191
	Effective area	1.20	0.189
	Parabolic assumption	1.29	0.312

Table 7.2 Effect of the definition of corroded area on model error parameter c.

Parameter	Distribution Type	Mean	Coefficient of Variation
Depth	Lognormal	1.8 (mm)	0.45
Maximum Length	Lognormal	60 (mm)	0.2
Depth Growth Rate	Normal	0.1 (mm)	0.5
Length Growth Rate	Normal	2 (mm)	0.5
Yield Strength	Lognormal	455.4 (MPa)	0.035

Table 7.3 Probability distributions of the corrosion parameters used in the example in Section 7.2.5

Failure Cause		Failure Rate (incidents/km yr)	Failure Mode		
			Small Leak	Large Leak	Rupture
Outside Force	mechanical damage	3.0×10^{-4}	25 %	50 %	25 %
	ground movement	3.0×10^{-5}	20 %	40 %	40 %
Crack-like Defects	environmentally induced	2.0×10^{-5}	60 %	30 %	10 %
	mechanically induced	1.0×10^{-4}	60 %	30 %	10 %
Other Causes		2.0×10^{-4}	80 %	10 %	10 %

Table 7.4 Average pipeline failure rates by cause and failure mode

8.0 CONDITIONS AT FAILURE

8.1 Overview

The Conditions at Failure node group (group 2) is highlighted in the version of the compound node influence diagram in Figure 8.1. This node group includes parameters describing the conditions associated with a possible failure of the pipeline, including weather conditions (*i.e.*, season, ambient temperature, atmospheric stability and wind direction) and product in the line for the pipeline section at which the failure occurs, and the specific failure location within that section.

Nodes within this group belong to the consequence analysis portion of the influence diagram and were therefore discussed in detail in PIRAMID Technical Reference Manual No. 3.2 (Stephens *et al.* 1996). The node group is included in the present document because one of its nodes, namely node 2.6 representing the Failure Section, was modified as a consequence of incorporating the corrosion analysis portion of the influence diagram. This node is discussed in detail in Section 8.2.

8.2 Failure Section

The Failure Section node (node 2.6) and its direct predecessor node are highlighted in the version of the basic node consequence analysis influence diagram shown in Figure 8.2. The node parameter represents the pipeline section containing the failure location. It is noted that pipeline sections for this node correspond to lengths of the pipeline for which *the line attributes affecting failure consequences* are uniform (see PIRAMID Technical Reference Manual No. 3.2 for a detailed listing of these attributes). The sections corresponding to this node are therefore different than those corresponding to the Defect Section node for which sectioning is based on the attributes affecting failure probability due to corrosion. Some line attributes affect both probabilities and consequences and are therefore included in the sectioning criteria for both the Defect Section and Failure Section nodes. As shown in Table 4.1, these common attributes are wall thickness, operating pressure and operating temperature. Attributes that affect probability but not consequences include line age and soil corrosivity for instance, whereas examples of attributes that affect consequences but not probabilities are pipeline diameter and orientation.

It would have been possible to combine the Defect Section and Failure Section nodes into one node for which the individual sections are uniform with respect to all attribute parameters. This approach is simpler than the one adopted in PIRAMID, however it is not as computationally efficient. Figure 8.3 illustrates the difference between the two approaches. The figure shows a pipeline that has 3 Defect Sections (*i.e.*, sections with uniform probability-related attributes) and 4 Failure Sections (*i.e.*, sections with uniform consequence-related attributes). The approach adopted in PIRAMID requires the probability analysis to be carried out for the 3 Defect Sections

and the consequence analysis to be carried out for the 4 Failure Sections. If the pipeline were divided into uniform sections with respect to all attributes combined, it would have 6 different sections, requiring both probability and consequence analyses to be carried out 6 times.

An arrow was added to the consequence analysis influence diagram to account for conditional dependence of the Failure Section on Pipe Performance. This dependence means that the probability of a failure event occurring on a specific section of the line depends on whether the failure occurs by rupture, large leak or small leak. The reason for this new relationship is that, in this version of the program, the probabilities of different failure modes are calculated from the corrosion attributes corresponding to each individual section, and therefore the relative probabilities of small leak, large leak and rupture will vary from section to section. Since the probability of a given failure mode depends on the section, it follows that the probability of a specific section given failure depends on the failure mode.

The probabilities associated with this node can be calculated using Bayes' theorem which, in the context of the present problem, states that the probability of a specific section, i, given failure is proportional to the probability of failure occurring on that section

$$p(Sec_i|f_j)\,\alpha\, p(f_j|Sec_i) \qquad [8.1]$$

where j indicates a specific failure mode. The probability of failure given a specific Failure Section can be calculated as the sum of the probabilities of failure of all defects within that section. This leads to (refer to Figure 8.3):

$$p(f_j \mid Sec_i) = \sum pd_{jk}\ \rho_k\ l_{ik} \qquad [8.2]$$

where pd_{jk} is the probability of failure mode j for a randomly selected defect on Defect Section k, ρ_k is the density of defects on Defect Segment k, and l_{ik} is the length of the portion of Defect Section k that overlaps Failure Section l. The summation in Equation [8.2] is for all Defect Sections overlapping the Failure Section being considered. Once Equation [8.2] is evaluated for all Failure Sections, the probability distribution of the Failure Section can be calculated by using Equation [8.1] and normalizing the probabilities of all sections to add up to 1. This leads to

$$p(Sec_i \mid f_j) = \frac{p(f_j \mid Sec_i)}{\sum_i p(f_j \mid Sec_i)} \qquad [8.3]$$

Figures

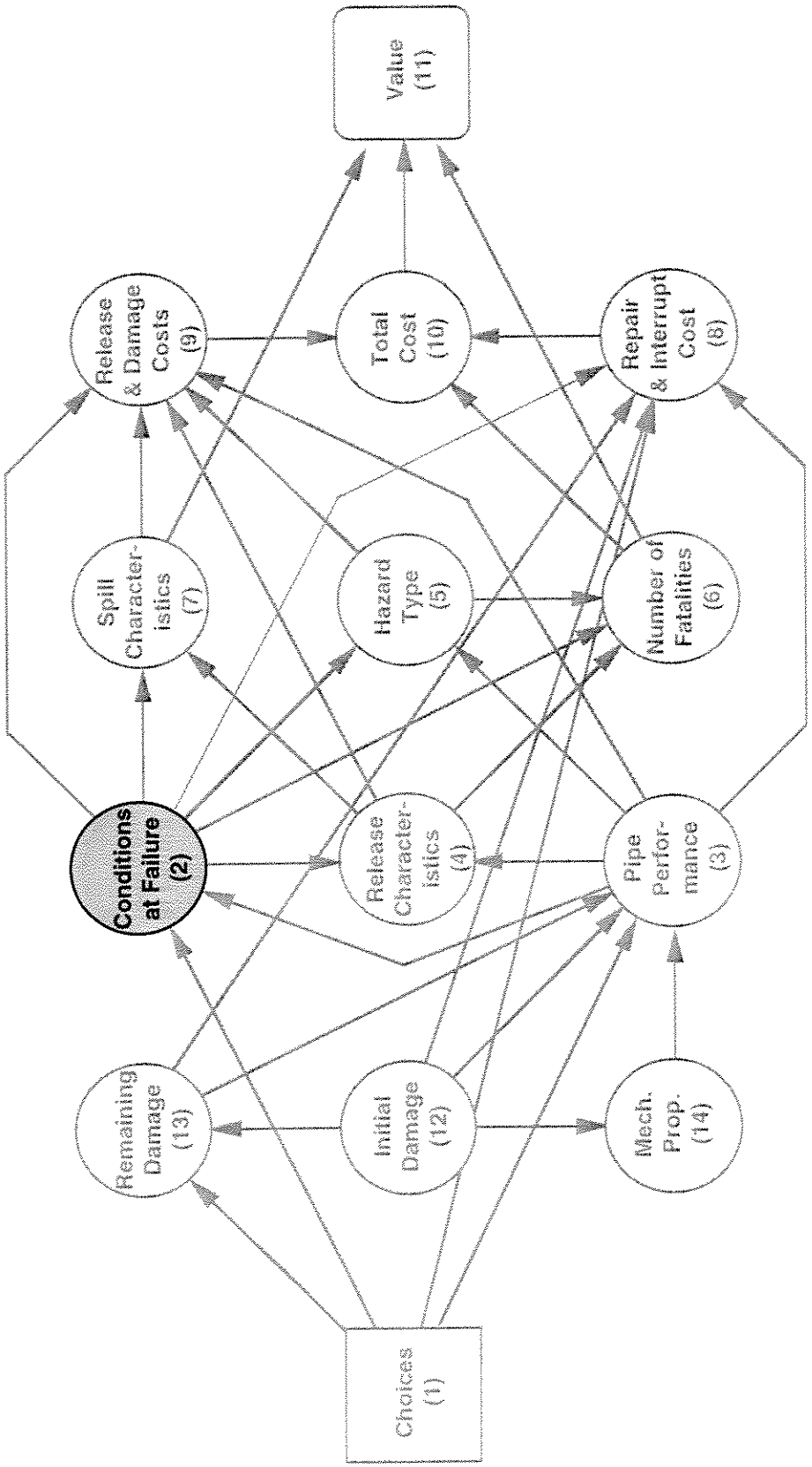

Figure 8.1 Compound node influence diagram highlighting Conditions at Failure node group

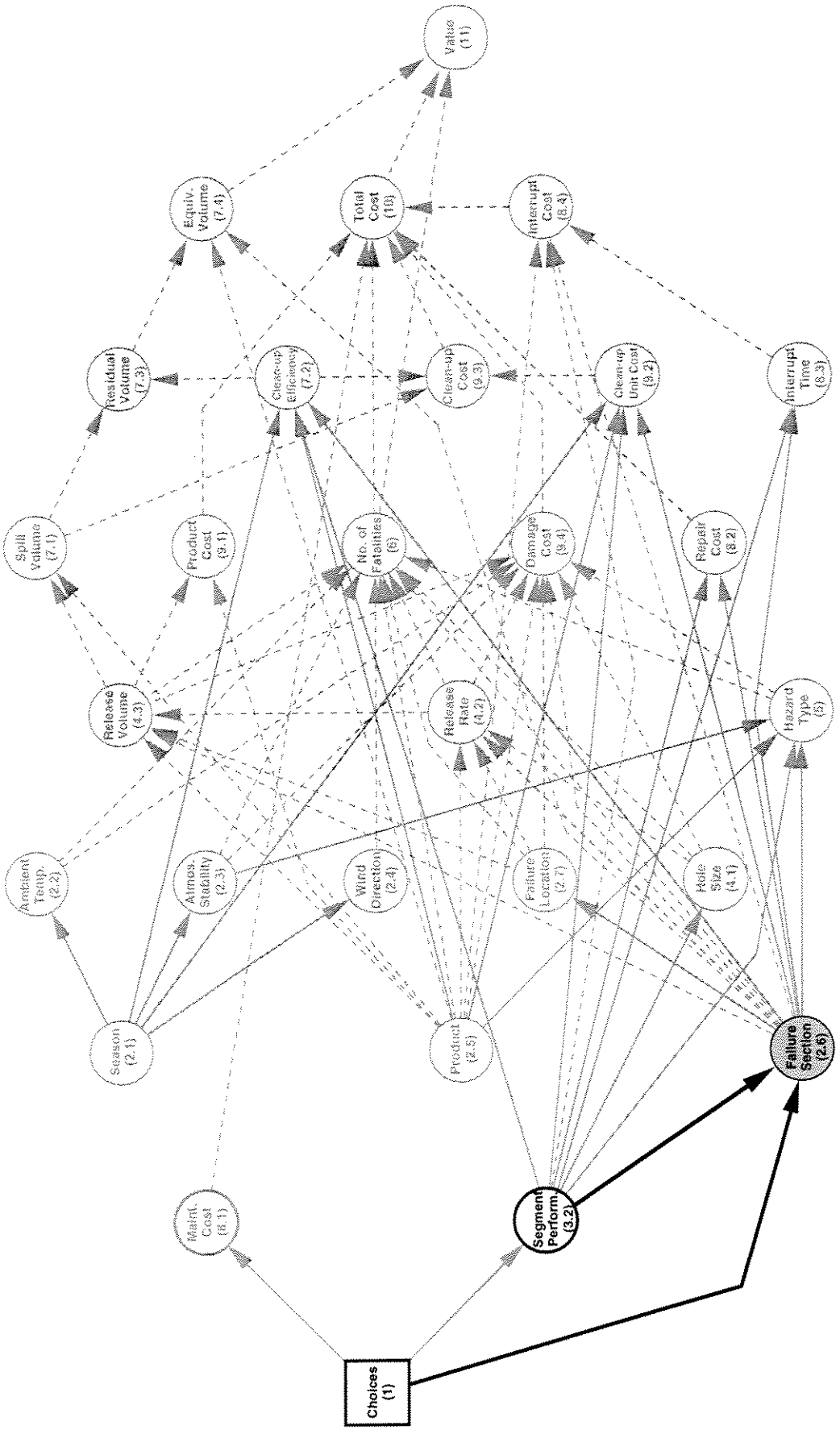

Figure 8.2 Basic node consequence influence diagram highlighting Failure Section node and its immediate predecessor nodes

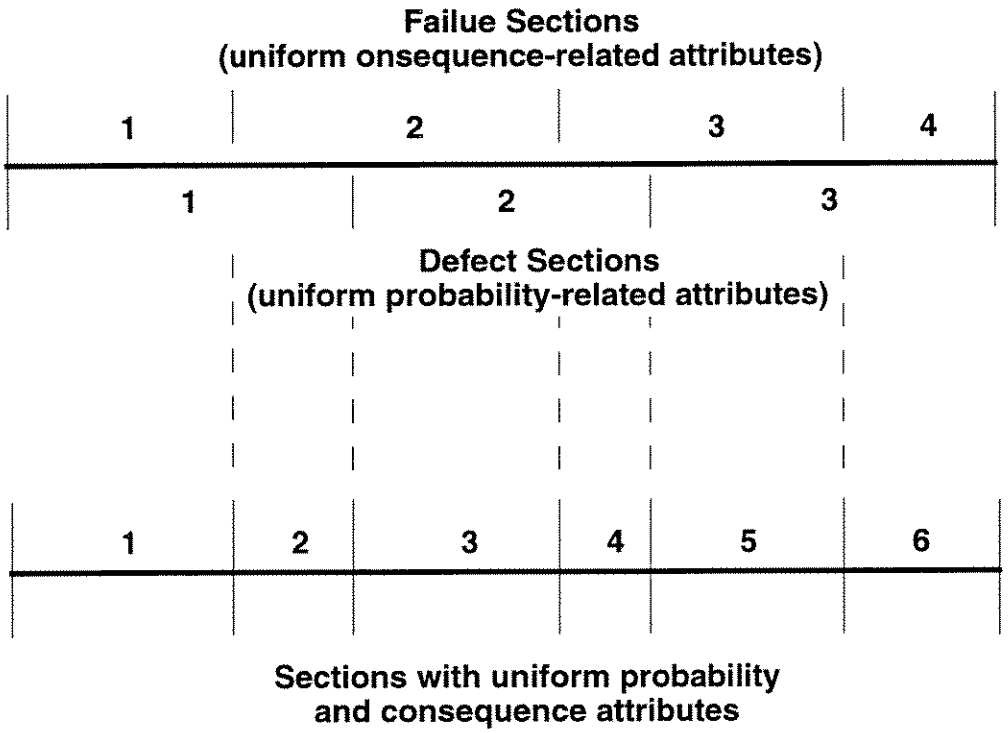

Figure 8.3 Illustration of pipeline segmentation with respect to probability-related and consequence-related attributes

9.0 REPAIR AND INTERRUPTION COST

9.1 Overview

The Repair and Interruption Cost node group (group 8) is highlighted in the version of the compound node influence diagram in Figure 9.1. This node group includes parameters describing the maintenance cost, failure repair cost, interruption time, and interruption cost. Nodes within this group belong to the consequence analysis portion of the influence diagram and were therefore discussed in detail in PIRAMID Technical Reference Manual No. 3.2 (Stephens *et al.* 1996). The node group is included in the present document because one of its nodes, namely node 8.1 representing the Maintenance Cost, was modified as a consequence of incorporating the corrosion analysis portion of the influence diagram. This node is discussed in detail in Section 9.2.

9.2 Maintenance Cost

The Maintenance Cost node (node 8.1) and its direct predecessor node are highlighted in the version of the basic node consequence analysis influence diagram shown in Figure 9.2. The node parameter represents the total annual maintenance cost for the whole pipeline segment in present value currency. As discussed in Section 2.3, this node requires information from two nodes in the corrosion analysis influence diagram, namely the probabilities of defect excavation and defect repair from node 13.5 titled Repair Action, and the defect density from node 12.1 titled Defect Section.

The calculation procedure for this node has been updated in PIRAMID Corrosion because the corrosion analysis portion of the influence diagram produces information that can be used to calculate the maintenance cost. This information includes the probability of excavating and repairing a randomly selected defect, which can be used in combination with the number of defects and the unit repair and excavation costs to calculate the total maintenance cost. Note that repair costs in this node refer to corrosion defect repairs, which are considered to be part of the maintenance cost. They should not be confused with failure repair costs which are defined as part of the Repair Cost node (node 8.2).

The total maintenance cost CM_t can be calculated from

$$CM_t = CI + \sum_i ce_i\, ne_i + \sum_i cr_i\, nr_i \qquad [9.1]$$

where

CI is the total inspection cost.

Repair and Interruption Cost

ce_i is the cost of excavation at a single location within section i of the pipeline, assuming that repair at that location will not be required. This situation occurs if in situ measurement of the defect size after excavation shows that the repair is smaller than estimated by the inspection tool and therefore pipe repair is not necessary. It is assumed however, that the pipe will be cleaned and re-coated to ensure that further defect growth does not occur. The costs associated with these activities are included in the value of ce_i. The excavation cost is defined as a function of the pipe section because it depends on such parameters as pipe diameter, accessibility of location and terrain/crossing type.

ne_i is the total number of excavations.

cr_i is the cost of repairing the pipeline at a single location within section i of the pipeline. This includes only the cost associated with pipe body repairs (*e.g.*, cut-out replacement or sleeve repair), since all other costs associated with excavation, cleaning and re-coating are included in ce_i. The repair cost is defined as a function of section because it depends on such parameters as pipe diameter, accessibility of location and terrain type (including crossings).

nr_i is the total number of repairs.

The number of repairs nr_i is given by

$$nr_i = l_i \, \rho_{ai} \, pr_i \qquad [9.2]$$

where

l_i is the length of the section.

ρ_{ai} is the actual density of corrosion defects.

pr_i is the probability that a defect will require excavation and repair. This probability is obtained directly from the Repair Action node (13.5).

The number of excavations is given by

$$ne_i = l_i \delta_{di} \, re_i \qquad [9.3a]$$

for the case of coating damage surveys, and by

$$ne_i = l_i \rho_{di} (pe_i + pr_i) \qquad [9.3b]$$

for the case of in-line inspection, where

δ_{di} is the detected (measured) density of coating damage. This is related to the actual density by an Equation analogous to Equation [4.1].

re_i is the ratio of coating damage defects that are to be excavated as defined by the user.

Repair and Interruption Cost

ρ_{di} is the detected (measured) density of corrosion defects. This can be calculated from the actual defects using Equation [4.1].

pe_i is the probability that a defect within section i will require excavation but will be found not to require pipe repair based on in situ measurement of its size. This probability is obtained directly from the Repair Action node (node 13.5).

The total cost of a given maintenance event must be evaluated in light of the interval to next inspection in order to create a fair basis for comparison between different possibilities. For example, an expenditure of $2 million for a maintenance event that has an associated interval of 10 years is likely to be more attractive than an expenditure of $1 million for a maintenance event that has an associated interval of 3 years. To account for this, the total maintenance cost is annualized by treating it as a loan that is amortized over the inspection interval. Based on this, the annual maintenance cost CM_a can be calculated from

$$CM_a = \frac{CM_t\, r}{[1-(1+r)^{\tau}]} \qquad [9.4]$$

where r is the real interest rate, defined as the actual interest rate less the inflation rate, and τ is the inspection interval.

Figures

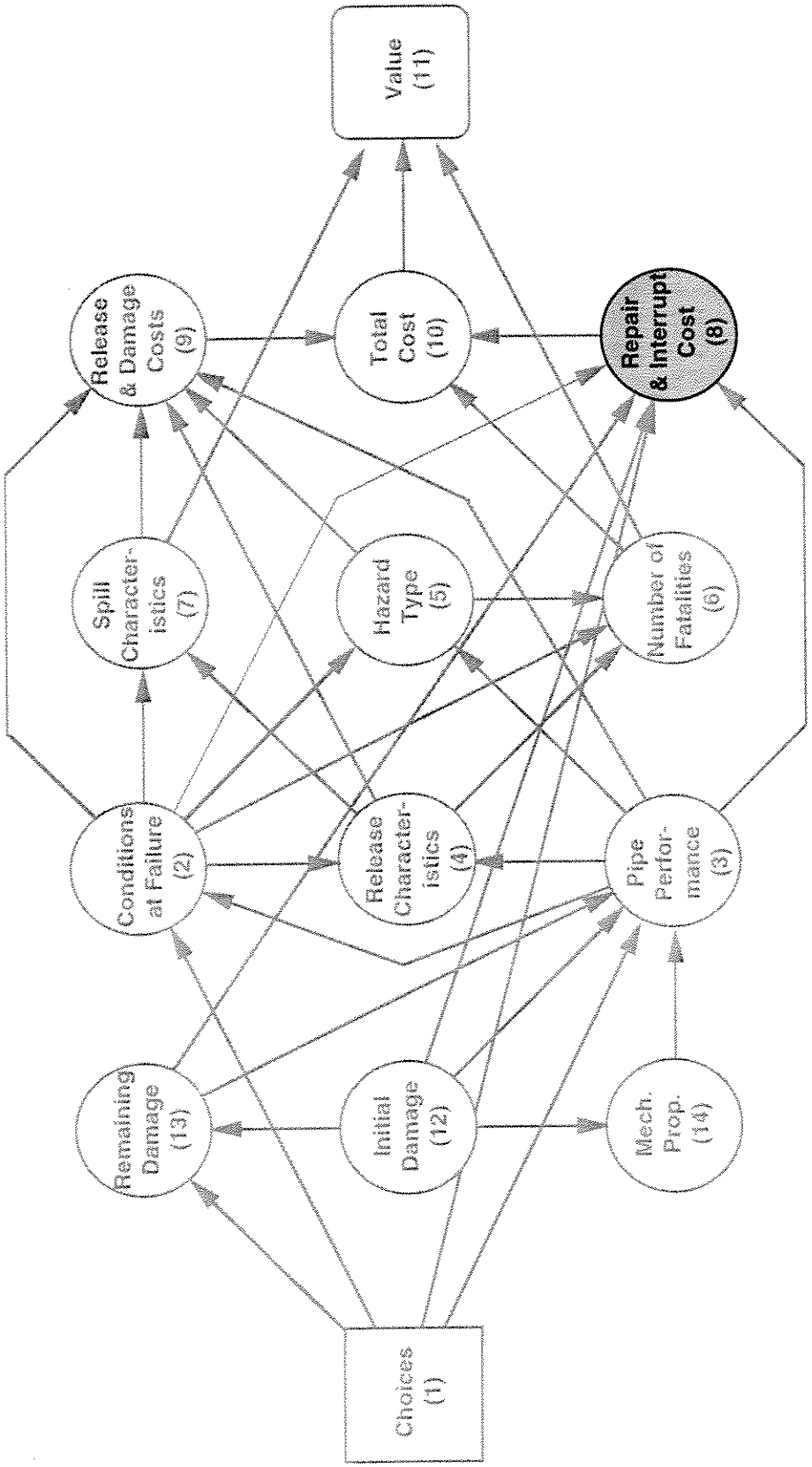

Figure 9.1 Compound node influence diagram highlighting Repair and Interruption Costs node group

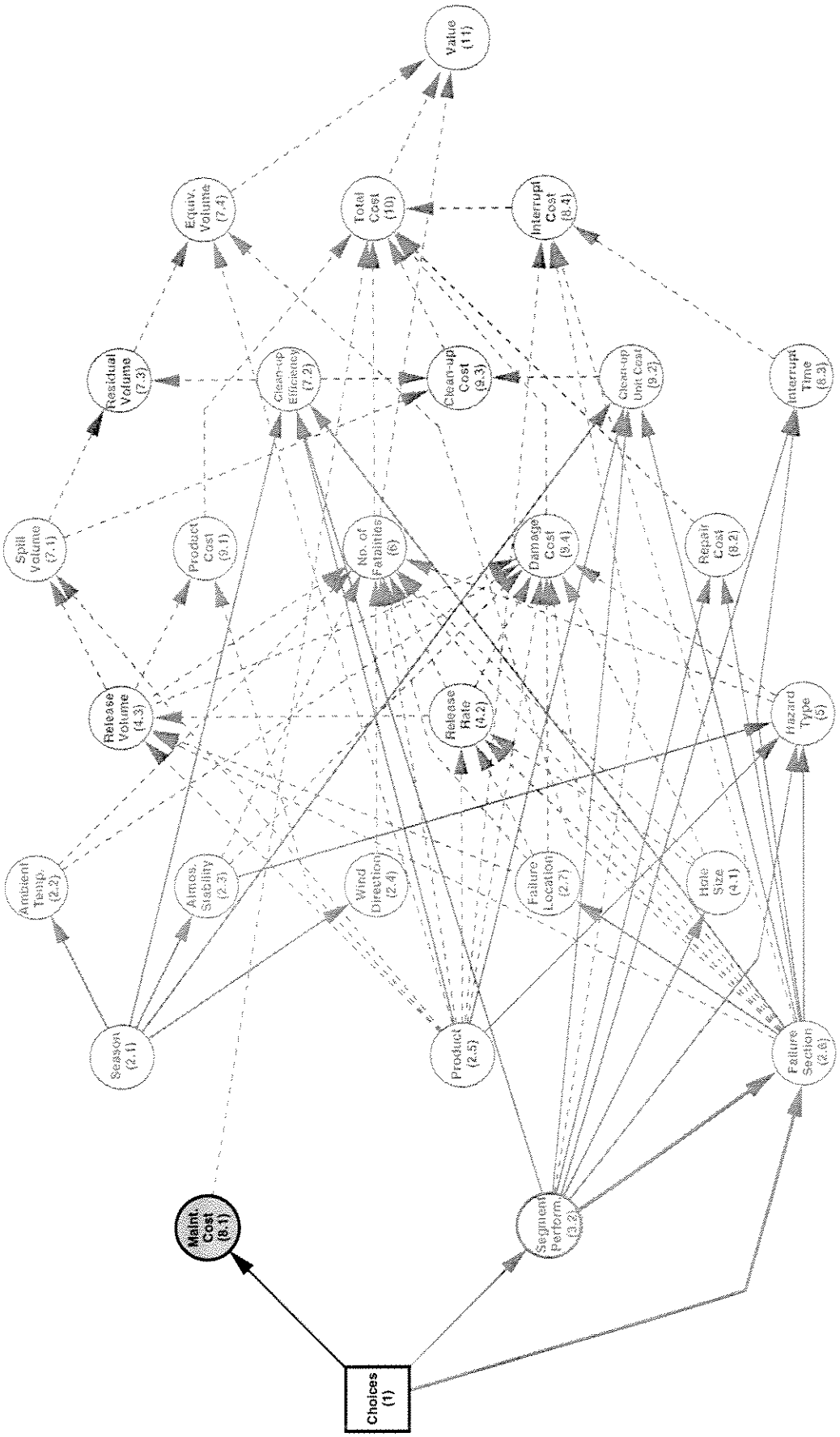

Figure 9.2 Basic node consequence influence diagram highlighting Maintenance Cost node and its immediate predecessor node

10.0 VALUE

The Value node (node 11) and its direct predecessor nodes are highlighted in the versions of the influence diagram shown in Figures 10.1 and 10.2. The value node defines the criterion used to evaluate maintenance choices taking into account the safety, environmental protection and financial objectives of the decision-maker. Depending on the preferences of the user, the specific parameter of the node is either the utility or the total cost. For the utility option, value is defined as a function of the number of fatalities, the equivalent spill volume and the total cost, which are the three parameters measuring human safety, environmental protection and financial objectives. The utility function is defined as an all-inclusive criterion for ranking different combinations of these three parameters, taking into account the decision-maker's attitudes toward risk and tradeoffs between life safety, environmental impact and costs. The purpose of the influence diagram in this case is to maximize the expected utility.

For the total cost option, the node parameter is defined as the total cost. In this case, the influence diagram is used to identify the minimum cost choice subject to user-defined constraints regarding the maximum allowable levels of safety and environmental risks. Details of the inputs and calculations associated with this node are given in PIRAMID Technical Reference Manual No. 3.2 (Stephens *et al.* 1996). That document describes value optimization for a single choice node that includes a set of discrete options.

For the corrosion maintenance problem there are three choice nodes, namely inspection method, repair criterion, and inspection interval. The repair criterion and inspection interval choices derive from continuous parameters. To ensure clarity of presentation of the output, special output formats have been developed for the value node in the corrosion maintenance optimization module. Figure 10.3 shows the utility output format. In this format, one plot is presented for each inspection method considered, and for the "no inspection" option as well. Each plot gives the utility as a function of time for the different repair criteria considered. The optimal combination of repair criterion and inspection interval for a given inspection method is the combination associated with the highest expected utility as shown in Figure 10.3. The optimal inspection method can be identified as the one that has the highest value among the maximum expected utility values for the different inspection methods. It is noted that for the "no inspection" option, there will be no repair and therefore the utility plot will include only one curve showing the expected utility as a function of the inspection interval.

Figure 10.4 shows the output format for the constrained cost optimization method (based on a life safety constraint). For each inspection method the expected cost is given as a function of the individual risk for different combinations of repair criterion and inspection interval. Each curve in the figure corresponds to a given repair criterion and the inspection intervals considered are marked on each curve. The optimal combination of repair criterion and inspection interval for a given inspection method is the lowest cost combination that meets the constraint (see Figure 10.4). The optimal inspection method can be identified as the one that has the lowest value among the minimum expected cost values for the different inspection methods. Similar to

Value

the utility case, the plot associated with the "no inspection" option will only one curve because repair criteria are not relevant unless the pipeline is inspected. It is noted, that similar outputs are also available for cost optimization with environmental constraints.

Figures

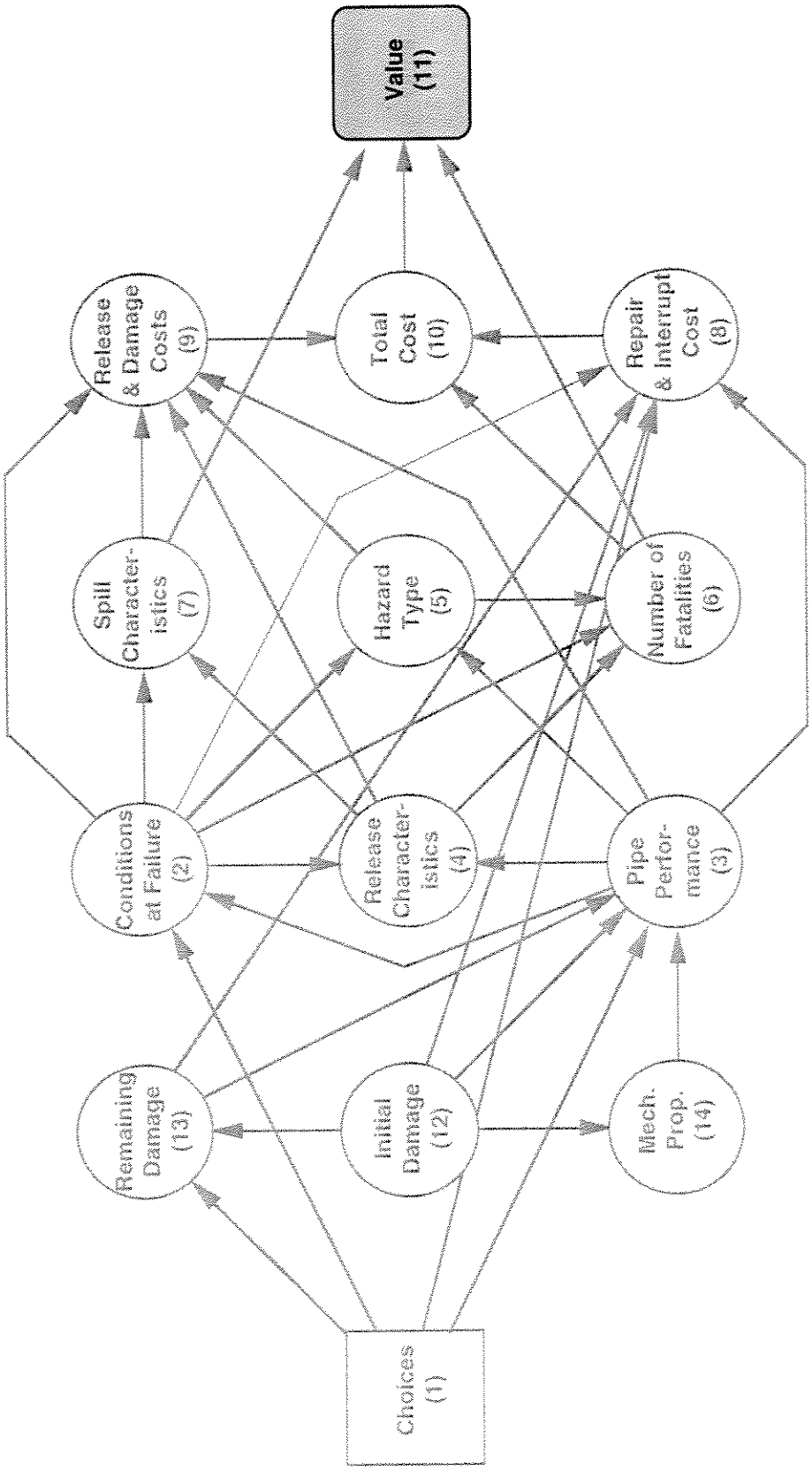

Figure 10.1 Compound node influence diagram highlighting Value node group

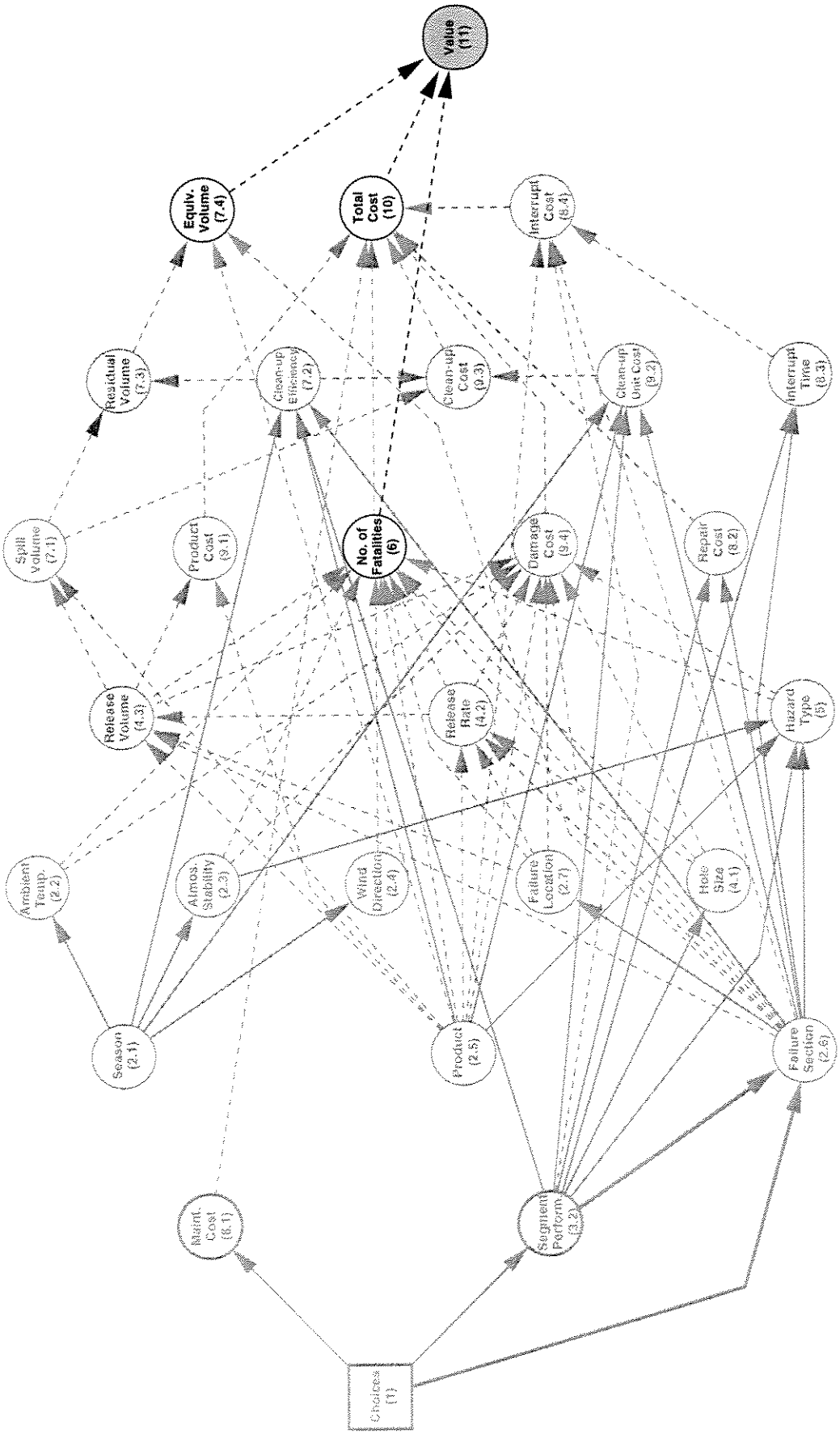

Figure 10.2 Basic node consequence influence diagram highlighting Value node and associated immediate predecessor nodes

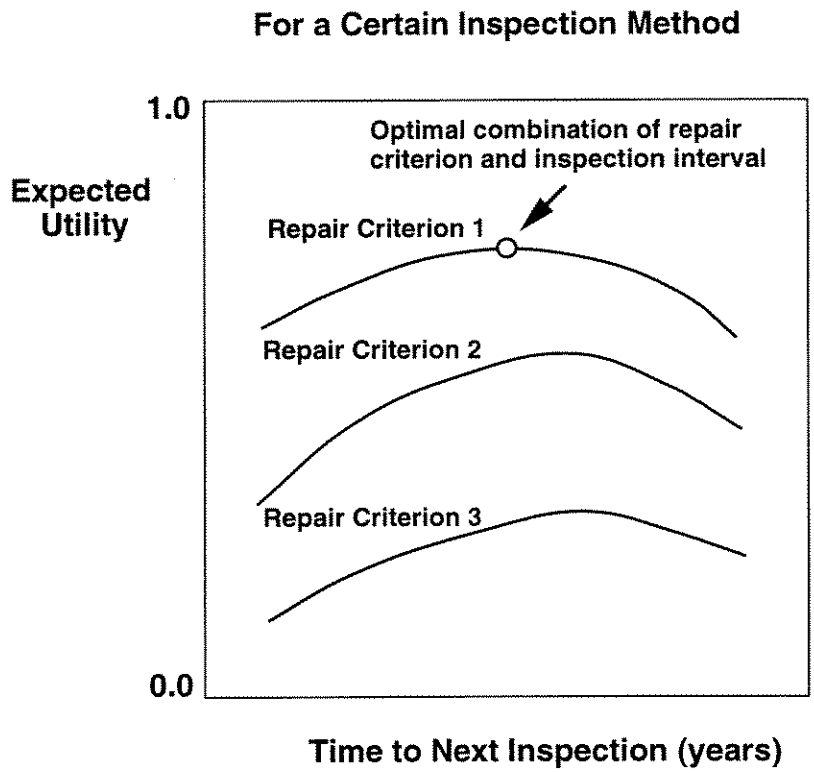

Note: For the "No inspection" option there will be only one curve and no repair criterion

Figure 10.3 Utility plots as a function of repair criterion and inspection interval

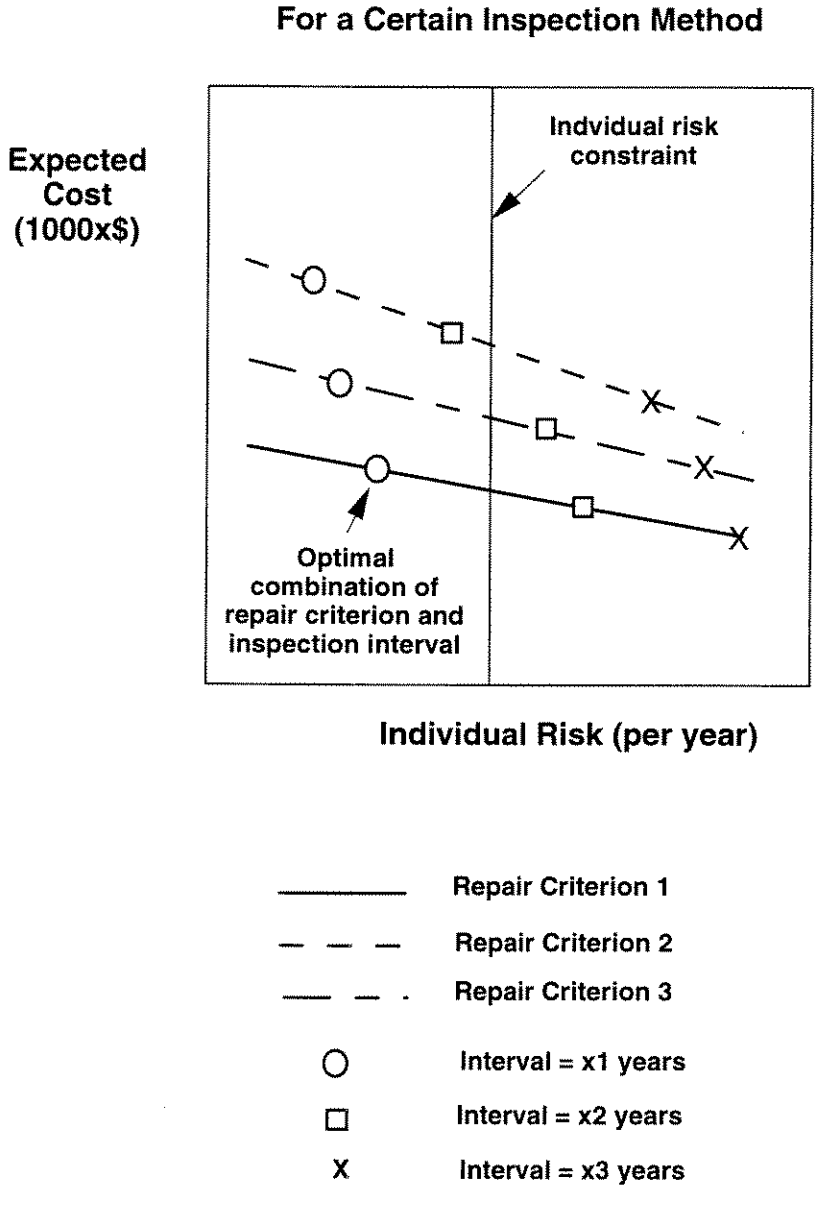

Figure 10.4 Constrained cost optimization plots as a function of repair criterion and inspection interval

11.0 REFERENCES

Abrams, H. and Hansen, S. S. 1984. Optimization of Composition and Processing to Satisfy X-70 Linepipe Property Requirement. Proceedings of International Conference on Technology and Applications of HSLA Steels, Philadelphia.

American Society of Mechanical Engineers 1991. ASME B31G Manual for determining the Remaining Strength of Corroded Pipelines. A Supplement to ASME B31 Code for Pressure Piping.

Brown, M., Nessim, M. and Greaves, H. 1995. Pipeline Defect Assessment: Deterministic and Probabilistic Considerations. Second International Conference on Pipeline Technology, Ostend, Belgium, September.

Bubenik, T. A., Olson, R. J., Stephens, D. R. and Francini, R. B. 1992. Analyzing the Pressure Strength of Corroded Line Pipe. Proceedings of the Eleventh International Conference on Offshore Mechanics and Arctic Engineering, Volume V-A, Pipeline Technology ASME.

C-FIT 1995. A Powerful New Tool for Fitting Probability Distributions to Statistical Data - User Guide. Centre For Engineering Research Inc., Edmonton, Alberta

Dally, J. W., Riley, W. F. and McConnell, K. G. 1983. Instrumentation for Engineering Measurements. John Wiley & Sons, Inc.

EGIG 1993. Gas Pipeline Incidents Report 1970-1992, European Gas Pipeline Incident Data Group.

Folias, E. S. 1964. The Stresses in a Cylindrical Shell Containing an Axial Crack. ARL 64-174, Aerospace Research Laboratories, October.

Harvey, D. W. 1994. Maintaining Integrity on Buried Pipelines. Materials Performance, August.

Jiao, G., Sotberg, T. and Bruschi, R. 1992. Probabilistic Assessment of the Wall Thickness Requirement for Pressure Containment of Offshore Pipelines. Proceedings of the Eleventh International Conference on Offshore Mechanics and Arctic Engineering, June, Vol. V-A, Pipeline Technology, pp. 249 - 255.

Kiefner, J. F. and Vieth, P. H. 1989. Project PR 3-805: A modified Criterion for Evaluating the Remaining Strength of Corroded Pipe. A Report for the Pipeline Corrosion Supervisory Committee of the Pipeline Research Committee of the American Gas Association.

Kiefner, J. F. 1969. Fracture Initiation. 4th Symposium on Line Pipe Research, Paper G, American Gas Association Catalogue No. L30075, November.

References

Kiefner, J. F., Maxey, W. A., Eiber, R. J. and Duffy, A. R. 1973. Failure Stress Levels of Flaws in Pressurized Cylinders. Progress in Flaw Growth and Fracture Toughness Testing, ASTM STP 536, American Society for Testing and Materials, pp. 461 - 481.

Madsen, H. O., Krenk, S. and Lind, N. C. 1986. Method of Structural Safety. Prentice-Hall Inc., Englewood Cliffs, New Jersey.

Mok, D. R. B., Pick, R. J. and Glover, A. G. 1990. Behavior of Line Pipe with Long External Corrosion. Materials Performance, May.

Nessim, M. A. and Hong, H. P. 1995. Probabilistic Decision Analysis Using Influence Diagrams - PIRAMID Technical Reference Manual No. 2.1. Confidential to C-FER's Pipeline Program Participants, C-FER Report 94022, October.

Rodriguez III, E. S. and Provan J. W. 1989. Development of a General Failure Control System for Estimating the Reliability of Deteriorating Structures. Corrosion, Vol. 45, No. 3., pp. 193 - 206.

Shannon, R. W. E. 1974. The Failure Behaviour Line Pipe Defects. International Journal of Pressure Vessel and Piping, Vol. 2, pp. 243 - 255.

Shannon, R. W. E. 1986. Buried Pipeline Monitoring - A Review of British Gas Experience with On-Line Inspection and Above Ground Methods. American Gas Association, Seventh Symposium.

Sheikh, A. K., Boah, J. K. and Hansen, D. A. 1990. Statistical Modeling of Pitting Corrosion and Pipeline Reliability. Corrosion, Vol. 46, No. 3, March.

Stephens, M. J. 1996. Prioritization of On Shore Pipeline Systems for Integrity Maintenance: PIRAMID Technical Reference Manual No. 4.1. Confidential to C-FER's Pipeline Program Participants, C-FER Report 95007, November.

Stephens, M. J., Nessim, M. A. and Chen, Q. 1995. A Methodology for Risk-Based Optimization of Pipeline Integrity Maintenance Activities - PIRAMID Technical Reference Manual No. 1.2. Confidential to C-FER's Pipeline Program Participants, C-FER Report 94006, October.

Stephens, M. J., Nessim, M. A. and Chen. Q. 1996. Probabilistic Assessment of Onshore Pipeline Failure Consequences: PIRAMID Technical Reference Manual No. 3.2. Confidential to C-FER's Pipeline Program Participants, C-FER Report 94035, November.

APPENDIX A

Estimating of Actual Defect Dimensions from Inspection Results

Appendix A

A.1 Notation

The following notation is used in this Appendix:

E_h	measurement error for defect depth
E_l	measurement error for defect length
H	actual depth of all defects
H_d	actual depth of detected defects
H_m	measured defect depth
L	actual length of all defects
L_d	actual length of detected defects
L_m	measured defect length
p_d	probability of detection
μ	mean value
σ	standard deviation

A.2 Problem Definition

Assume that the probability distributions of H_m, L_m, E_h, and E_l are given. These distributions are denoted $f_{Hm}(h)$, $f_{Lm}(l)$, $f_{Eh}(e)$, and $f_{El}(l)$. Also assume that the probability of detection is defined as a function of the defect depth, $p_d(h)$. This Appendix describes how this information is used to derive the probability distributions of H and L, $f_H(h)$ and $f_L(l)$.

A.3 Calculation Procedure for Defect Depth

The actual depth of defects that were detected and measured can be expressed as the measured depth minus the measurement error. This leads to

$$H_d = H_m - E_h \qquad [A.1]$$

Based on Equation [A.1] the mean and standard deviation of H_d can be calculated from

$$\mu_{Hd} = \mu_{Hm} - \mu_{Eh}, \qquad \mu_{Hm} > \mu_{Eh} \qquad [A.2a]$$

$$\sigma_{Hd} = \sqrt{(\sigma_{Hm})^2 - (\sigma_{Eh})^2}, \qquad \sigma_{Hm} > \sigma_{Eh} \qquad [A.2b]$$

Using Equations [A.2a] and [A.2b], and assuming that the distribution type of H_d is the same as that of H_m $f_{Hd}(h)$ is fully defined.

The probability distributions of H_d and H are related as follows:

$$f_H(h) \propto \frac{f_{Hd}(h)}{p_d(h)} \qquad [A.3]$$

or

$$f_H(h) = \frac{1}{K} \frac{f_{Hd}(h)}{p_d(h)} \qquad [A.4a]$$

where

$$K = \int_0^\infty \frac{f_{Hd}(h)}{p_d(h)}\, dh \qquad [A.4b]$$

Equations [A.4] provide the required probability distribution of H. Since these equations cannot be solved analytically, and since a numerical solution is time consuming, the actual solution adopted is to use Equations [A.4] to derive the mean and standard deviation of H and assume that the distribution type of H is the same as that for H_d. The mean and standard deviation are given by:

$$\mu_H = \int_0^\infty \frac{h}{K} \frac{f_{Hd}(h)}{p_d(h)}\, dh \qquad [A.5a]$$

$$\sigma_H = \sqrt{\int_0^\infty \frac{(h-\mu_H)^2}{K} \frac{f_{Hd}(h)}{p_d(h)}\, dh} \qquad [A.5b]$$

A.4 Calculation Procedure for Defect Length

The actual length of defects that were detected and measured can be expressed as the measured length minus the measurement error. This leads to

$$L_d = L_m - E_l \qquad [A.6]$$

Based on Equation [A.6] the mean and standard deviation of L_d can be calculated from

$$\mu_{Ld} = \mu_{Lm} - \mu_{El}, \qquad \mu_{Lm} > \mu_{El} \qquad [A.7a]$$

$$\sigma_{Ld} = \sqrt{(\sigma_{Lm})^2 - (\sigma_{El})^2}, \qquad \sigma_{Lm} > \sigma_{El} \qquad [A.7b]$$

Using Equations [A.7a] and [A.7b], and assuming that the distribution type of L_d is the same as that of L_m, $f_{Ld}(l)$ is fully defined.

Appendix A

Because the probability of detection is assumed to be independent of defect length, the probability distribution of L is identical to that of L_d.

APPENDIX B

Calculation of the Probability Distribution of Depth and Length After Repair Action

Appendix B

B.1 Notation

H	actual depth of all defects
H_d	depth of detected defects
H_u	depth of undetected defects
H_{du}	depth of detected unrepaired defects
H_a	depth of all defects after repair
L	actual length of all defects
L_d	length of detected defects
L_u	length of undetected defects
L_{du}	length of detected unrepaired defects
L_a	length of all defects after repair
p_d	probability of detection
$p_{(e\cap r)\|d}(h)$	probability of excavation and repair given defect depth h
$p_{(e\cap r)\|d}(l)$	probability of excavation and repair given defect length l

B.2 Purpose

Calculation of the probability distributions of the defect depth and length after repair action was discussed in Sections 5.4 and 5.5 of this document. This Appendix provides the mathematical details of the calculations described in that section.

The probability distributions of H, H_d, H_u, H_{du}, H_a, L, L_d, L_u, L_{du} and L_a are denoted by $f_H(h)$, $f_{Hd}(h)$, $f_{Hu}(h)$, $f_{Hdu}(h)$, $f_{Ha}(h)$, $f_L(l)$, $f_{Ld}(l)$, $f_{Lu}(l)$, $f_{Ldu}(l)$ and $f_{La}(l)$, respectively. $f_H(h)$, and $f_L(l)$ are assumed to be known (see Appendix A). The probability of detection is defined as a function of the defect depth, $p_d(h)$.

Note that since the updated distribution of a random variable expressed in analytical form as shown in this section cannot be represented by a standard distribution type, an approximation is adopted in which the updated distribution is assumed to have the same type as the original distribution (*i.e.*, only the mean and standard deviation of the random variable are updated).

As mentioned in Section 5.4, some of the calculations described in this Appendix are only relevant to specific inspection tools. This is indicated in the appropriate subsection titles in this Appendix.

B.3 Calculation Procedure for Detected Defect Depth (In-line Tools Only)

The probability distribution of H_d and H are related as follows:

Appendix B

$$f_{Hd}(h) \propto p_d(h) f_H(h) \qquad [B.1]$$

or

$$f_{Hd}(h) = \frac{1}{K_d} p_d(h) f_H(h) \qquad [B.2]$$

where

$$K_d = \int_0^\infty p_d(h) f_H(h) dh \qquad [B.3]$$

Note that the overall probability of detection is given by $p_d = K_d$.

The mean and the standard deviation of H_d are given by:

$$\mu_{Hd} = \frac{1}{K_d} \int_0^\infty h p_d(h) f_H(h) dh \qquad [B.4a]$$

and

$$\sigma_{Hd} = \sqrt{\frac{1}{K_d} \int_0^\infty (h - \mu_{Hd})^2 p_d(h) f_H(h) dh} \qquad [B.4b]$$

B.4 Calculation Procedure for Undetected Defect Depth (In-line Tools Only)

The probability distribution of H_u and H are related as follows:

$$f_{Hu}(h) \propto (1 - p_d(h)) f_H(h) \qquad [B.5]$$

or

$$f_{Hu}(h) = \frac{1}{1 - K_d} (1 - p_d(h)) f_H(h) \qquad [B.6]$$

The mean and the standard deviation of H_u are given by:

$$\mu_{Hu} = \frac{1}{1 - K_d} \int_0^\infty h(1 - p_d(h)) f_H(h) dh \qquad [B.7a]$$

and

Appendix B

$$\sigma_{Hu} = \sqrt{\frac{1}{1-K_d}\int_0^{\infty}(h-\mu_{Hu})^2(1-p_d(h))f_H(h)dh} \qquad [B.7b]$$

B.5 Calculation Procedure for Detected and Undetected Defect Length (All Tools)

Because the probability of detection is independent of defect length, and the defect length is assumed to be independent of defect depth, the probability distributions of detected and undetected defect length are the same as the distribution of L (*i.e.*, $f_{Ld}(l) = f_L(l) = f_{Lu}(l)$).

B.6 Calculation Procedure for Depth of Detected Unrepaired Defects (All Tools)

The probability distribution of H_{du} and H_d are related as follows:

$$f_{Hdu}(h) \propto (1 - p_{(e\cap r)|d}(h))f_{Hd}(h) \qquad [B.8]$$

or

$$f_{Hdu}(h) = \frac{1}{1-K_{(e\cap r)|d}}(1 - p_{(e\cap r)|d}(h))f_{Hd}(h) \qquad [B.9]$$

where

$$K_{(e\cap r)|d} = \int_0^{\infty}(1 - p_{(e\cap r)|d}(h))f_{Hd}(h)dh \qquad [B.10]$$

The probability of excavation and repair given detection for a defect with depth h, $p_{(e\cap r)|d}(h)$, can be calculated from Equations [C.6] to [C.9] by substituting h for H_d. Note that $K_{(e\cap r)|d} = 1 - p_{(e\cap r)|d}$.

The mean and the standard deviation H_{du} are given by:

$$\mu_{Hdu} = \frac{1}{1-K_{(e\cap r)|d}}\int_0^{\infty}h(1 - p_{(e\cap r)|d}(h))f_{Hd}(h)dh \qquad [B.11a]$$

and

$$\sigma_{Hdu} = \sqrt{\frac{1}{1-K_{(e\cap r)|d}}\int_0^{\infty}(h-\mu_{Hdu})^2(1 - p_{(e\cap r)|d}(h))f_{Hd}(h)dh} \qquad [B.11b]$$

Appendix B

B.7 Calculation Procedure for Length of Detected Unrepaired Defects (All Tools)

The probability distribution of L_{du} and L_d are related as follows:

$$f_{Ldu}(l) \propto (1 - p_{(e\cap r)|d}(l)) f_{Ld}(l) \qquad [B.12]$$

or

$$f_{Ldu}(l) = \frac{1}{1 - K_{(e\cap r)|d}} (1 - p_{(e\cap r)|d}(l)) f_{Ld}(l) \qquad [B.13]$$

The probability of excavation and repair given detection for a defect with length l, $p_{(e\cap r)|d}(l)$, can be calculated from Equations [C.6] to [C.9] by substituting l for L_d.

The mean and the standard deviation L_{du} are given by:

$$\mu_{Ldu} = \frac{1}{1 - K_{(e\cap r)|d}} \int_0^\infty l(1 - p_{(e\cap r)|d}(l)) f_{Ld}(l) dl \qquad [B.14a]$$

and

$$\sigma_{Ldu} = \sqrt{\frac{1}{1 - K_{(e\cap r)|d}} \int_0^\infty (l - \mu_{Ldu})^2 (1 - p_{(e\cap r)|d}(l)) f_{Ld}(l) dl} \qquad [B.14b]$$

B.8 Calculation Procedure for Defect Depth After Repair (All Tools)

The probability distribution of H_a H_{du} and H_d are related as follows:

$$f_{Ha}(h) = \left((1 - p_d) f_{Hu}(h) + p_d (1 - p_{(e\cap r)|d}) f_{Hdu}(h)\right) \Big/ \left(1 - p_{(e\cap r)|d}\right) \qquad [B.15]$$

The mean and standard deviation of H_a are given by:

$$\mu_{Ha} = \frac{1}{1 - p_{(e\cap r)|d}} \int_0^\infty h\left((1 - p_d) f_{Hu}(h) + p_d (1 - p_{(e\cap r)|d}) f_{Hdu}(h)\right) dh \qquad [B.16a]$$

and

$$\sigma_{Ha} = \sqrt{\frac{1}{1 - p_{(e\cap r)|d}} \int_0^\infty (h - \mu_{Ha})^2 \left((1 - p_d) f_{Hu}(h) + p_d (1 - p_{(e\cap r)|d}) f_{Hdu}(h)\right) dh} \qquad [B.16b]$$

Appendix B

B.9 Calculation Procedure for Defect Length After Repair (All Tools)

The probability distribution of L_a and L_{du} and L_d are related as follows:

$$f_{La}(l) = \Big((1-p_d)f_{Hu}(l) + p_d(1-p_{(e\cap r)|d})f_{Ldu}(l)\Big)\Big/\Big(1-p_{(e\cap r)|d}\Big) \qquad [B.17]$$

The mean and standard deviation of L_a are given by:

$$\mu_{La} = \frac{1}{1-p_{(e\cap r)|d}}\int_0^\infty l\Big((1-p_d)f_{Lu}(l) + p_d(1-p_{(e\cap r)|d})f_{Ldu}(l)\Big)dl \qquad [B.18a]$$

and

$$\sigma_{La} = \sqrt{\frac{1}{1-p_{(e\cap r)|d}}\int_0^\infty (l-\mu_{La})^2\Big((1-p_d)f_{Lu}(l) + p_d(1-p_{(e\cap r)|d})f_{Ldu}(l)\Big)dl} \qquad [B.18b]$$

APPENDIX C

Calculation of the Probability Distribution of Repair Action

Appendix C

C.1 Notation

d pipe diameter
d_n nominal pipe diameter
E_h measurement error for defect depth obtained from in-line inspection
E_l measurement error for defect length obtained from in-line inspection
H depth of defects
H_d depth of detected defects
H_m measured depth of detected defects (from in-line inspection)
h_e depth threshold for pipe excavation (low resolution in-line inspection)
L_d length of defect defects
L_m measured length of defect defects (from in-line inspection)
m Folias factor
p pipeline maximum operating pressure
p_{na} probability of no action
p_d Probability of detection
p_e probability of excavation (and coating repair)
p_r probability that pipe body repair is required
p_{nr} probability that pipe body repair is not required
$p_{a|b}$ probability of a given b
$p_{a\cap b}$ probability of a and b (intersection of a and b)
r_e resistance threshold for pipe excavation (high resolution in-line inspection)
r_r resistance threshold for pipe repair
s yield strength
s_n specified minimum yield strength
t pipe wall thickness
t_n nominal pipe wall thickness

C.2 Problem Definition

Given the probability distributions of H_d, L_d (or H_m, L_m), E_h, and E_l, and a function that calculates the pipe resistance in the form

$$r = r(p, h, l, s, t, d) \qquad [C.1]$$

calculate p_{na}, $p_{e\cap nr}$, and $p_{e\cap r}$. The pressure resistance function used in the analysis is Equation [7.15] in Section 7.2.4.2.

C.3 Basic Model

The required probabilities are: 1) the probability of no action, p_{na}; 2) the probability of excavation without pipe body repair, $p_{e\cap nr}$; and 3) the probability of excavation with pip body repair, $p_{e\cap r}$. These probabilities can be calculated as follows:

$$p_{e\cap r} = p_{(e\cap r)|d}\, p_d \qquad [C.2]$$

$$p_{e\cap nr} = p_e - p_{e\cap r} = p_{e|d}\, p_d - p_{e\cap r} \qquad [C.3]$$

$$p_{na} = 1 - (p_{e\cap nr} + p_{e\cap r}) \qquad [C.4]$$

These equations acknowledge that excavation and repair are conditional on defect detection. Three quantities are needed to calculate the required probabilities using Equations [C.2] through [C.4]. These are the probability of detection, p_d, the probability of excavation given detection, $p_{e|d}$ and the joint probability of excavation and repair given detection, $p_{(e\cap r)|d}$. Calculation methods for these probabilities are described in the following sections.

C.4 Probability of Detection

For in-line inspection tools, the overall probability of detection can be calculated by integration of the probability of detection as a function of defect depth over the probability distribution of the defect depth. This leads to

$$p_d = \int_0^\infty p_d(h)\, f_H(h)\, dh \qquad [C.5]$$

For coating damage surveys, the probability of detection is defined by the user.

C.5 Probability of Excavation Given Detection

For high resolution in-line inspection tools, the probability of excavation given detection can be calculated as the probability that the calculated resistance of a detected defect is lower than the excavation criterion. The pressure calculation uses the measured defect dimensions, which are subject to measurement error, and the nominal values of the yield strength, pipe diameter and wall thickness. In a pre-inspection run (*i.e.*, inspection data not available), the required probability can be calculated from

$$p_{e|d} = p(r < r_e) = p\big(g = [r\{p,(H_d + E_h),(L_d + E_l),s,t,d\} - r_e] < 0\big) \qquad [C.6a]$$

In a post-inspection run, the probability can be calculated from

$$p_{e|d} = p(r < r_e) = p\left(g = [r\{p, H_m, L_m, s, t, d\} - r_e] < 0\right) \qquad \text{[C.6b]}$$

For low resolution in-line inspection tools, the probability of excavation is calculated as the probability that the defect depth exceeds the excavation threshold. This is given by:

$$p_{e|d} = p(H_m \geq h_e) \qquad \text{[C.6c]}$$

The probability in Equations [C.6] can be evaluated using FORM (see Madsen *et al.* 1986). The solution will provide the probability value, the associated reliability index, β_e and a set of sensitivity factors a_{ei}, corresponding to each of the input random variables in Equations [C.6].

For coating damage survey methods, the ratio of defects to be detected in defined by the user as input.

C.6 Joint Probability of Excavation and Repair Given Detection

The probability that a detected defect requires repair can be calculated as the probability that the calculated resistance of a detected defect is lower than the excavation criterion. This calculation is similar to that of the probability of excavation given detection, except that the actual (instead of measured) depth and length of detected defects can be used based on the assumption that an in situ measurement will be made before the repair decision is made. For a pre-inspection run (*i.e.*, inspection measurements not available) this gives

$$p_{r|d} = p(r < r_r) = p\left(g = r\{p, H_d, L_d, s, t, d\} - r_r < 0\right) \qquad \text{[C.7a]}$$

For a post-inspection run the probability is given by

$$p_{e|d} = p(r < r_e) = p\left(g = [r\{p, (H_m + E_h), (L_m + E_l), s, t, d\} - r_r] < 0\right) \qquad \text{[C.7b]}$$

The probability in Equations [C.7] can be evaluated using FORM (Madsen *et al.* 1986). The solution will provide the probability value, the associated reliability index, β_r and a set of sensitivity factors a_{ri}, corresponding to the each of the input random variables in Equations [C.7].

The required probability is in fact a joint probability that a detected defect will be both excavated and repaired. Using the outcome of Equations [C.6] and [C.7], this joint probability can be calculated from (see Madsen *et al.* 1986 pp. 110)

$$p_{(e \cap r)|d} = \Phi(-\beta_e)\,\Phi(-\beta_r) + \int_0^{\rho} \phi(-\beta_e, -\beta_r, r)\, dr \qquad \text{[C.8]}$$

where Φ is the standard normal cumulative distribution function, ϕ is the bivariate normal density function, and ρ is the correlation coefficient for the two response surfaces representing the excavation and repair criteria. This is given by

$$\rho = \sum a_{ei} a_{rj} \qquad [C.9]$$

where the summation is for all values of i and j corresponding to the same random variable.

C.7 Reference

Madsen, H. O., Krenk, S. and Lind, N. C. 1986. Method of Structural Safety. Prentice-Hall Inc., Englewood Cliffs, New Jersey.

APPENDIX D

Calculation of the Probabilities of Different Failure Modes

Appendix D

D.1 Notation

a_{1i} sensitivity factors associated with pipe body failure criterion
a_{2j} sensitivity factors associated small leak criterion
g_1 pipe body failure function ($g_1 < 0$ represents failure by large leak or rupture)
g_2 small leak failure function ($g_2 < 0$ represents failure by small leak)
p_f total probability of failure
p_{sl} probability of small leak
p_{lr} total probability of failure
f_{sl} relative frequency of small leak
f_{ll} relative frequency of large leak
f_r relative frequency of rupture
f_{lr} relative frequency of large leak or rupture
β_1 reliability index associated with g_1
β_2 reliability index associated with g_2
ρ_{12} correlation coefficient between g_1 and g_2
$a \cap b$ probability of a and b
$a \cup b$ probability of a and/or b

D.2 Purpose

Calculation of the probability of failure of a pipeline at a given corrosion defect was discussed in Section 7.2 of this document. This Appendix provides the mathematical details of the calculations described in theat section.

D.3 Calculation of the Total Probability of Failure

The total probability of failure is defined as the joint probability of a small leak, large leak or rupture. Two failure criteria are used in the calculation, one for pipe body failures (large leaks and ruptures combined), g_1, and the other for small leaks, g_3, (see Section 7.2.3 and Figure D.1). The probabilities of exceeding each of these individual criteria can be calculated using the FORM methodology. As discussed in Appendix C, the FORM calculation for each criterion provides the probability of failure, p, the reliability index, β, and a set of sensitivity factors, a_i for each random variable used in the criterion. The total probability of failure can be calculated as the joint probability of a small leak and a pipe body failure (see Figure D.1)

$$p_f = p_{sl \cup lr} = p_{sl} + p_{lr} - p_{sl \cap lr} \qquad [D.1]$$

Appendix D

where

$$p_{sl\cap lr} = \Phi(-\beta_3)\Phi(-\beta_1) + \int_0^{\rho_{12}} \phi(-\beta_3, -\beta_1, r)\, dr \qquad [D.2]$$

and

$$\rho_{12} = \sum a_{1i} a_{2j} \qquad [D.3]$$

where the summation is for values of a that correspond to the same random variable.

D.4 Calculation of the Relative Probabilities of the Different Failure Modes

The relative frequencies of the different failure modes at any point in time are calculated from the probabilities associated with a defect crossing the failure boundary at the locations corresponding to the different failure modes. Figure D.1 shows these locations as AB for large leaks and ruptures, and BC for small leaks. Calculation of these probabilities is described in the following (see Madsen *et al.* 1986).

The probability of a crossing over the small leak boundary, p_{csl} is proportional to the probability of $p(g_1 > 0 \mid g_2 = 0)$. This is given by

$$p_{csl} \propto \Phi(\beta_{12}), \quad \text{where} \quad \beta_{12} = \frac{\beta_1 - \rho_{12}\beta_2}{\sqrt{1-\rho^2_{12}}} \qquad [D.4]$$

where Φ is the standard cumulative probability distribution function.

The probability of a crossing over the pipe body failure boundary, p_{clr} is proportional to the probability of $p(g_2 > 0 \mid g_1 = 0)$. This is given by

$$p_{clr} \propto \Phi(\beta_{21}), \quad \text{where} \quad \beta_{21} = \frac{\beta_2 - \rho_{12}\beta_1}{\sqrt{1-\rho^2_{12}}} \qquad [D.5]$$

The relative frequencies are then obtained by normalizing the results in [D.4] and [D.5] using

$$f_{sl} = \frac{p_{csl}\,\phi(\beta_{12})}{p_{csl}\,\phi(\beta_{12}) + p_{clr}\,\phi(\beta_{21})} \qquad [D.6]$$

$$f_{lr} = \frac{p_{clr}\,\phi(\beta_{21})}{p_{csl}\,\phi(\beta_{12}) + p_{clr}\,\phi(\beta_{21})} \qquad [D.7]$$

Appendix D

Finally the relative probabilities of large leaks and ruptures are calculated based on a fixed ratio of 9 to 1. This leads to

$$f_{ll} = 0.75\, f_{lr} \qquad [D.8]$$

$$f_{r} = 0.25\, f_{lr} \qquad [D.9]$$

D.5 Reference

Madsen, H. O., Krenk, S. and Lind, N. C. 1986. Method of Structural Safety. Prentice-Hall Inc., Englewood Cliffs, New Jersey.

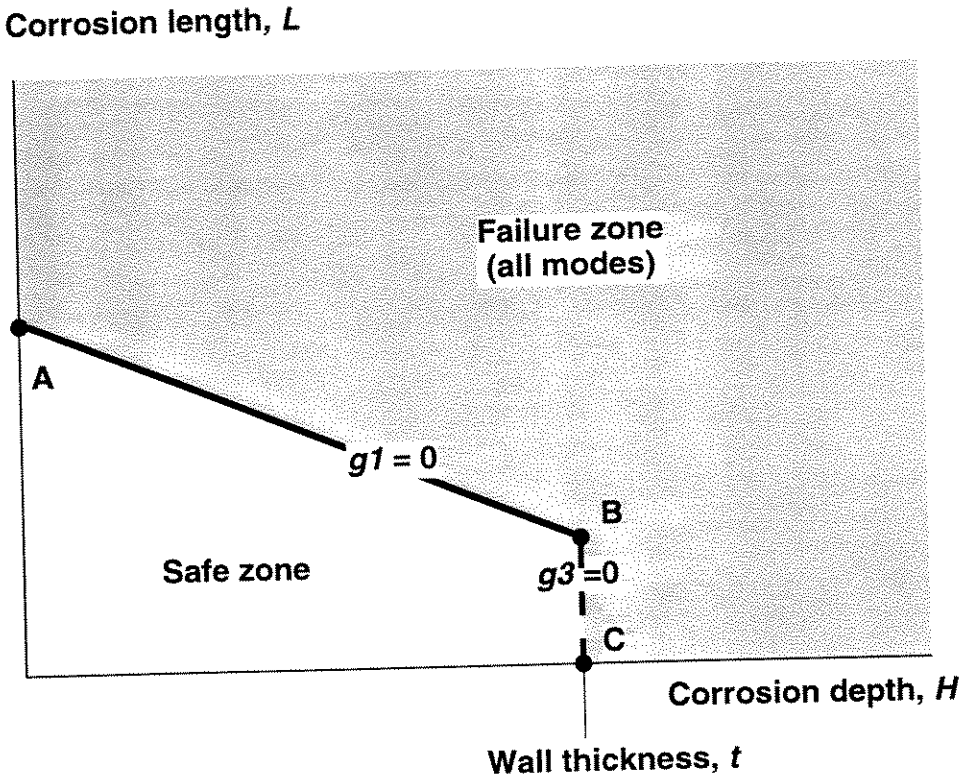

Large leak or rupture crossing zone

Small leak crossing zone

Figure D.1 Illustration of the calculation of Rupture, Large leak and Small leak

APPENDIX E

Burst Test Data for Corroded Pipe

No.	OD (in)	t (in)	Fy (psi)	SMYS (psi)	L-tot (in)	d-max (in)	d-avg (in)	A-tot (in^2)	failure press. (psi)	Leak/ Rupt.
1	30	0.370	58700	52000	2.50	0.146	0.093	0.233	1623	L
2	30	0.370	58700	52000	2.25	0.146	0.097	0.219	1620	L
3	30	0.370	58700	52000	4.25	0.157	0.069	0.292	1700	R
4	30	0.375	63800	52000	5.50	0.240	0.086	0.472	1670	R
5	30	0.375	58800	52000	4.75	0.209	0.127	0.605	1525	R
6	24	0.365	40500	35000	3.00	0.271	0.200	0.601	1100	L
7	24	0.365	40500	35000	4.75	0.251	0.176	0.836	1165	L
8	24	0.365	40500	35000	5.25	0.251	0.186	0.974	1220	R
9	24	0.380	41800	35000	5.00	0.271	0.180	0.899	1510	R
10	30	0.375	62000	52000	2.75	0.375	0.142	0.392	1745	R
11	30	0.375	61300	52000	5.50	0.146	0.059	0.324	1840	R
12	30	0.375	62000	52000	4.50	0.115	0.071	0.319	1895	R
13	30	0.375	66200	52000	4.00	0.230	0.105	0.421	1775	R
14	30	0.375	70600	52000	1.60	0.209	0.114	0.183	2140	L
15	30	0.375	66500	52000	2.00	0.209	0.104	0.209	2000	R
16	20	0.325	41000	35000	5.75	0.209	0.104	0.598	1150	L
17	20	0.325	41100	35000	6.50	0.219	0.081	0.528	1695	L
18	16	0.310	28600	25000	4.50	0.230	0.132	0.596	1100	L
19	16	0.310	28600	25000	5.00	0.240	0.129	0.643	1270	L
20	16	0.310	28600	25000	6.00	0.282	0.165	0.990	820	R
21	16	0.310	28600	25000	2.75	0.272	0.136	0.375	890	L
22	16	0.310	28400	25000	6.25	0.199	0.120	0.748	1290	L
23	24	0.417	50200	35000	13.00	0.290	0.176	2.291	1395	R
24	24	0.410	46800	35000	8.00	0.380	0.237	1.896	1660	R
25	24	0.396	50200	35000	5.75	0.360	0.191	1.099	930	L
26	24	0.444	50200	35000	8.25	0.220	0.167	1.378	1900	R
27	24	0.366	53900	35000	15.00	0.275	0.118	1.763	1469	R
28	24	0.364	52000	35000	13.00	0.254	0.131	1.707	1264	R
29	24	0.355	52000	35000	6.50	0.289	0.127	0.823	1505	L
30	24	0.319	47500	35000	5.50	0.216	0.086	0.475	1732	L
31	24	0.332	45000	35000	4.50	0.220	0.117	0.527	1752	L
32	24	0.375	53800	35000	16.00	0.295	0.231	3.700	742	R
33	24	0.375	48800	37000	9.00	0.320	0.230	2.073	788	R
34	20	0.312	50000	35000	12.00	0.252	0.228	2.740	713	R
35	20	0.305	55100	35000	10.50	0.210	0.150	1.580	1673	R
36	24	0.361	47400	35000	10.50	0.319	0.105	1.108	1290	L
37	24	0.361	41200	35000	12.50	0.285	0.067	0.831	1475	L
38	24	0.355	50300	35000	8.50	0.243	0.057	0.485	1741	L
39	24	0.371	45000	35000	10.50	0.276	0.110	1.157	1357	L
40	24	0.371	45000	35000	10.50	0.291	0.107	1.124	1357	L
41	24	0.372	48200	35000	22.00	0.284	0.061	1.333	1599	L
42	24	0.364	48100	35000	8.50	0.224	0.136	1.154	1645	R
43	24	0.366	43000	35000	12.50	0.242	0.059	0.737	1808	L
44	24	0.366	51500	35000	4.00	0.191	0.181	0.725	1583	R
45	24	0.368	47700	35000	28.00	0.288	0.062	1.726	1530	L
46	20	0.274	40500	35000	12.00	0.130	0.067	0.800	1739	R
47	20	0.311	35300	35000	8.50	0.239	0.030	0.254	1694	L
48	20	0.311	35300	35000	11.00	0.105	0.033	0.358	1694	L
49	20	0.266	40200	35000	15.50	0.144	0.065	1.007	1507	L
50	20	0.309	41900	35000	12.00	0.218	0.039	0.471	1816	L
51	30	0.372	60750	52000	36.00	0.130	0.076	2.750	1844	R
52	30	0.376	52000	52000	12.00	0.230	0.156	1.868	1515	R
53	30	0.375	60264	52000	12.00	0.140	0.109	1.310	1815	R
54	30	0.382	63542	52000	20.00	0.145	0.065	1.290	1902	R
55	30	0.376	59030	52000	20.00	0.130	0.080	1.600	1785	R
56	30	0.378	62082	52000	33.00	0.110	0.070	2.320	1916	R
57	30	0.379	65419	52000	14.00	0.170	0.094	1.310	1775	R
58	30	0.381	52000	52000	12.00	0.300	0.129	1.550	1120	L
59	30	0.378	61221	52000	8.00	0.170	0.088	0.700	1720	L
60	30	0.377	61794	52000	12.00	0.160	0.092	1.108	1789	R
61	30	0.373	60173	52000	9.00	0.110	0.083	0.750	1840	R
62	24	0.375	42000	37000	33.50	0.322	0.210	7.025	804	R
63	30	0.365	58600	52000	16.00	0.229	0.178	2.841	987	R
64	30	0.375	68770	52000	27.00	0.245	0.208	5.603	992	R
65	30	0.375	64400	56000	7.50	0.150	0.076	0.567	1970	R
66	20	0.260	61000	52000	16.00	0.218	0.174	2.789	835	R
67	36	0.330	65000	65000	16.00	0.218	0.155	2.472	775	R
68	30	0.298	71000	60000	63.00	0.269	0.146	9.216	815	R
69	22	0.198	60967	52000	6.00	0.148	0.089	0.535	828	R

Table E.1 Test data for pipes with actual corroded flaws